

OCEANOGRAPHIC AND CLIMATIC DRIVERS AND PRESSURES

Elliott L. Hazen¹, Isaac D. Schroeder¹, Jay Peterson², Bill Peterson², William J. Sydeman³, Sarah A. Thompson³, Brian K. Wells¹, Steven J. Bograd¹, N. Garfield¹

1. NOAA Fisheries, Southwest Fisheries Science Center
2. NOAA Fisheries, Northwest Fisheries Science Center
3. Farallon Institute for Advanced Ecosystem Research, P.O. Box 750756, Petaluma, CA 94952, USA

TABLE OF CONTENTS

Table of Contents 2

List of Tables and Figures 3

 Sound Bite 8

 Executive Summary 8

 Detailed Report.....10

 Oceanographic and climatic drivers and pressures10

 Implications of Climate Drivers for Coastal and Marine Spatial Planning11

 Change in Sea Level.....12

 Change in Sea Surface Temperature.....15

 Water Column Structure.....23

 Changes in California current transport and mesoscale activity.....30

 Timing and Strength of Upwelling.....33

 Timing and Frequency of El Niño Events43

 Changes in source waters.....46

 Ocean Acidification.....54

 Dissolved Oxygen and Hypoxic Events.....54

 Multivariate Ocean Climate Index – MOCI58

 Spatial Satellite Sea Surface Temperature and Chlorophyll-a61

 Effects of Anthropogenic Climate Change65

 Links to data, as appropriate67

 References cited70

LIST OF TABLES AND FIGURES

Figure E1. Winter (Jan-Mar) 2013 anomaly maps (deviation from mean over 2003-2013) of sea surface temperature (SST; left) and surface chlorophyll-a (chl-a; right). Points above or below 1 standard deviation are marked in grey. 9

Figure E2. The Total Upwelling Magnitude Index (TUMI; top) and Spring Transition Index (STI, bottom) at 39°N..... 9

Figure OC 1. Coastal sea level heights from 1967-2013 for monthly, winter, and summer means. Monthly values are included to show seasonal cycles and a continuous time series, and the blue line shows a running annual average. South Beach, Oregon coastal sea level illustrates patterns in the northern portion of the CCLME.....13

Figure OC 2. Coastal sea level heights from 1898-2013 for monthly, winter and summer means. Monthly values are included to show seasonal cycles and a continuous time series, and the blue line shows a running annual average. San Francisco coastal sea level illustrates patterns in the central portion of the CCLME.....14

Figure OC 3. Coastal sea level heights from 1906-2013 for monthly, winter and summer means. Monthly values are included to show seasonal cycles and a continuous time series, and the blue line shows a running annual average. San Diego coastal sea level illustrates patterns in the southern portion of the CCLME.....15

Figure OC 4. Sea surface temperature (SST) buoy data from early 1990 -2013 for monthly, winter and summer means. Monthly values are included to show seasonal cycles and a continuous time series, and the blue line shows a running annual average. Buoy 46050 illustrates patterns in the northern portion of the CCLME.....17

Figure OC 5. Sea surface temperature (SST) buoy data from early 1990 -2013 for monthly, winter and summer means. Monthly values are included to show seasonal cycles and a continuous time series, and the blue line shows a running annual average. Buoy 46014 illustrates patterns in the central portion of the CCLME.....18

Figure OC 6. Sea surface temperature (SST) buoy data from 1990-2013 for monthly, winter and summer means. Monthly values are included to show seasonal cycles and a continuous time series, and the blue line shows a running annual average. Buoy 46025 illustrates patterns in the southern portion of the CCLME.....19

Figure OC 7. Pacific Decadal Oscillation (PDO) index values from 1900-2013 for monthly, winter and summer means. For the monthly PDO the blue line shows a running annual average.....20

Figure OC 8. Northern Oscillation Index (NOI) values from 1948-2013 for monthly, winter and summer means. Monthly values are included to show seasonal cycles and a continuous time series, and the blue line shows a running annual average.....22

Figure OC 9. Pycnocline depth data from 1998-2013 for monthly, winter and summer means. Monthly values are included to show seasonal cycles and a continuous time series, and the blue line shows a running annual average. Newport line station NH25, illustrates patterns in the northern portion of the CCLME.....24

Figure OC 10. Pycnocline depth data from 1998-2013 (where available) and for monthly, winter and summer. Monthly values are included to show seasonal cycles and a continuous time series, and the blue line shows a running annual average. Station 67.55 illustrates patterns in the central portion of the CCLME.....25

Figure OC 11. Pycnocline depth data from 1950-2012 and for monthly, winter and summer means. Monthly values are included to show seasonal cycles and a continuous time series, and the blue line shows a running annual average. Station 93.30 illustrates patterns in the southern portion of the CCLME. Dashed lines show data gaps of greater than 2 years.26

Figure OC 12. Pycnocline strength data from 1998-2013 for monthly, winter and summer means. Monthly values are included to show seasonal cycles and a continuous time series, and the blue line shows a running annual average. Newport line station NH25 illustrates patterns in the northern portion of the CCLME.....27

Figure OC 13. Pycnocline strength data from 1998-2013 for monthly, winter and summer means. Monthly values are included to show seasonal cycles and a continuous time series, and the blue line shows a running annual average. Station 67.55 illustrates patterns in the central portion of the CCLME.....28

Figure OC 14. Pycnocline strength data from 1950-2012 for monthly, winter and summer means. Monthly values are included to show seasonal cycles and a continuous time series, and the blue line shows a running annual average. Station 93.30 illustrates patterns in the southern portion of the CCLME. Dashed lines identify data gaps of greater than 2 years.29

Figure OC 15. Satellite altimetry determined Eddy Kinetic Energy from 1992-2012 at 45°N for monthly, winter and summer means. Monthly values are included to show seasonal and long term variability. The region centered on 45°N illustrates patterns in the northern portion of the CCLME..31

Figure OC 16. Eddy Kinetic Energy satellite data from 1992-2013 at 39°N for monthly, winter and summer means. Monthly values are included to show seasonal cycles and a continuous time series, and the blue line shows a running annual average. The region centered on 39°N illustrates patterns in the central portion of the CCLME.32

Figure OC 17. Eddy Kinetic Energy satellite data from 1992-2013 at 33°N for monthly, winter and summer means. Monthly values are included to show seasonal cycles and a continuous time series, and the blue line shows a running annual average. The region centered on 33°N illustrates patterns in the southern portion of the CCLME.....33

Figure OC 18. The Upwelling Index calculated from 1967-2013 at 45°N for monthly, winter and summer means. Monthly values are included to show seasonal cycles and a continuous time series, and the blue line shows a running annual average. The UI at 45°N was illustrates patterns in the northern portion of the CCLME.....35

Figure OC 19. The Upwelling Index calculated from 1967-2013 at 39°N for monthly, winter and summer means. Monthly values are included to show seasonal cycles and a continuous time series, and the blue line shows a running annual average. The UI at 39°N illustrates patterns in the central portion of the CCLME.....36

Figure OC 20. The Upwelling Index calculated from 1967-2013 at 33°N for monthly, winter and summer means. Monthly values are included to show seasonal cycles and a continuous time series, and the blue line shows a running annual average. The UI at 33°N illustrates patterns in the southern portion of the CCLME.....37

Figure OC 21. The Spring Transition Index (STI) calculated yearly from 1967-2013 at 45°N and 39°N. The STI at 33°N is not included because there is not an extended downwelling phase during a year at this latitude.38

Figure OC 22. The Length of the Upwelling Season Index (LUSI) calculated yearly from 1967-2013 at 45°N and 39°N. The LUSI at 33°N is not included because there is not an extended downwelling phase during a year at this latitude.....39

Figure OC 23. The total upwelled magnitude index (TUMI) calculated yearly from 1967-2013 at 45°N, 39°N and 33°N.40

Figure OC 24. Alongshore, meridional winds buoy data from early 1990 -2013 for monthly, winter and summer means. Monthly values are included to show seasonal cycles and a continuous time series, and the blue line shows a running annual average. Buoy 46050 was chosen to illustrate patterns in the northern portion of the CCLME.....41

Figure OC 25. Alongshore, meridional winds buoy data from early 1990 -2013 for: monthly, winter and summer means. Monthly values are included to show seasonal cycles and a continuous time series, and the blue line shows a running annual average. Buoy 46014 was chosen to illustrate patterns in the central portion of the CCLME.42

Figure OC 26. Alongshore, meridional winds buoy data from early 1990 -2013 for: monthly, winter and summer means. Monthly values are included to show seasonal cycles and a continuous time series, and the blue line shows a running annual average. Buoy 46025 was chosen to illustrate patterns in the southern portion of the CCLME.....43

Figure OC 27. Multivariate ENSO Index values (MEI) from 1950-2013 for monthly, winter and summer means. For the monthly MEI the blue line shows a running annual average.45

Figure OC 28. North Pacific Gyre Oscillation values (NPGO) from 1950-2013 for monthly, winter and summer means. For the monthly NPGO the blue line shows a running annual average.47

Figure OC 29. Nutrient data (nitrate + nitrite) at 150 m from 1997-2013 at station NH25 from the Newport line in the northern CCLME for monthly, winter and summer means. Monthly values are included to show seasonal cycles and a continuous time series, and the blue line shows a running annual average. Station NH25 illustrates patterns in the northern portion of the CCLME. Dashed lines show data gaps of greater than 2 years.48

Figure OC 30. Nutrient data (nitrate + nitrite) at 150 m from 1997-2013 at CalCOFI station 67.55 representing central California for monthly, winter and summer means. Monthly values are included to show seasonal cycles and a continuous time series, and the blue line shows a running

annual average. Station 67.55 illustrates patterns in the central portion of the CCLME. For the last 3 years sampling has not done at station 67.55 in the summer (Jun-Aug). 49

Figure OC 31. Nutrient data (nitrate + nitrite) at 150 m from 1997-2013 at CalCOFI station 93.30 representing southern California for: monthly, winter and summer means. Monthly values are included to show seasonal cycles and a continuous time series, and the blue line shows a running annual average. Station 93.30 illustrates patterns in the southern portion of the CCLME. Dashed lines show data gaps of greater than 2 years. 50

Figure OC 32. Top. total copepod biomass, and bottom. monthly anomaly of the copepod community index from 1996-2013 in the northern California current. The blue line shows a running annual average. 52

Figure OC 33. Northern Copepod Biomass Anomaly index monthly from 1996-2012 in the northern California current. The blue line shows a running annual average. 53

Figure OC 34. Southern Copepod Biomass Anomaly index monthly from 1996-2013 in the northern California current. The blue line shows a running annual average. 53

Figure OC 35. Newport line (Newport, Oregon NH25) dissolved oxygen at 150 m from 1999-2013 for monthly, winter and summer means. Monthly values are included to show seasonal cycles and a continuous time series, and the blue line shows a running annual average. Station NH25 illustrates patterns in the northern portion of the CCLME. Dashed lines show data gaps of greater than 2 years. 56

Figure OC 36. CALCOFI station 67.55 dissolved oxygen at 150 m from 1998-2012 for monthly, winter and summer means. Monthly values are included to show seasonal cycles and a continuous time series, and the blue line shows a running annual average. Station 67.55 illustrates patterns in the central portion of the CCLME. 57

Figure OC 37. CALCOFI station 93.30 dissolved oxygen at 150 m from 1950-2012 for monthly, winter and summer means. Monthly values are included to show seasonal cycles and a continuous time series, and the blue line shows a running annual average. Station 93.30 illustrates patterns in the southern portion of the CCLME. Dashed lines show data gaps of greater than 2 years. 58

Figure OC 38. Multivariate Ocean Climate Index, axis 1, for winter, spring, summer and fall for the central-northern ecoregion of the CCLME from 1990-2010. 60

Figure OC 39. Blended satellite SST for: (left) winter 2013 SST anomalies, (middle) 5-year (2009-2013) winter SST means relative to the long-term standard deviation and (right) 5-year (2009-2013) winter SST trends relative to the long-term standard deviation. The value of each grid cell in the mean (center) and trend (right) maps has been normalized by the long-term standard deviation of the winter time series at that grid cell. In the anomaly map the zero contour is drawn in black and a gray dot marks a grid cell where the 2013 anomaly exceeds 1 standard deviation of the long-term mean. The plus/minus 1 contour is drawn in black for the trend map and a gray dot marks any grid location that has a trend exceeding 1 standard deviation from the long-term value. 62

Figure OC 40. Blended satellite SST for: (left) summer 2013 SST anomalies, (middle) 5-year (2009-2013) summer SST means relative to the long-term standard deviation and (right) 5-year

(2009-2013) summer SST trends relative to the long-term standard deviation. The value of each grid cell in the mean (center) and trend (right) maps has been normalized by the long-term standard deviation of the summer time series at that grid cell. In the anomaly map the zero contour is drawn in black and a gray dot marks a grid cell where the 2013 anomaly exceeds 1 standard deviation of the long-term mean. The plus/minus 1 contour is drawn in black for the trend map and a gray dot marks any grid location that has a trend exceeding 1 standard deviation from the long-term value.....63

Figure OC 41. Aqua MODIS satellite chl-a for: (left) winter 2013 chl-a anomalies, (middle) 5-year (2009-2013) winter chl-a means relative to the long-term standard deviation and (right) 5-year (2009-2013) winter chl-a trends relative to the long-term standard deviation. The value of each grid cell in the mean (center) and trend (right) maps has been normalized by the long-term standard deviation of the winter time series at that grid cell. In the anomaly map the zero contour is drawn in black and a gray dot marks a grid cell where the 2013 anomaly exceeds 1 standard deviation of the long-term mean. The plus/minus 1 contour is drawn in black for the trend map and a gray dot marks any grid location that has a trend exceeding 1 standard deviation from the long-term value.....64

Figure OC 42. Aqua MODIS satellite chl-a for: (left) summer 2013 chl-a anomalies, (middle) 5-year (2009-2013) summer chl-a means relative to the long-term standard deviation and (right) 5-year (2009-2013) summer chl-a trends relative to the long-term standard deviation. The value of each grid cell in the mean (center) and trend (right) maps has been normalized by the long-term standard deviation of the summer time series at that grid cell. In the anomaly map the zero contour is drawn in black and a gray dot marks a grid cell where the 2013 anomaly exceeds 1 standard deviation of the long-term mean. The plus/minus 1 contour is drawn in black for the trend map and a gray dot marks any grid location that has a trend exceeding 1 standard deviation from the long-term value.....65

Table OC 1. Top indicators for ocean and climatic pressures. Three stations were chosen when possible for northern, central, and southern portions of the California current. Time series availability often differed across the three locations.....67

SOUND BITE

The past year (2013) was characterized by record cumulative upwelling in the central CCLME leading to below average SSTs and localized regions of high Chlorophyll-a biomass, although the ecosystem implications of these anomalies remain unclear. Recent data from the equatorial Pacific suggest that an El Niño will affect the CCLME in the coming year.

EXECUTIVE SUMMARY

The California Current Large Marine Ecosystem (CCLME) is primarily driven by bottom-up physical processes; thus trends in the physical and biogeochemical state can inform the management of ecosystem services. The Pacific Decadal Oscillation (PDO) and the North Pacific Gyre Oscillation (NPGO), respectively indicators of sea surface temperature and changes in source water, continue to describe a cool phase that has largely persisted since 1999 in the CCLME (Figure E1). From late 2009 to early 2010, a short duration El Niño with stronger than average downwelling-favorable winds was observed and was quickly followed by La Niña conditions in the summer of 2010. Currently, an El Niño event is developing in the equatorial Pacific that will likely have ecosystem implications in the coming year. From 2009 to 2013, the CCLME has been characterized by periods of strong and persistent upwelling from central California to Oregon (Figure E2). In 2013, an early onset and long upwelling season led to the highest cumulative annual upwelling index (TUMI) on record, resulting in negative SST anomalies and a few localized areas of increased chlorophyll-a (chl-a), overlaid on a background of generally decreased chl-a (Figure E2). The full ecosystem implications of these upwelling anomalies are as yet unclear; although most of the physical indicators suggest that primary productivity should have been high during 2013, chl-a biomass was below average most areas. There may be an optimal window in both the timing and magnitude of upwelling that maximizes ecosystem productivity, and the extremely high upwelling during 2013 may have actually led to increased offshore transport and loss of plankton to coastal food webs. The trend of decreasing oxygen content (DO) continues to suggest increased habitat compression for pelagic species and more severe hypoxic events on the shelf that can lead to physiological stress or large scale die-offs.

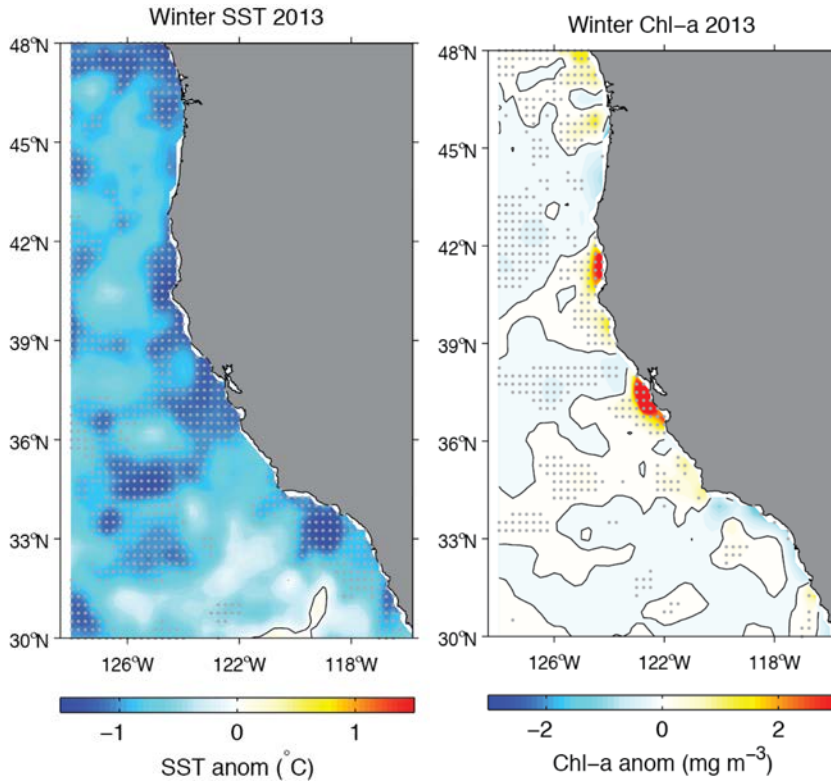


Figure E1. Winter (Jan-Mar) 2013 anomaly maps (deviation from mean over 2003-2013) of sea surface temperature (SST; left) and surface chlorophyll-a (chl-a; right). Points above or below 1 standard deviation are marked in grey.

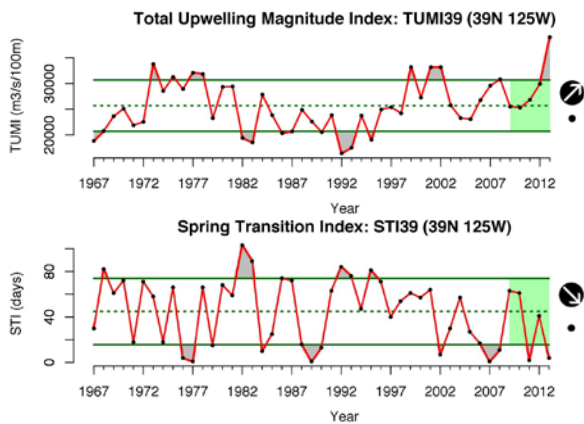


Figure E2. The Total Upwelling Magnitude Index (TUMI; top) and Spring Transition Index (STI, bottom) at 39°N.

DETAILED REPORT

The ultimate aim of the California Current Integrated Ecosystem Assessment (IEA) is to quantify the web of interactions that links drivers and pressures to ecosystem-based management (EBM) components and to forecast how changing environmental conditions and management actions affect the status of EBM components. In order to capture the breadth of pressures acting on the California Current Large Marine Ecosystem (CCLME), a lengthy list of drivers and pressures was developed and consolidated. Drivers are defined as the top-level forcing factors that result in pressures which in turn cause changes in the ecosystem. For example, coastal development is a driver that results in increased coastal armoring and the loss of associated intertidal habitat. For this CCIEA, both natural and anthropogenic drivers are considered. An example of the former is climate variability and the latter include the human population size in the coastal zone and associated coastal development, and the demand for seafood. Other anthropogenic pressures include coastal pollution, habitat loss and degradation, and fishing effort that can be mapped to specific drivers. In principle, anthropogenic drivers can be assessed and controlled. Natural environmental fluctuation cannot be controlled but must be incorporated and accounted for in management efforts.

Indicators are proxies that serve as measures of either drivers or pressures. Indicators were developed by first identifying a suite of drivers and pressures that were most closely associated with impacts and changes to the different EBM components in the California Current IEA. We used several publications (Halpern et al. 2008, Sydeman and Elliott 2008, Halpern et al. 2009, Sydeman and Thompson 2010, Teck et al. 2010, Peterson et al. 2012) to develop potential pressures on the CCLME. During reviews of the literature, we identified 32 primary groups of pressures on the CCLME, and these were categorized as “oceanographic and climatic” or “anthropogenic.” Indicators for each of these pressures were then evaluated using the indicator selection framework developed by Levin et al. (2011) and Kershner et al. (2011) and used in the previous version of NOAA’s Integrated Ecosystem Assessment for the California Current (Levin and Schwing 2011). The second step was to develop time-series for each of the top indicators for each pressure. These time-series were used to determine the current status, short-term trends, and five-year anomalies for each pressure in the CCLME. In this IEA, we use the same indicators as the 2013 CCIEA, along with a new additional multivariate ocean climate index (MOCI)(Sydeman et al. 2014), and spatially explicit satellite remote sensed sea surface temperature (SST) and chlorophyll-a (chl-a). **Changes in the current IEA versus previous reports are highlighted by BOLD**, with new interpretations in italics.

OCEANOGRAPHIC AND CLIMATIC DRIVERS AND PRESSURES

Three broad pressures associated with climate change were described by Teck et al. (2010) as physical state variables: increasing ocean acidification, sea level rise, and changes in sea surface temperature. Climate change includes long-term natural variability, short-term event driven variability, and an anthropogenic global warming signal, but separating anthropogenic from natural processes is difficult in the California Current. The CCLME is an eastern boundary current system largely driven by upwelling, so we have included a few additional pressures (9 total) presented below and summarized in Table OC1. It is important to mention that this document is not aimed to provide extensive reviews of the state of the California Current, but instead cataloguing and presenting existing information in a Driving Forces-Pressures-State-Impacts-Responses framework (e.g. Levin et al. 2009) as a foundation for forthcoming IEA sections. There are a number of high quality status reports for the California Current including the state of the California Current (Bjorkstedt et al. 2011), PICES Ecosystem status report (Bograd 2010), and ocean ecosystem

indicators (<http://www.nwfsc.noaa.gov/research/divisions/fed/oeip/a-ecinhome.cfm>), among others.

We have used long term running means of the whole dataset, and highlight deviations from the mean and trends over the past 5 years for conformity across IEA figures, however many of the state variables fluctuate at decadal to multi-decadal scales. The 5-year window is used to show short-term trends and anomalies in the environmental indicator. On each figure, the dotted line represents the long-term mean of the time series with the green lines representing 1 standard deviation above and below. The arrows represent positive (↗), negative (↘) or lack of (↔) trend over the past 5 years while a +, -, or • indicate that the mean of the past 5 years is greater than, less than, or within 1 standard deviation from the long-term mean respectively.

There is a close mechanistic link between coastal upwelling and ecosystem productivity on seasonal, annual, and interannual scales (Hickey 1979, Checkley and Barth 2009). Upwelling in the central-northern CCLME occurs in two distinct seasonal modes (winter and summer), with certain biological processes being more sensitive to one or the other (Black et al. 2011, Thompson et al. 2012). Thus in this section we present indicators when there is monthly data as winter and summer means. Summer means were calculated from June 1st - August 31st and winter means were calculated from January 1st - March 31st of the current year; thus *winter precedes summer for each index*. Indicator selection followed the IEA framework and identified datasets with the most relevance to the pressure, and had the longest and most complete time series. Indicator evaluation, data indices and sources are summarized in Table OC1.

IMPLICATIONS OF CLIMATE DRIVERS FOR COASTAL AND MARINE SPATIAL PLANNING

There are regional differences within the CCLME in climate forcing (Mendelssohn et al. 2003, García-Reyes and Largier 2012) and ecosystem response (Checkley and Barth 2009). Therefore, patterns in the southern California Current region may vary substantially from patterns in the northern California Current. When considering an overall IEA for the CCLME, it may prove most useful to separately evaluate each ecoregion/subecosystem initially. In no single region, however, are all the desired physical and biological attributes available for comprehensive analyses. Therefore, to understand ecosystem form, function, and controls, to the extent possible we must combine information between regions. We have examined three primary regions in the CCLME using cruise data such as CALCOFI (California Cooperative Oceanic and Fisheries Investigations) off southern and central California and the Newport line off Oregon. More holistic data are provided by buoy data (National Buoy Data Center), and satellite products.

The central and northern CCLME is dominated by strong seasonal variability in winds, temperature, upwelling, and plankton production (Huyer 1983). In addition to weak, delayed, or otherwise ineffectual upwelling, warm-water conditions in this region could result from either onshore transport of offshore subtropical water or northward transport of subtropical coastal waters (King et al. 2011). Low copepod species richness and high abundance of northern boreal copepods is associated with cold, subarctic water masses transported to the northern CCLME from the Gulf of Alaska (Peterson and Schwing 2003, Hooff and Peterson 2006, Peterson 2009, Bi et al. 2011, Keister et al. 2011). Therefore, copepod community composition may be used as an indicator of this physical oceanographic process.

Evidence suggests covariation between the central and northern ecoregions. As an example, when fatty, subarctic northern boreal copepods are present in the northern CCLME during cool-water conditions, the productivity of the planktivorous Cassin's auklet in the central subregion increases. Conversely, when the less fatty subtropical copepods dominate the system in warm-water years (i.e., a higher southern copepod anomaly index), Cassin's auklet breeding success is reduced (Sydeman et al. 2011).

CHANGE IN SEA LEVEL

BACKGROUND

Sea level rise from climate change is expected to accelerate in the next century. The International Panel on Climate Change (IPCC) estimates that the global average sea level will rise further between 0.6 and 2 feet (0.18 to 0.59 meters) in the next century (IPCC 2007) as a result of natural processes and anthropogenic global warming. These estimates of sea level rise excluded any increases due to glacial melt. At its simplest, sea level rise is due to the thermal expansion of seawater (Domingues et al. 2008) and increased freshwater inputs from melting polar and glacier ice from the continents (Radić and Hock 2011). To best estimate the rate of sea level rise vertical movements of the land such as post-glacial rebound need to be considered to get an adequate rate (Douglas 1991). Multiple time scales are associated with sea level rise; on multi decadal timescales steric changes in the density field are often attributed to climate variability, while seasonal to interannual time scales variations are due to atmospheric and oceanic effects that can result in geostrophic readjustments.

Coastal sea level is used as a proxy for nearshore surface current strength and direction. In the winter, sea levels are high due to the poleward flowing counter current (Davidson Current). With the onset of upwelling winds in the spring, sea levels lower and the current is directed equatorward; the equatorward flow is dominant in the spring and summer (King et al. 2011).

EVALUATION AND SELECTION OF INDICATORS

Records of sea level rise must be multiple decades in length to distinguish changes over naturally occurring low-frequency signals that derive from atmospheric and oceanic forcing (Parker 1991). Three tidal gauge locations along the CCS achieve the criteria of being exceptionally long in length thus good indicators of change in sea level. They are: San Diego, CA (1906-present), San Francisco, CA (1897-present), and South Beach, OR (1967-present). Combining coastal tide gauges with satellite altimetry (Saraceno et al. 2008) can provide a more direct measure of stratification and circulation however these time series are limited by satellite altimetry availability.

STATUS AND TRENDS

Since 1950, there have been increasing sea level trends, particularly until 1977 with more numerous and extreme positive anomalies (Figures OC1 – OC3). Over the past five summers, the San Diego station values have been greater than one standard deviation from the mean although there were no significant short-term trends throughout the California Current. Coastal sea level trends have been somewhat muted since 1980 due to wind changes and the Pacific Decadal Oscillation (PDO) masking any upper-ocean temperature steric effect (Bromirski et al. 2012). The summer

records show a long-term trend of sea level rising at about 2 mm yr⁻¹. This trend isn't evident in either the monthly or winter plots. **The greatest difference between this year's and last year's status, is that sea level in winter 2012/2013 at South Beach OR was much lower than the immediate previous years**, however, the following summertime sea level at this location was similar to previous years. *This observation is most likely due to an earlier onset of upwelling at this location, as evidenced by an earlier STI during 2013 (Fig OC21).*

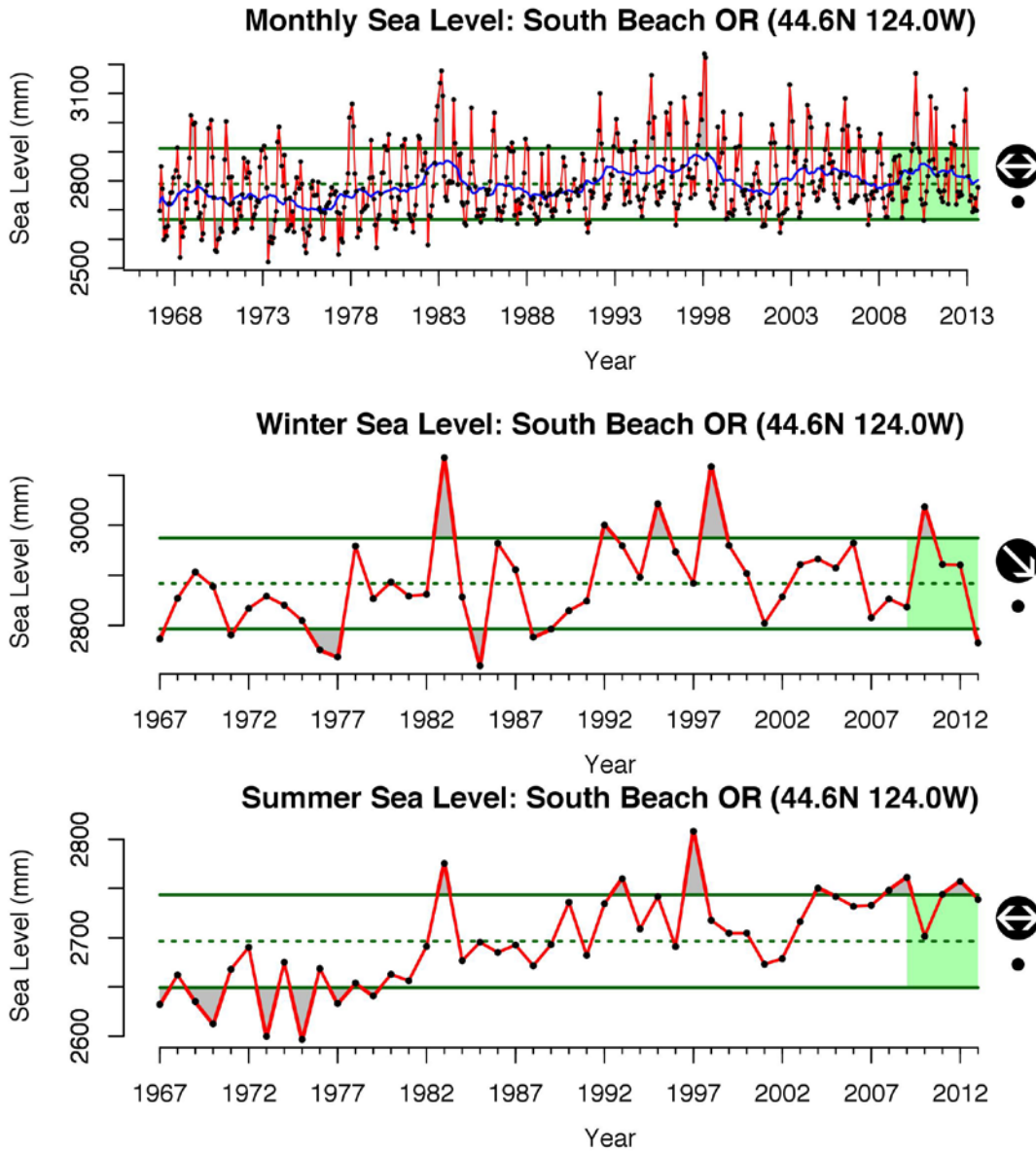


Figure OC 1. Coastal sea level heights from 1967-2013 for monthly, winter, and summer means. Monthly values are included to show seasonal cycles and a continuous time series, and the blue line shows a running annual average. South Beach, Oregon coastal sea level illustrates patterns in the northern portion of the CCLME.

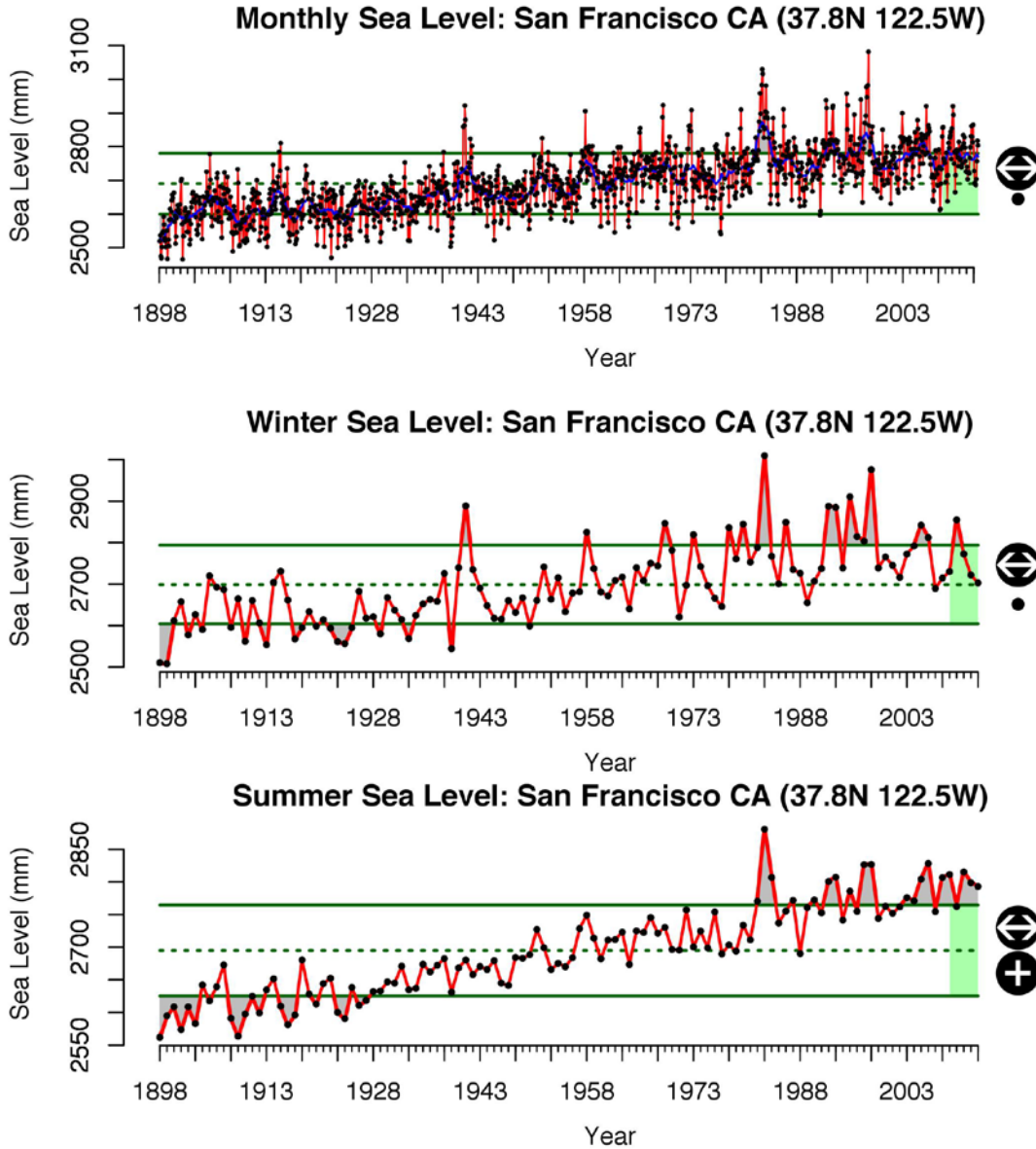


Figure OC 2. Coastal sea level heights from 1898-2013 for monthly, winter and summer means. Monthly values are included to show seasonal cycles and a continuous time series, and the blue line shows a running annual average. San Francisco coastal sea level illustrates patterns in the central portion of the CCLME.

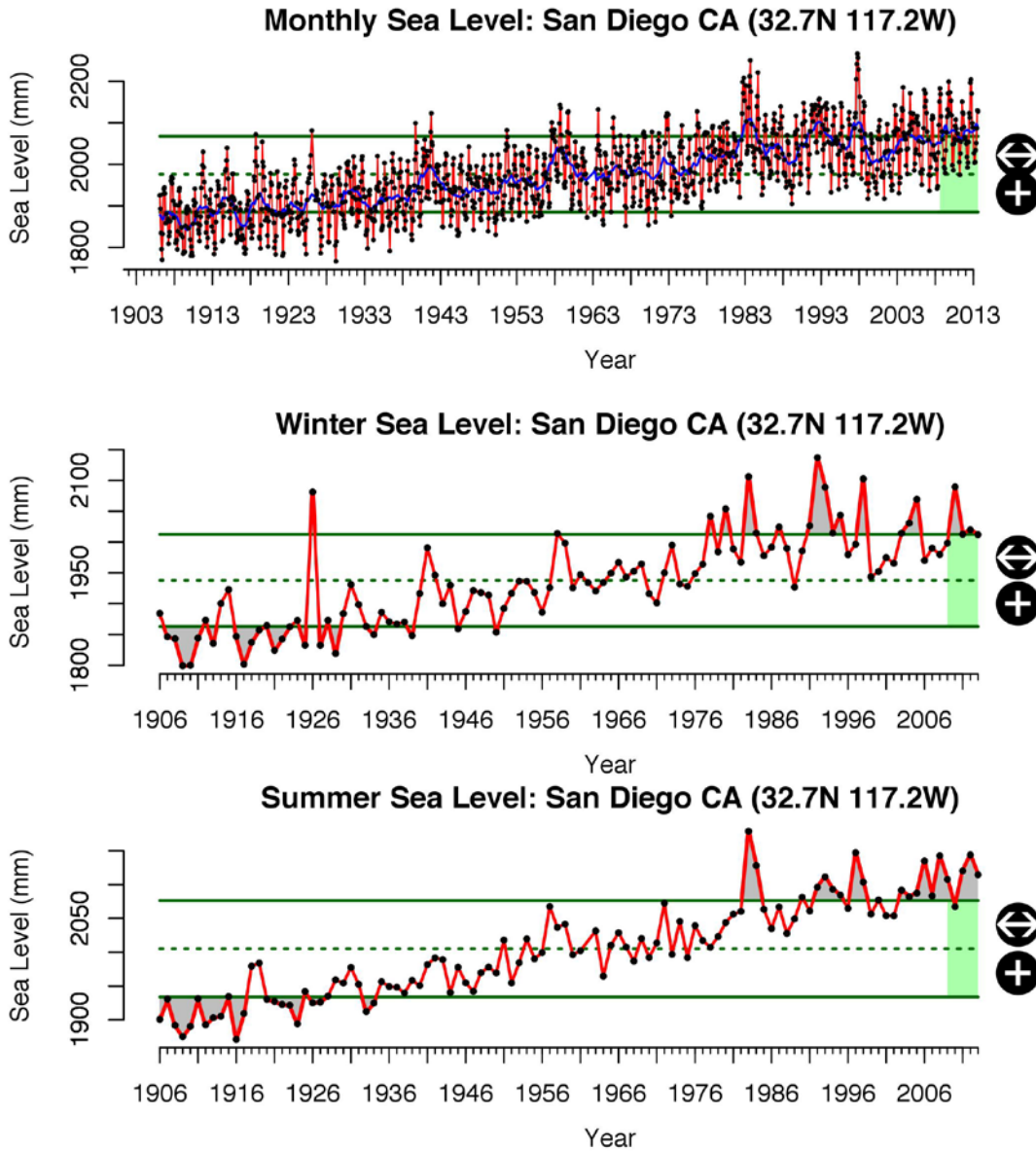


Figure OC 3. Coastal sea level heights from 1906-2013 for monthly, winter and summer means. Monthly values are included to show seasonal cycles and a continuous time series, and the blue line shows a running annual average. San Diego coastal sea level illustrates patterns in the southern portion of the CCLME.

CHANGE IN SEA SURFACE TEMPERATURE

BACKGROUND

Water temperatures in the California current vary at multiple time scales: seasonally due in large part to upwelling, inter-annually due to regional-scale forcing, and at the broadest scales due to natural low frequency variability and anthropogenic climate change. Upwelling timing and strength

greatly influences the California ecosystem through productivity and temperature changes (see section below), and many species in the CCLME are thermally limited directly (Song et al. 2012) or indirectly through trophic interactions (Wells et al. 2008). ENSO events and climatic forcing has the greatest influence on interannual temperatures resulting in changes in species composition and biodiversity. At the broadest scales, temperatures in the world's oceans are predicted to warm up to 6 degrees Celsius by 2100 (IPCC 2007). The effects of ocean warming on marine ecosystems are being examined more in recent years, and multiple studies have observed or predicted range shifts in marine organisms over the next century (Hazen et al. 2012, Sunday et al. 2012), spatial changes in productivity and diversity (Rijnsdorp et al. 2009), and changes in timing of migration for oceanic and riverine fish (Spence and Hall 2010). Long term warming in the California current may be buffered by upwelling, but changes in source waters and stratification may limit any buffering effect.

EVALUATION AND SELECTION OF INDICATORS

There are numerous indicators of sea surface temperature at various spatial and temporal scales in the CCS. The Pacific decadal oscillation (PDO) index is used to show low frequency changes in sea surface temperature (SST) over the north Pacific (Mantua et al. 1997). When the PDO is positive, SST within the CCLME (especially the northern region) is warmer. The PDO does an inadequate job of describing SST variability in the coastal zone. The Multivariate ENSO index (MEI) represents patterns in six main observed variables over the tropical Pacific, to identify status of the El Niño southern oscillation, but the impact of ENSO on the CCLME varies. The Northern Oscillation Index (NOI) indexes the interannual changes of atmospheric forcing relevant to the CCLME, still a broad index. Thus, coastal zone water temperature change indicators are chosen via SST measured by NDBC buoys. SST winter/summer means are taken from three NDBC buoys in the CCLME. The three buoys are located in the California Bight, Central California and Oregon.

STATUS AND TRENDS

SST

Cold sea surface temperature (SST) from upwelled water often results in high productivity but nutrient content depends upon remotely forced state of the ocean, which can be indicated by large-scale climate indices (North Pacific gyre Oscillation (NPGO), PDO, MEI, and NOI). Negative NPGO, positive PDO, and positive MEI would act in concert to create an extremely warm, low-productivity regime in the CCLME. According to many long-term data sets from the open ocean, SSTs have increased by 0.5°C to 1.0°C over the past 50 years (IPCC 2007, Levitus et al. 2009). SST from three NOAA National Data Buoy Center (NDBC) buoys showed highs in 1983 and 1998 corresponding with increased MEI values (Figures OC4 – OC6). Most SST values in the past 5 years were lower than the 20-year mean average at all stations and for both seasons. The exceptions were warmer than average SSTs in winter 2010 at all three stations which had high SSTs due to the short duration El Niño, and the summer of 2011 in central California as well. **For 2013, SST values remained as cold or colder than the immediately previous years (except the winter SST for the northernmost station), reinforcing the evidence that 2013 had an early onset, and stronger overall upwelling than 2012.**

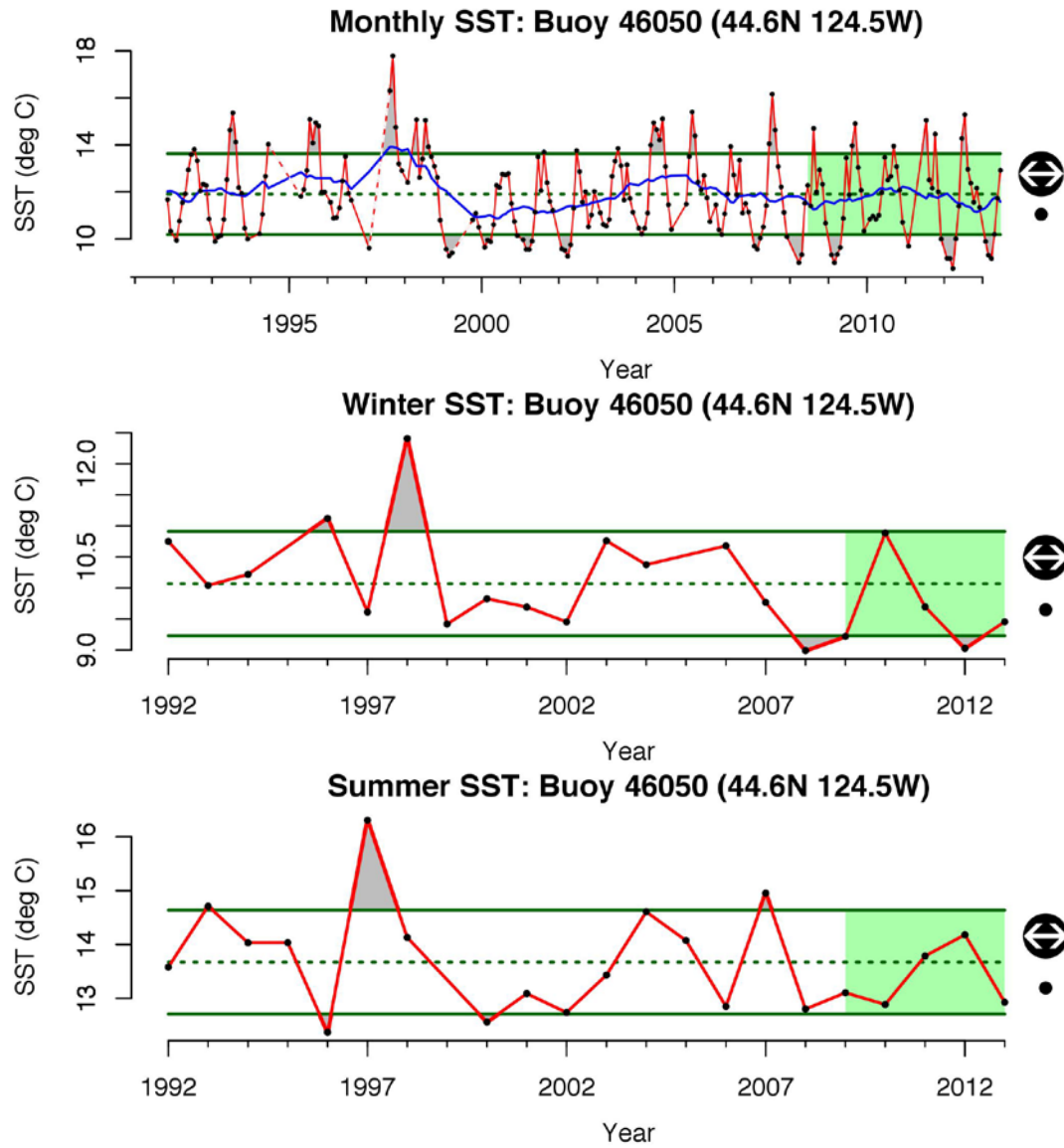


Figure OC 4. Sea surface temperature (SST) buoy data from early 1990 -2013 for monthly, winter and summer means. Monthly values are included to show seasonal cycles and a continuous time series, and the blue line shows a running annual average. Buoy 46050 illustrates patterns in the northern portion of the CCLME.

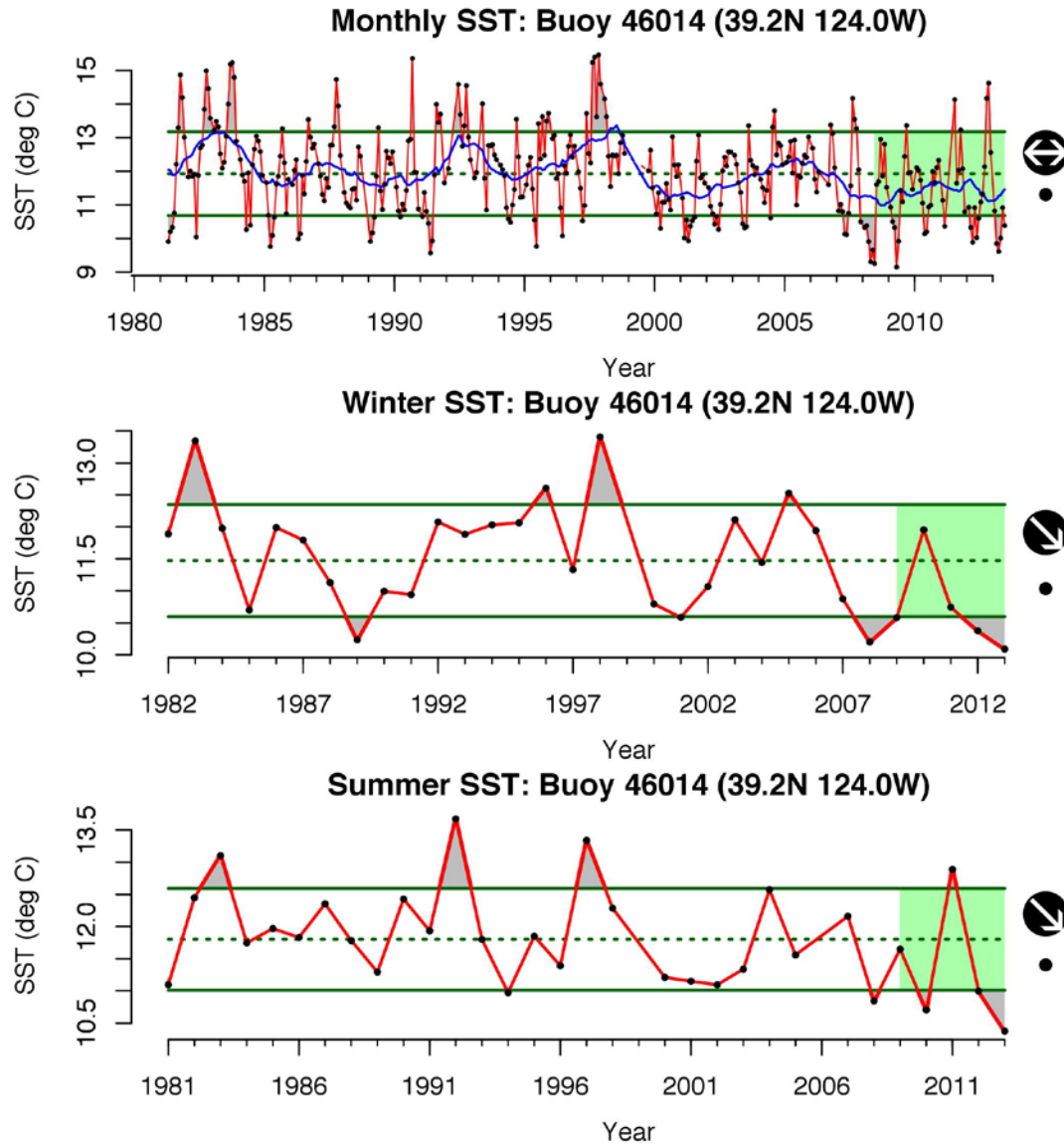


Figure OC 5. Sea surface temperature (SST) buoy data from early 1990 -2013 for monthly, winter and summer means. Monthly values are included to show seasonal cycles and a continuous time series, and the blue line shows a running annual average. Buoy 46014 illustrates patterns in the central portion of the CCLME.

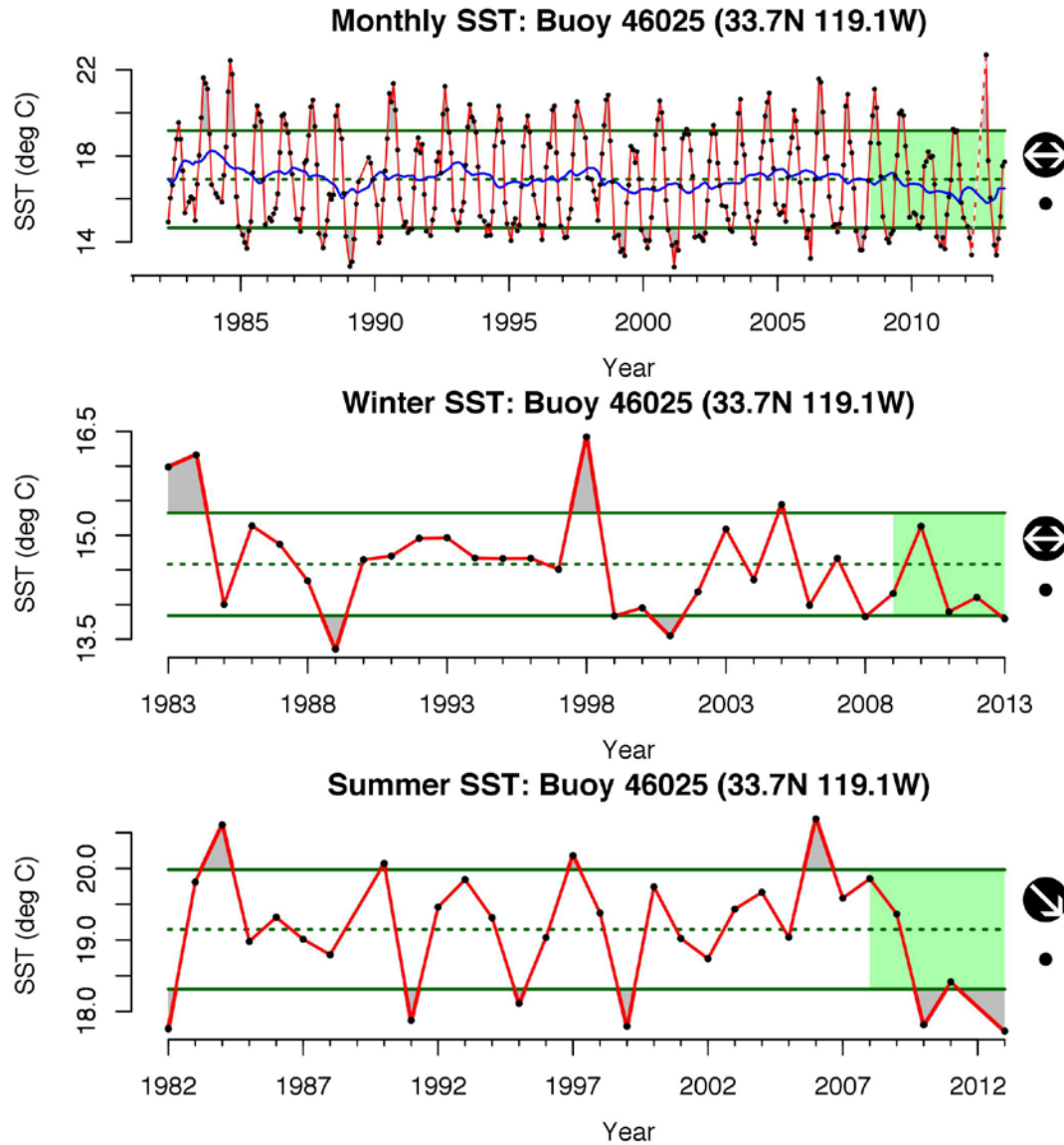


Figure OC 6. Sea surface temperature (SST) buoy data from 1990-2013 for monthly, winter and summer means. Monthly values are included to show seasonal cycles and a continuous time series, and the blue line shows a running annual average. Buoy 46025 illustrates patterns in the southern portion of the CCLME.

PDO

Pacific decadal oscillation (PDO) is a low frequency signal in North Pacific sea surface temperatures that affects biological productivity in the Northeast Pacific (Mantua et al. 1997). Cold (negative values of the PDO) periods are associated with enhanced productivity in the CCLME and vice versa (King et al. 2011). The PDO index has been largely in a positive (i.e., warm California Current and Northeast Pacific) state since late 1977, resulting in warmer waters along the coast of the CCLME with a negative phase since 1998 with occasional warm episodes from El Niños (Figure

OC7). Over the past 5 years, the winter and summer indices have remained relatively low, except a higher value in 2010 for winter. **Values for 2013 have remained low, similar to the immediately previous years, supporting the observations that 2013 was a strong upwelling year.**

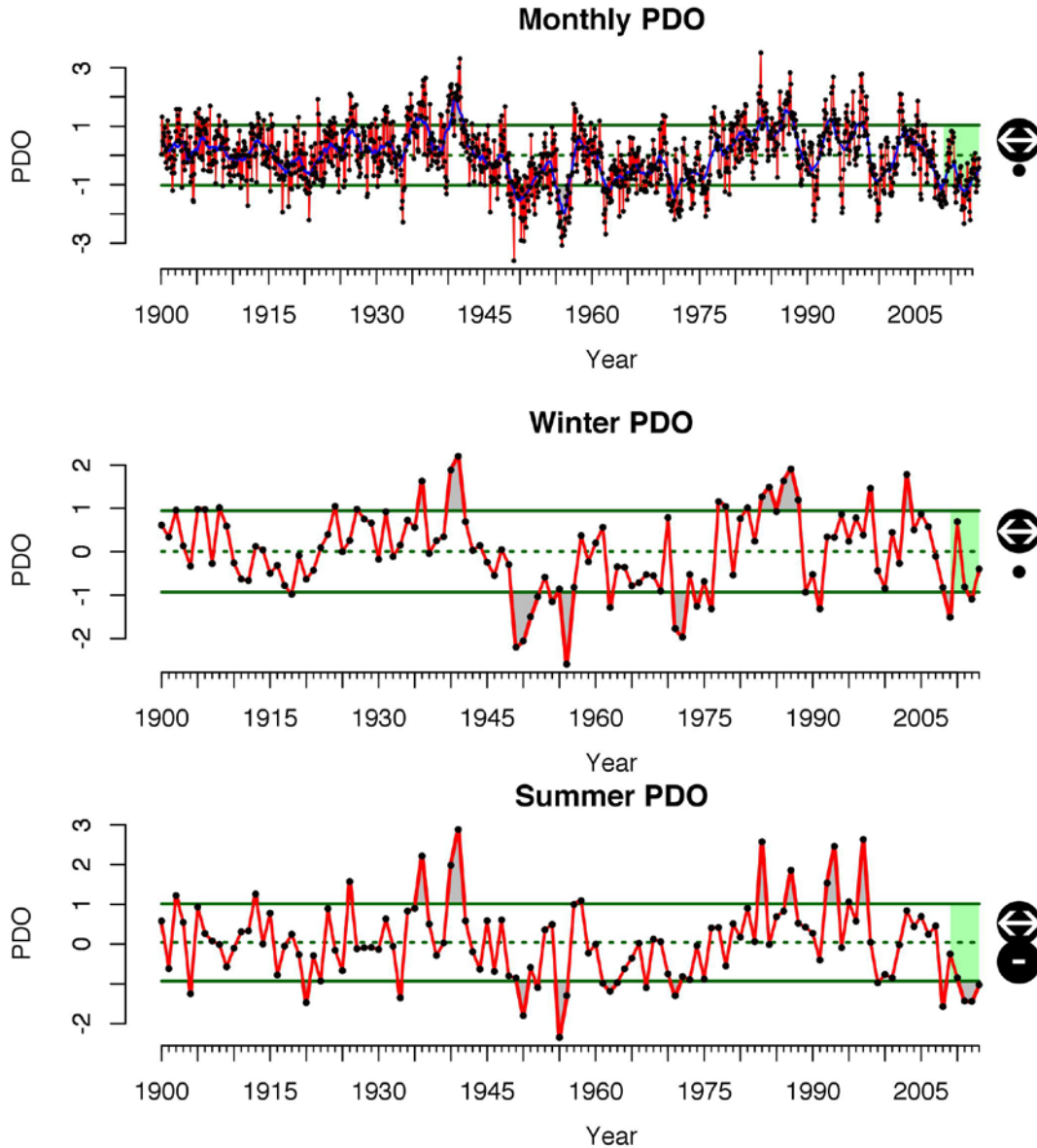


Figure OC 7. Pacific Decadal Oscillation (PDO) index values from 1900-2013 for monthly, winter and summer means. For the monthly PDO the blue line shows a running annual average.

NOI

Northern oscillation index (NOI) is the sea level pressure difference between the climatological mean position of the North Pacific High and Darwin, Australia (Schwing et al. 2002).

NOI describes the strength of atmospheric forcing between the equatorial Pacific and the North Pacific, particularly in terms with ENSO. Positive values of the NOI are related to a more intense North Pacific High and stronger north winds over the CCS, and stronger northeasterly trade winds in the subtropics resulting in cooler waters. NOI was largely positive from 1950 to 1977, and then switched to more negative values until 1998 (Figure OC8). In the winter, NOI values were positive from 2006 to 2009 with a drop and overall negative trend in 2010 representing the brief El Niño event. In the summer of 2010, NOI values became strongly positive which should result in increased coastal upwelling in the California Current, and have since returned to near neutral values. **In 2013, the NOI remained similar to the previous years, with a slight increase for the winter average;** *such atmospheric forcing is consistent with the early setup of upwelling and lower SST seen in 2013.*

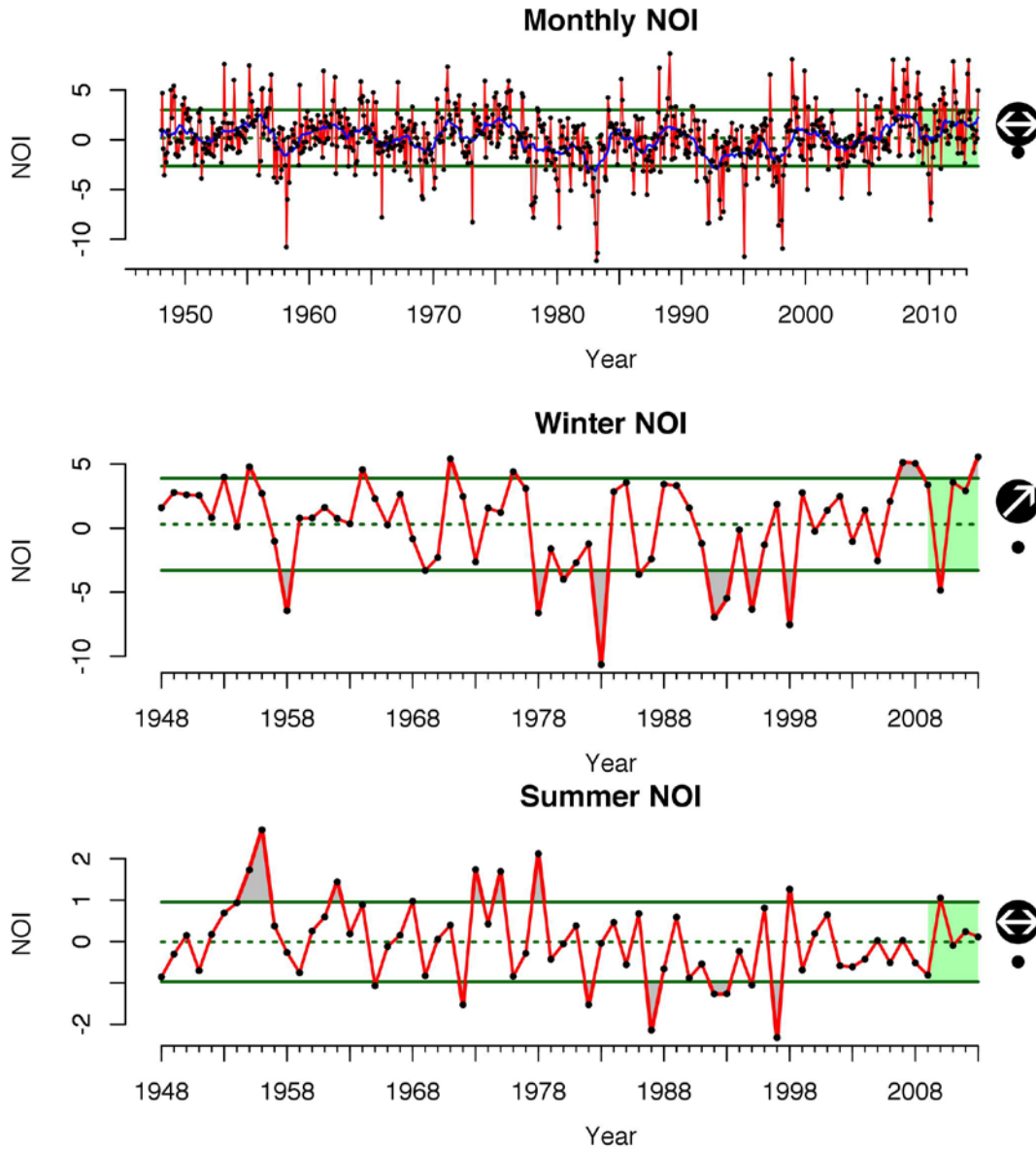


Figure OC 8. Northern Oscillation Index (NOI) values from 1948-2013 for monthly, winter and summer means. Monthly values are included to show seasonal cycles and a continuous time series, and the blue line shows a running annual average.

MEI

See Timing and Frequency of El Niño events.

WATER COLUMN STRUCTURE

BACKGROUND

The ocean is vertically stratified into large horizontal layers of water with different properties, such as nutrients, oxygen, temperature, salinity and density. For the water column structure attribute, we will focus on stratification due to density differences. Layers of more dense water lie below less dense water and the boundary between the layers acts as a barrier to mixing. Mixing between layers is easier when the density difference (e.g. the strength of stratification) between the layers is small. The formation of the layers is due to several different geo-physical processes, which act on different spatial and temporal timescales. For example, any physical processes that can change the water density, such as wind mixing of adjacent layers, fresh water inputs and atmospheric thermal heating/cooling, will affect water column stratification. The effectiveness of upwelling winds in the CCLME can be reduced if the water column is highly stratified thus limiting the injection of nutrients from deep water into the surface euphotic zone (Palacios et al. 2004, Behrenfeld et al. 2006). In this report we will characterize the water column structure by quantifying information of the upper surface water mass. Two variables of interest are the mixed layer depth (pycnocline depth) and the strength of the stratification (the gradient between the density of the surface layer and the adjacent lower layer). Buoyancy frequency, or Brunt-Väisälä frequency, can be used to define water column density stratification. The buoyancy frequency is proportional to vertical changes in density; the largest buoyancy frequency will mark the pycnocline (Pond and Pickard 1983). Upwelling can be constrained if the pycnocline depth is deep and the strength of stratification is strong.

EVALUATION AND SELECTION OF INDICATORS

Long time series of the strength of stratification and the mixed layer depth have been compiled at three stations for this report, but broader spatial coverage would be ideal for future IEAs. The MEI can provide a proxy for the pycnocline depth over interannual time scales because El Niño events result in a deepening of the pycnocline due to the propagation of Kelvin waves. Additionally, atmospheric teleconnections during an El Niño favor an intensified Aleutian Low pressure cell that is also displaced to the south and east of its climatological position. This pressure pattern favors intense south-southwesterly winds that cause intense coastal onshore Ekman transport and downwelling, and reduced heat fluxes from the ocean to the atmosphere. Together these two impacts lead to a warmer than average upper ocean over the continental shelf.

STATUS AND TRENDS

PYCNOCLINE DEPTH

Pycnocline depth, the depth at which there is the greatest rate of change in density in the vertical water column, represents the separation between warmer nutrient-poor surface waters and cooler nutrient-rich deep waters. The shallower the pycnocline, the more nutrients are available to the photic zone. From 2007-2011, pycnocline depth decreased steadily at station 67.55 in central California for both summer and winter (Figure OC10). In southern California (station 93.30), pycnocline depth is highly variable with no clear trend over this period (Figure OC11). In the northern California current (station NH25), the pycnocline has become deeper in the winter but has

no clear trend in the summer (Figure OC9). Note that at particular stations, either samples were not taken or data has yet to be processed at the time of writing of this report, thus limiting our ability to comment on the most recent trends in this indicator. **For 2013, where there are data, wintertime pycnocline depth remained similar to immediately previous years (NH 25 and CalCOFI 67.55), but markedly decreased during the summer at NH 25 (the only location with summer 2013 data).** *The shallower pycnocline depth during the summer at NH 25 supports the evidence for strong upwelling and likely enhanced productivity during summer 2013.*

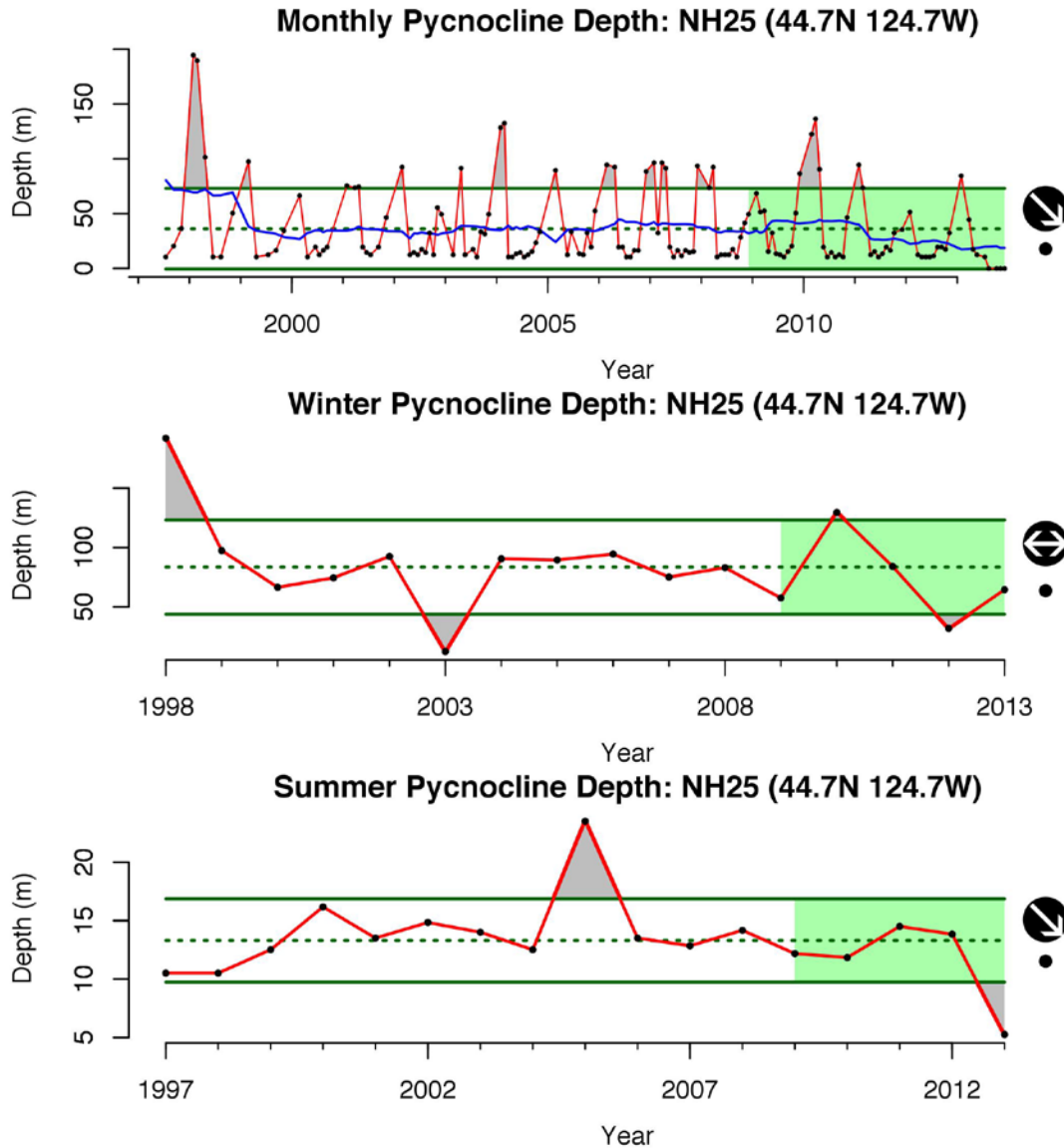


Figure OC 9. Pycnocline depth data from 1998-2013 for monthly, winter and summer means. Monthly values are included to show seasonal cycles and a continuous time series, and the blue line shows a running annual average. Newport line station NH25, illustrates patterns in the northern portion of the CCLME.

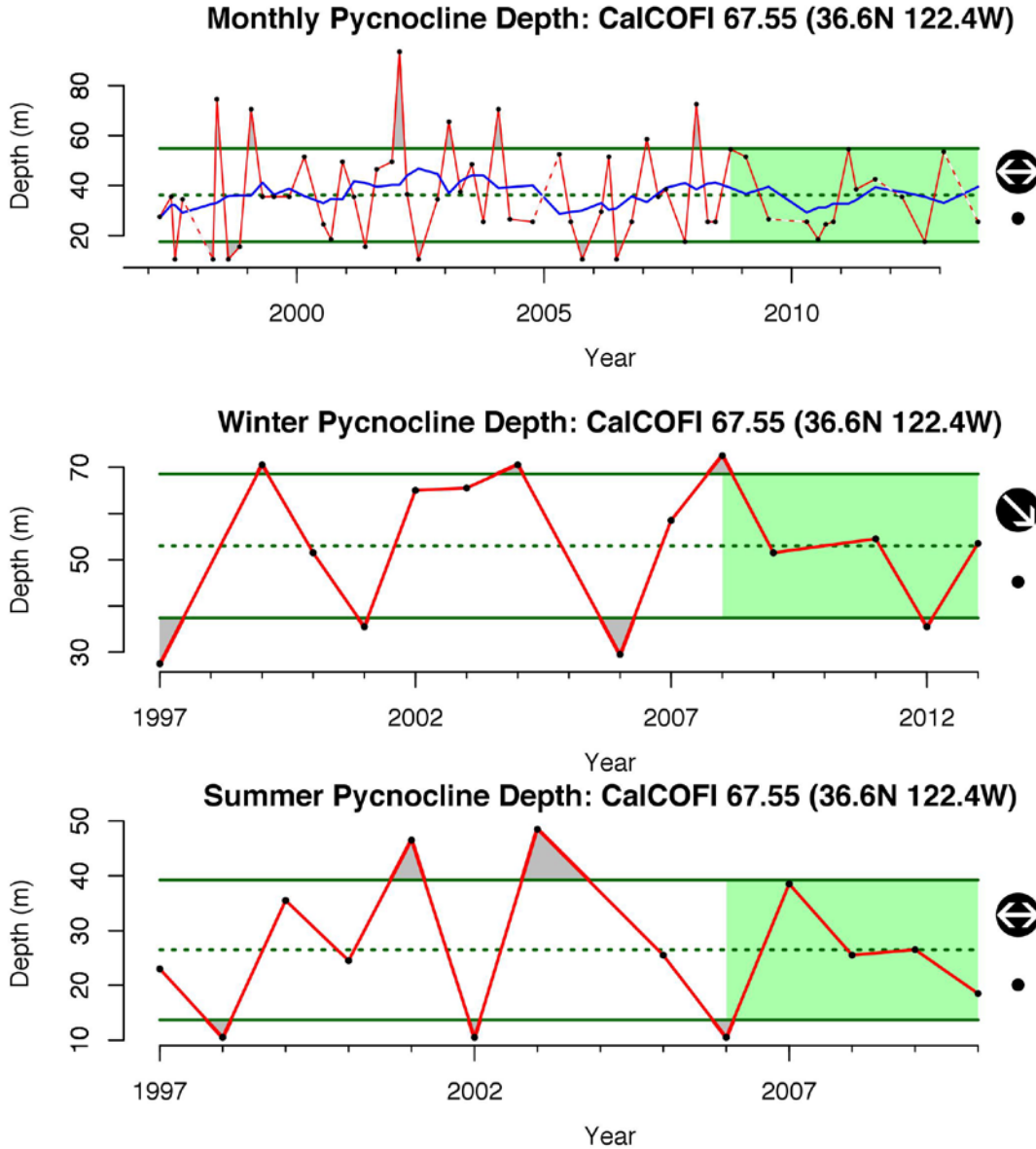


Figure OC 10. Pycnocline depth data from 1998-2013 (where available) and for monthly, winter and summer. Monthly values are included to show seasonal cycles and a continuous time series, and the blue line shows a running annual average. Station 67.55 illustrates patterns in the central portion of the CCLME.

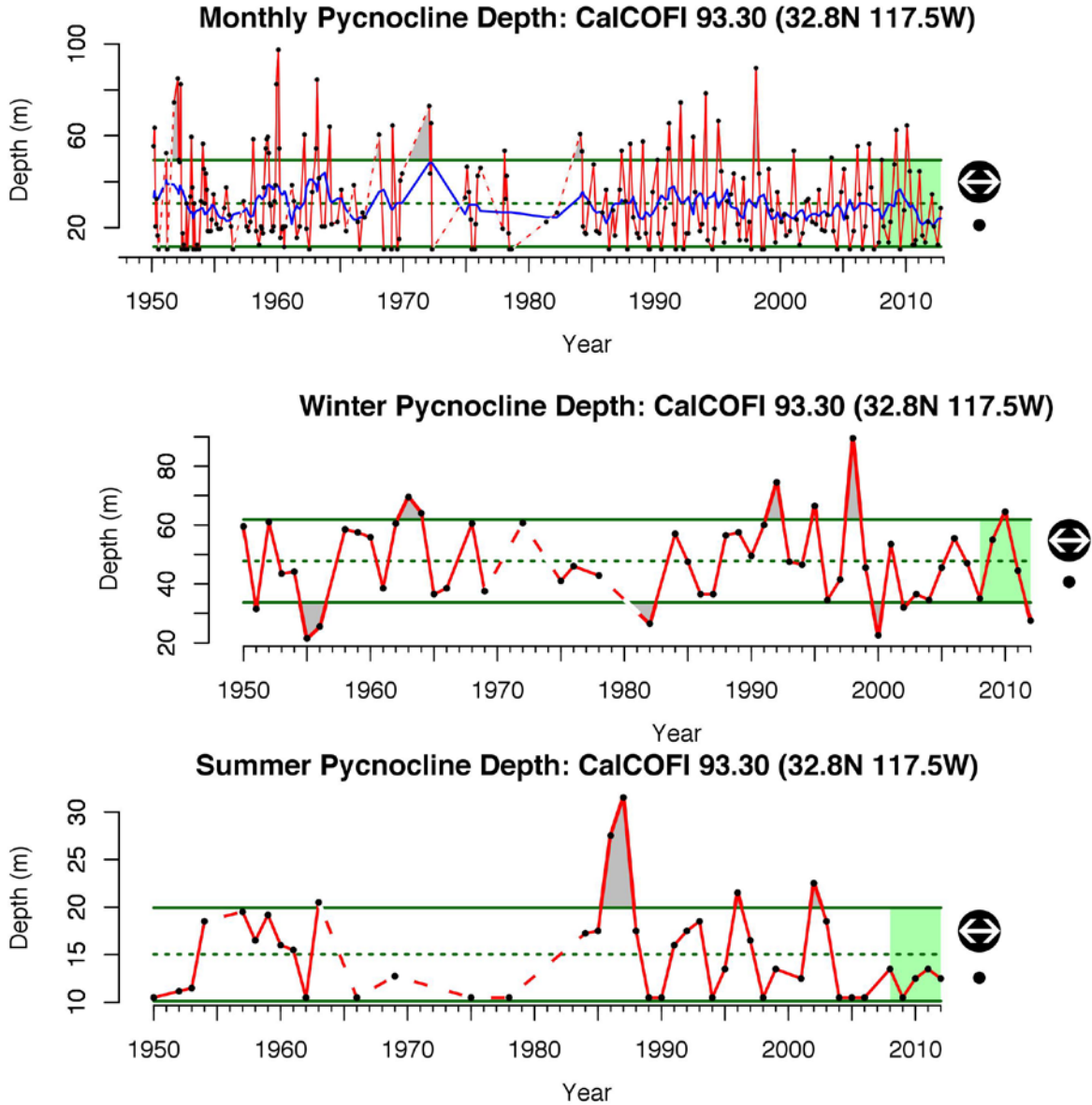


Figure OC 11. Pycnocline depth data from 1950-2012 and for monthly, winter and summer means. Monthly values are included to show seasonal cycles and a continuous time series, and the blue line shows a running annual average. Station 93.30 illustrates patterns in the southern portion of the CCLME. Dashed lines show data gaps of greater than 2 years.

PYCNOCLINE STRENGTH

The BVF (Brunt-Väisälä frequency) value indicates the strength of the density gradient in the vertical water column. The stronger the pycnocline, the less mixing of nutrients occurs across the pycnocline. From 2007-2011, pycnocline strength has increased steadily at station 67.55 in central California for both summer and winter (Fig. OC13). In southern California (station 93.30), thermocline strength has been highly variable with no clear trend over this same period (Fig. OC14).

In the northern California current (station NH25), the pycnocline has strengthened (Fig. OC12). As noted above, due to cruise limitations, more recent samples are missing from many stations, or have yet to be processed at the time of writing this report, hence limiting our ability to update these trends. **For 2013, where there are data (NH25 and Winter, CalCOFI 67.55) pycnocline strength decreased, as compared to 2012, and was particularly weak at NH25 during the summer.** Thus the increased upwelling during 2013 should have been very effective at carrying nutrients to the surface, and thus increasing productivity.

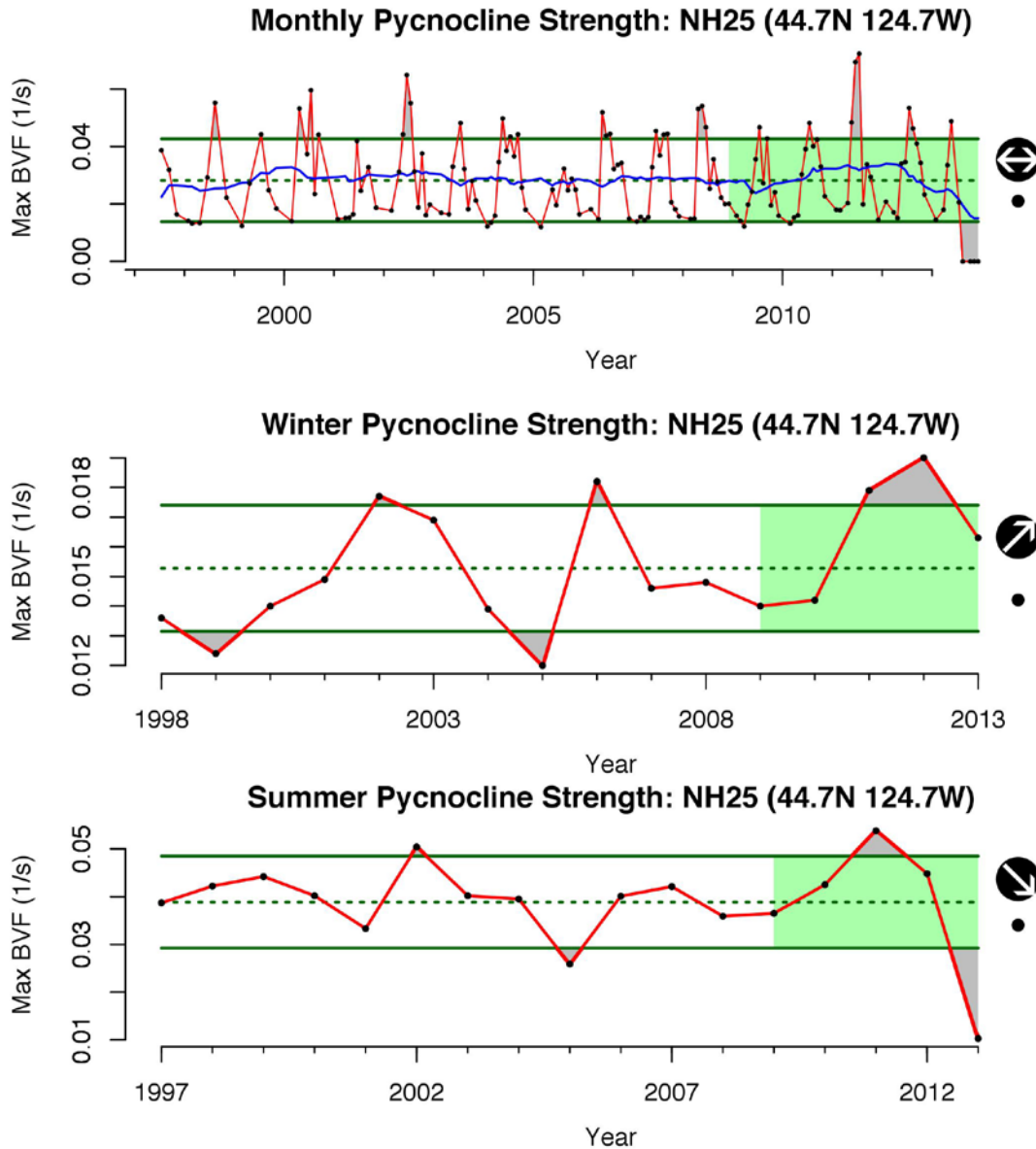


Figure OC 12. Pycnocline strength data from 1998-2013 for monthly, winter and summer means. Monthly values are included to show seasonal cycles and a continuous time series, and the blue line shows a running annual average. Newport line station NH25 illustrates patterns in the northern portion of the CCLME.

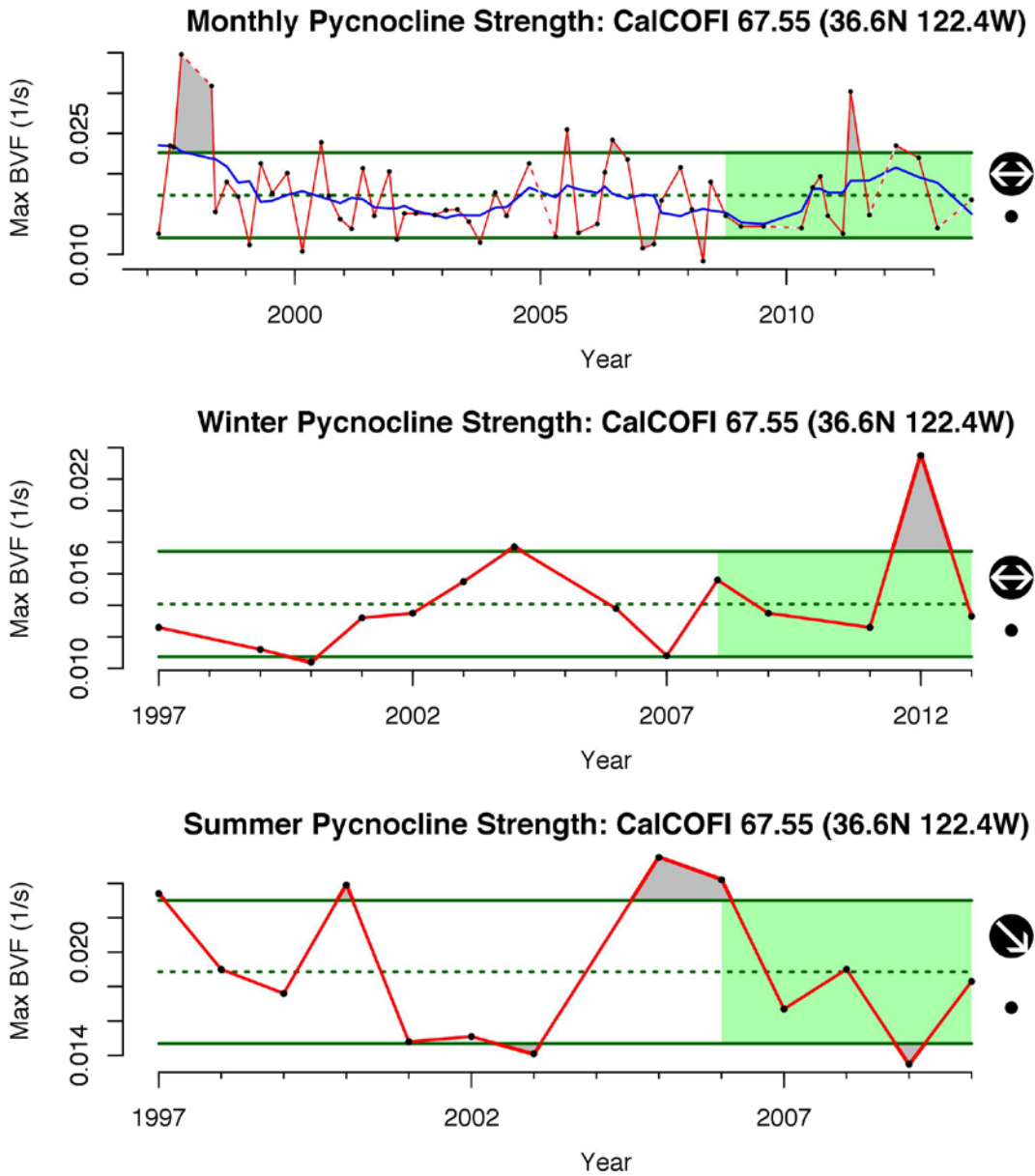


Figure OC 13. Pycnocline strength data from 1998-2013 for monthly, winter and summer means. Monthly values are included to show seasonal cycles and a continuous time series, and the blue line shows a running annual average. Station 67.55 illustrates patterns in the central portion of the CCLME.

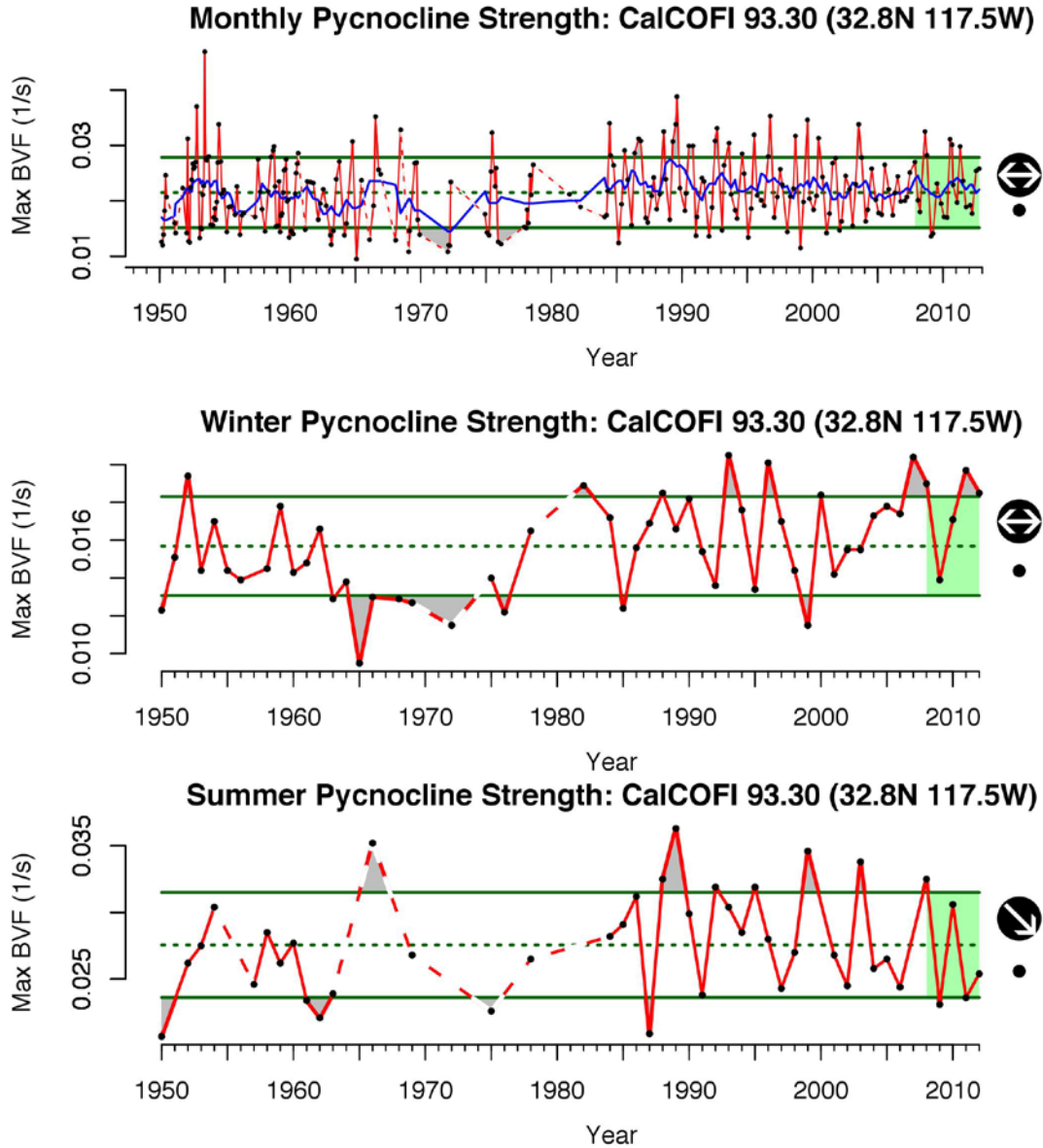


Figure OC 14. Pycnocline strength data from 1950-2012 for monthly, winter and summer means. Monthly values are included to show seasonal cycles and a continuous time series, and the blue line shows a running annual average. Station 93.30 illustrates patterns in the southern portion of the CCLME. Dashed lines identify data gaps of greater than 2 years.

MEI

See Timing and Frequency of El Niño events.

CHANGES IN CALIFORNIA CURRENT TRANSPORT AND MESOSCALE ACTIVITY

BACKGROUND

The major currents of the CCLME are the equatorward flowing California Current and coastal jet, the poleward flowing Undercurrent and Davidson Current, and the Southern California Eddy (Checkley and Barth 2009, King et al. 2011). These currents strengthen at particular times during the year due to local and remote forcing. Embedded in the slow flowing (<5 cm/s) California Current are mesoscale eddies, upwelling filaments, and jets (Checkley and Barth 2009). The geostrophically balanced California Current is present throughout the year, and is surface intensified. In winter, a broad northward flowing current, called the Davidson Current, forms when upwelling inducing winds diminish in strength. The source waters of the California Current and Undercurrent are different, with the California Current being fed by the low-salinity, high-oxygen and high-nitrate water from the North Pacific Current and the Undercurrent's source waters originating from the eastern tropical North Pacific, which are high-salinity, low-oxygen and low-nitrate. Changes in the volume transport of the California Current can result from changes to the North Pacific Current, which is affected by variations in the sea level height over the Northeast Pacific (Cummins and Freeland 2007). The North Pacific Gyre Oscillation (NPGO) index represents variations in the eastern and central regions of the North Pacific Gyre circulation. Since the NPGO is significantly correlated with nutrients and chl-a in the southern CCLME, it also provides a rough index of California Current transport (Di Lorenzo et al. 2008). Eddies and fronts provide important habitat for top predators in the California Current through prey aggregation (Wells et al. 2008, Kappes et al. 2010). We have indexed mesoscale activity using remotely-sensed measures of eddy kinetic energy (EKE) calculated from altimetry data (Strub and James 2000, Haney et al. 2001).

EVALUATION AND SELECTION OF INDICATORS

Winter and summer means of eddy kinetic energy from three locations in the CCLME are used as indicators of mesoscale activity in the CCLME (Strub and James 2000, Marchesiello et al. 2003). The three regions are the mean EKE over 6 degrees centered at latitudes 33, 39 and 45°N, with each region extending zonally from the shore to 300 km. Winter/summer means of the NPGO show low frequency variations of circulation in the CCLME. Positive (negative) values of the NPGO are linked to increased (decreased) upwelling, nitrate and chl-a, especially in the southern CCLME (Chenillat et al. 2012).

STATUS AND TRENDS

EKE

Eddy Kinetic Energy (EKE) is a measure of mesoscale activity calculated from the square of the zonal and meridional geostrophic flow. High EKE values indicate more mesoscale activity (front, eddies, jets) with much of the eastern Pacific having low EKE values (<300 cm²/s²). EKE has not shown a long-term trend at any of the three locations (33°N, 39°N, and 45°N) in winter or summer (Figures OC15 – OC17). Since 2009, EKE has been variable with no clear trend at 33°, decreased at 39°N, and decreased in the summer but not winter at 45°N. **Summer of 2013 showed generally decreased EKE at all three stations as compared to the immediately previous years.** *These observations suggest that 2013 appears to have had lower than average mesoscale activity.*

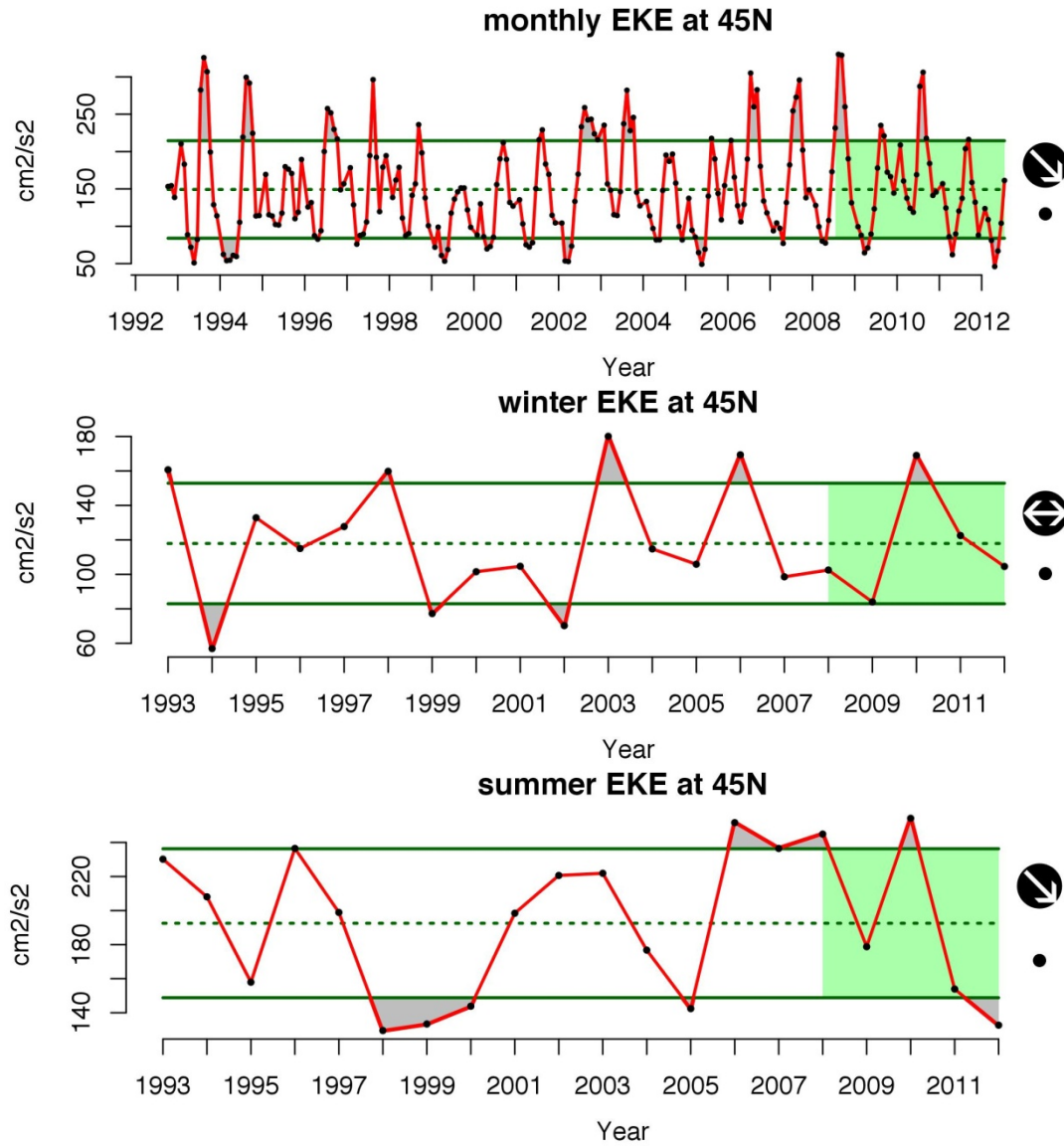


Figure OC 15. Satellite altimetry determined Eddy Kinetic Energy from 1992-2012 at 45°N for monthly, winter and summer means. Monthly values are included to show seasonal and long term variability. The region centered on 45°N illustrates patterns in the northern portion of the CCLME.

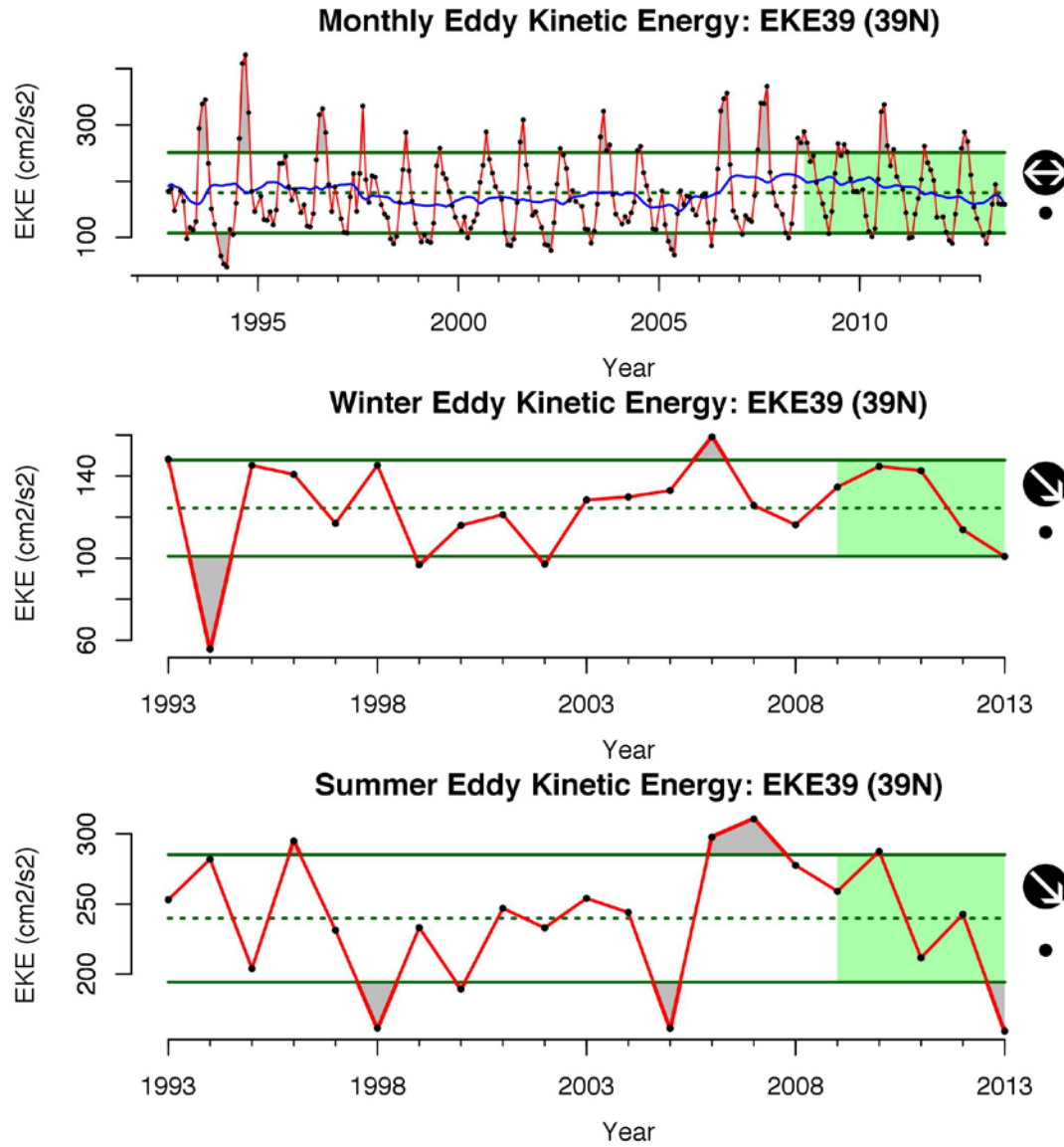


Figure OC 16. Eddy Kinetic Energy satellite data from 1992-2013 at 39°N for monthly, winter and summer means. Monthly values are included to show seasonal cycles and a continuous time series, and the blue line shows a running annual average. The region centered on 39°N illustrates patterns in the central portion of the CCLME.

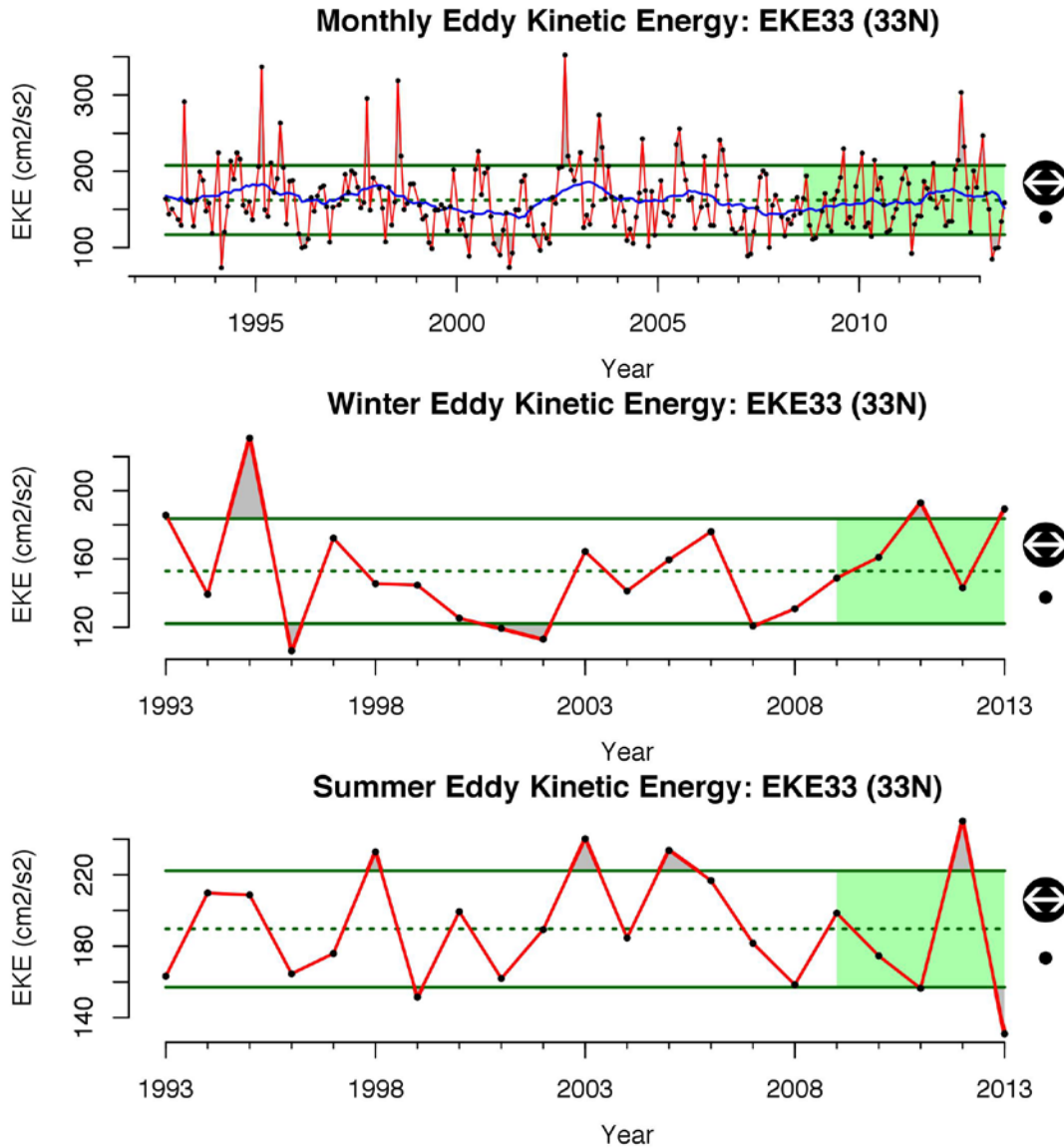


Figure OC 17. Eddy Kinetic Energy satellite data from 1992-2013 at 33°N for monthly, winter and summer means. Monthly values are included to show seasonal cycles and a continuous time series, and the blue line shows a running annual average. The region centered on 33°N illustrates patterns in the southern portion of the CCLME.

TIMING AND STRENGTH OF UPWELLING

BACKGROUND

Upwelling is critically important to productivity and ecosystem health in the CCLME (Huyer 1983). The strength and duration of upwelling in the CCLME is highly variable, and is forced by large-scale atmospheric pressure systems. More specifically, the pressure gradient between the oceanic North Pacific High and continental Low situated over the southwestern United States drives

upwelling-favorable northerly winds. The interaction (friction and Coriolis force) of the northerly winds and the water surface moves water offshore in the surface layer, and this water is replaced by water upwelled from depths of greater than 50 - 100 m. The upwelled water is cooler, saltier and higher in nutrient concentrations than the surface water it replaces. The onset and duration of the upwelling season varies latitudinally, starting earlier and lasting longer in the southern CCLME (Bograd et al. 2009).

Because of the close mechanistic and correlative link between coastal upwelling and ecosystem productivity on seasonal, annual, and interannual scales (Chavez et al. 2003), scientists have a strong need for operational products that quantify and forecast upwelling within marine ecosystems. However, it is extremely difficult to quantify upwelling directly, and measurements of coastal upwelling are scarce.

EVALUATION AND SELECTION OF INDICATORS

Timing and strength of upwelling were indexed using two sources: meridional winds from NDBC buoys and the atmospheric model-derived Upwelling Index (UI) (Bakun 1975). Given the importance of upwelling favorable winds to the ecosystem, both are included to provide the raw data and derived product often used for measuring upwelling in the CCLME. The NOI can also serve as a broad-scale proxy for winds as positive values mean that winds from the north are typically more intense. The meridional winds from buoys are winter/summer means from three locations along the CCLME. Three derived products (STI, TUMI and LUSI) using the UI identify the timing and strength and duration of upwelling in the CCLME (Bograd et al. 2009). The spring transition index (STI) identifies the time when upwelling starts and varies with latitude in the CCLME. The units for STI are days and a year with a small STI value will have an earlier start to the onset of upwelling winds. The length of upwelling season index (LUSI) will provide information on the duration of upwelling during a particular year. The units for LUSI are days and a larger LUSI value indicates that the upwelling season for the given year is long. The total upwelling magnitude (TUMI) measures the ultimate amount of upwelling. There may be years of short but intense periods of upwelling, or longer but weaker upwelling seasons. Time series of STI and LUSI will be at three locations in the CCLME.

STATUS AND TRENDS

UI

Upwelling index (UI). The 2005 upwelling season was unusual in terms of its initiation, duration, and intensity. In 2005 upwelling was delayed or interrupted and SSTs were approximately 2-6°C warmer than normal (Barth et al. 2007). The situation in the southern ecoregion was different in both 2005 and 2006, as average upwelling and SST prevailed (Peterson et al. 2006). Other than a brief period of weaker than normal upwelling in the summer of 2008, west coast upwelling has been increasing since the late summer of 2006 (Figures OC18 – OC20). Wind patterns in early 2009 reflect anomalously strong high pressure over the Northeast Pacific and very high upwelling while early to mid 2010 appears to be a below average upwelling year at lat 35–45°N. **For 2013, the UI increased or stayed relatively high for all stations, as compared to the immediately previous years. This supports the evidence that 2013 was a year of strong upwelling.**

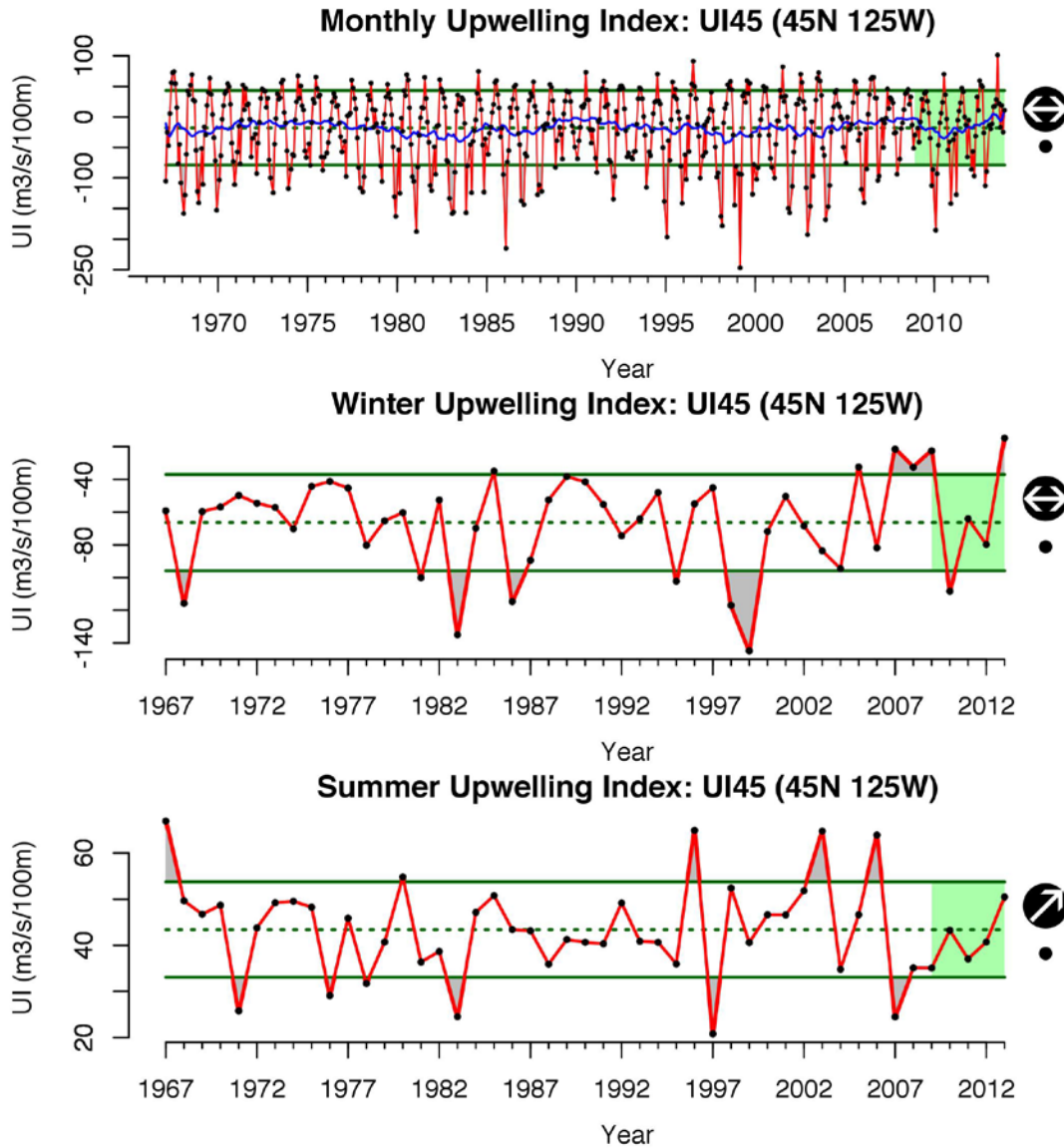


Figure OC 18. The Upwelling Index calculated from 1967-2013 at 45°N for monthly, winter and summer means. Monthly values are included to show seasonal cycles and a continuous time series, and the blue line shows a running annual average. The UI at 45°N illustrates patterns in the northern portion of the CCLME.

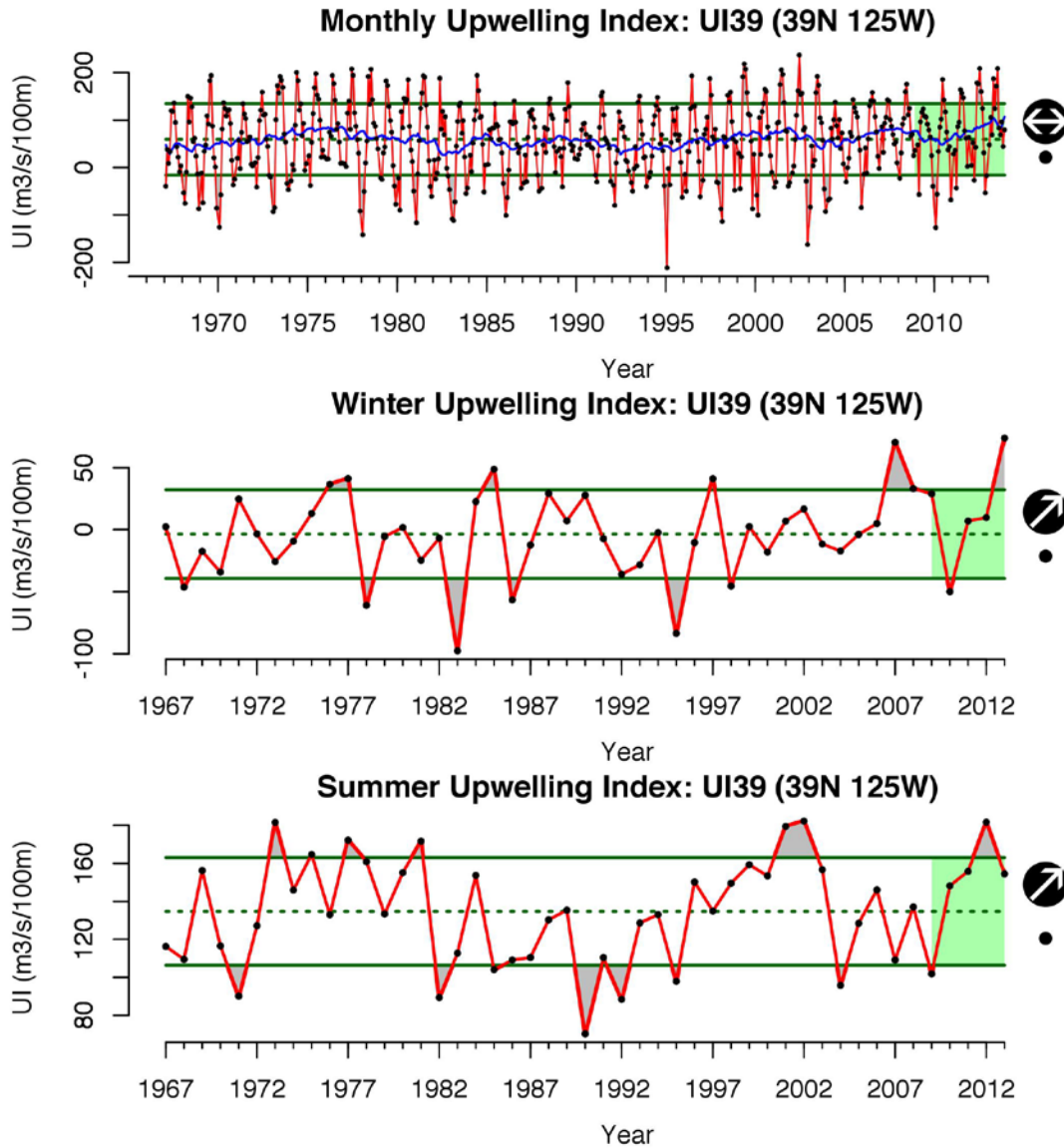


Figure OC 19. The Upwelling Index calculated from 1967-2013 at 39°N for monthly, winter and summer means. Monthly values are included to show seasonal cycles and a continuous time series, and the blue line shows a running annual average. The UI at 39°N illustrates patterns in the central portion of the CCLME.

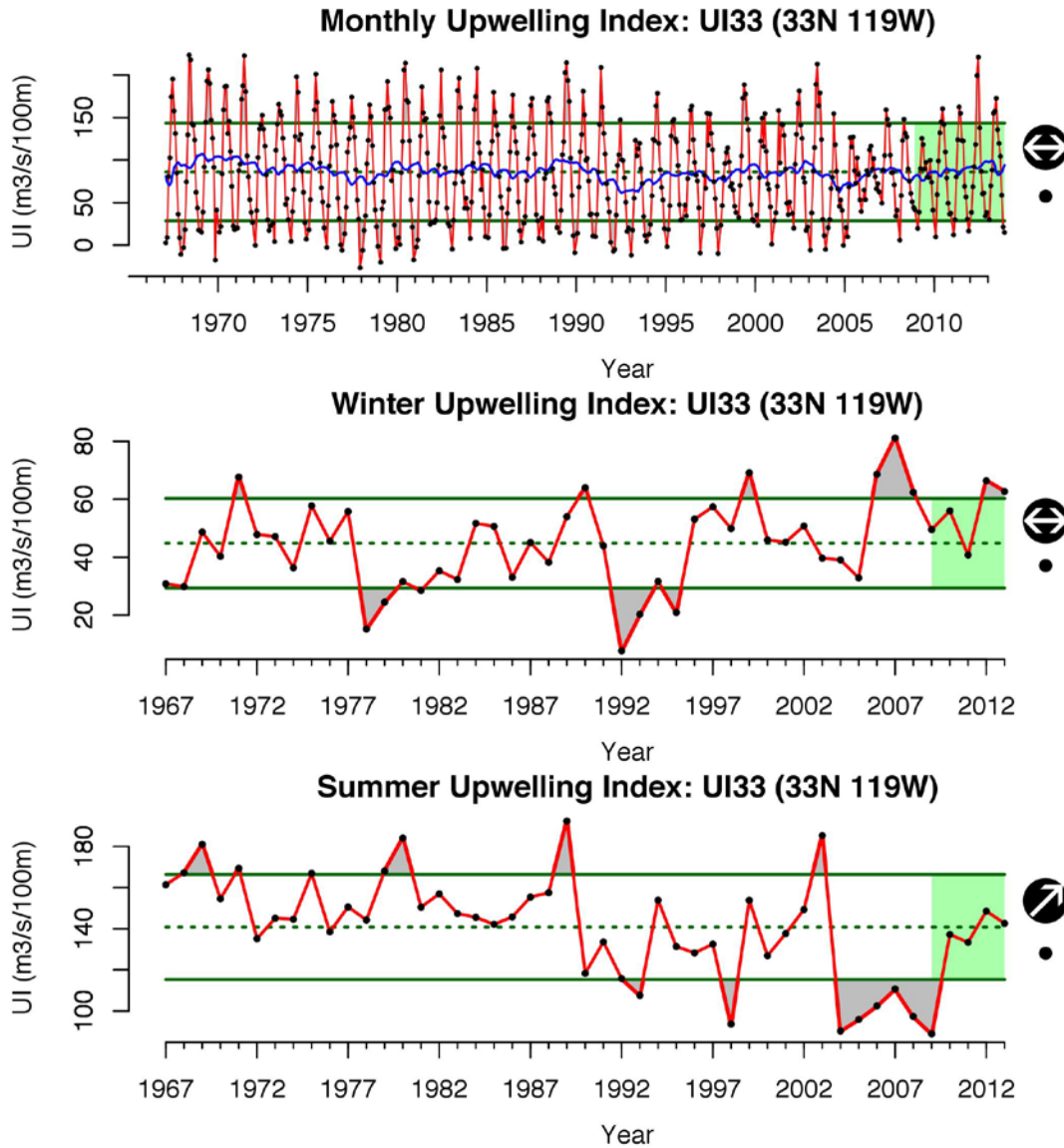


Figure OC 20. The Upwelling Index calculated from 1967-2013 at 33°N for monthly, winter and summer means. Monthly values are included to show seasonal cycles and a continuous time series, and the blue line shows a running annual average. The UI at 33°N illustrates patterns in the southern portion of the CCLME.

STI

The spring transition index (STI) indicates roughly the start of the upwelling season. It is defined by the date the annual cumulative upwelling index (CUI) reaches its minimum value (Bograd et al. 2009). The STI fluctuates around 10 days past March 1st with a few extremely early or late years. In the early 90's and in 2005 anomalously late upwelling occurred with a severe effect on many biological time series. The past 5 years have had variable STI values ranging from ± 1 standard deviation (Figure OC21). Given the UI often remains positive at 33°, confounding the calculation of

the STI, we have excluded this time series. **For 2013, the STI decreased for both locations as compared to 2012.** The earlier transition to upwelling in 2013 supports the evidence that total upwelling during 2013 was higher than previous years.

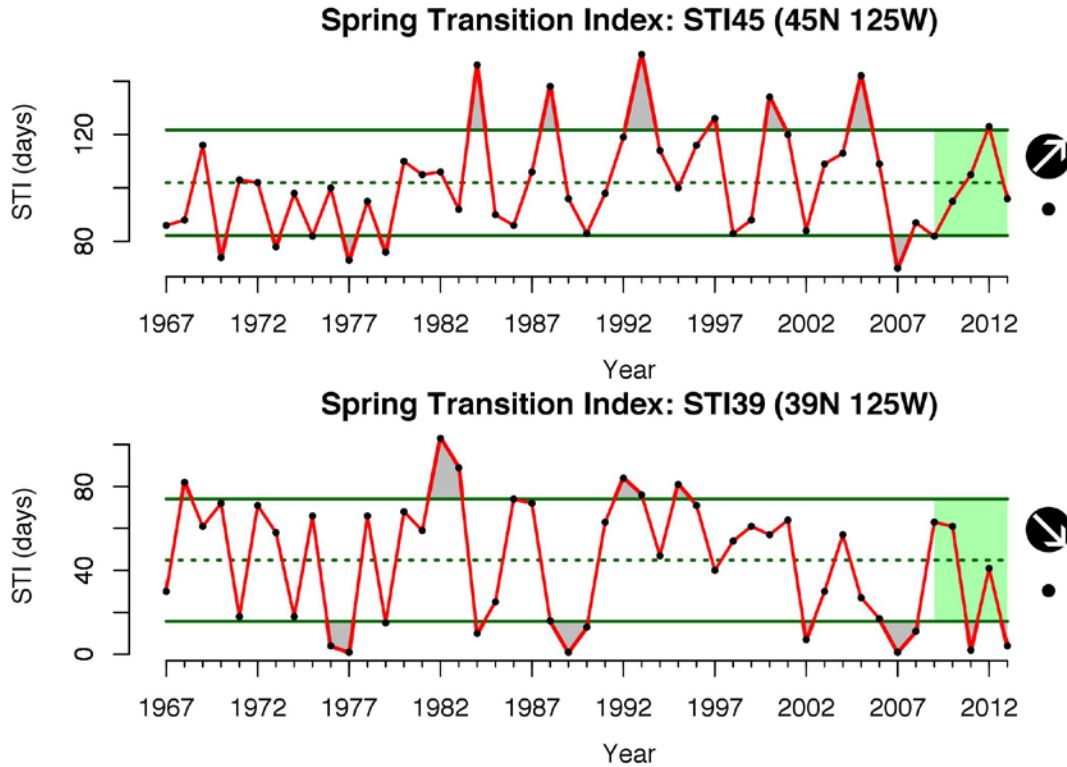


Figure OC 21. The Spring Transition Index (STI) calculated yearly from 1967-2013 at 45°N and 39°N. The STI at 33°N is not included because there is not an extended downwelling phase during a year at this latitude.

LUSI

The length of the upwelling season (LUSI) is determined by the date of the STI until the date of the CUI maximum. This length of upwelling season indicates how long the upwelling favorable conditions persisted over the year. Over the past 5 years, LUSI has been highly variable at 39° while showing a declining trend at 45°N (Figure OC22). **For 2013 vs 2012, the length of the upwelling season was longer at the southern station, and similar at the northern station.** This supports the evidence that 2013 was in general a stronger year of upwelling, although the intensification seems to have been greater in the southern portions of the current.

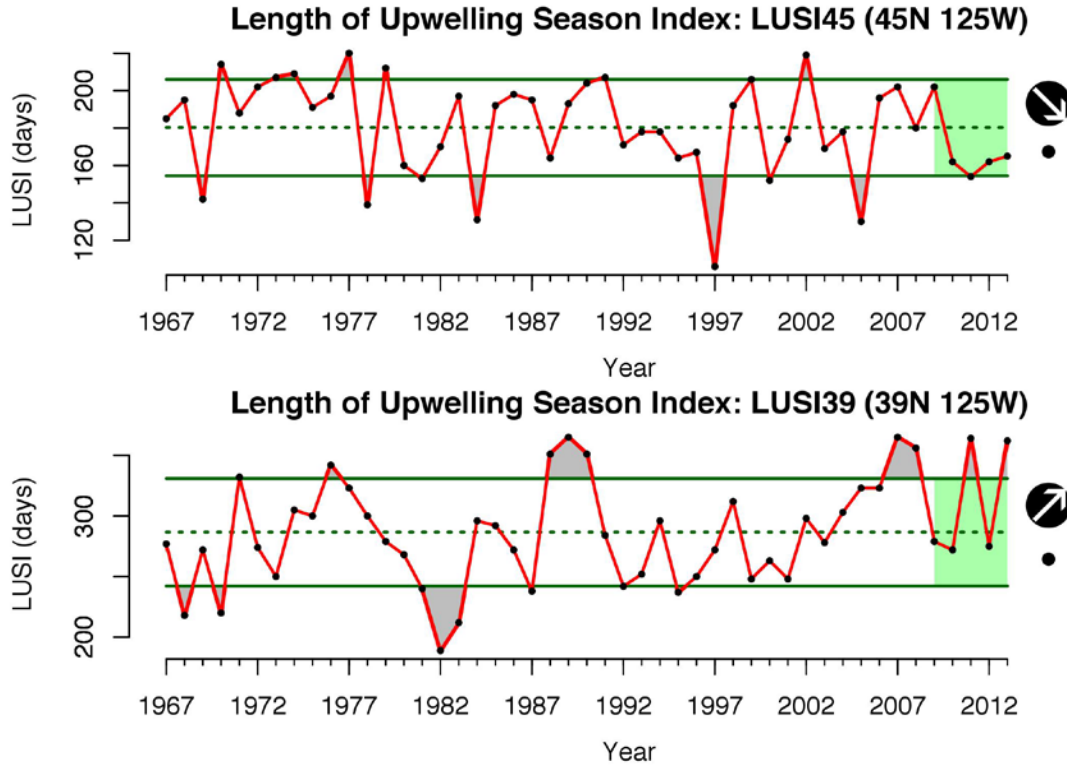


Figure OC 22. The Length of the Upwelling Season Index (LUSI) calculated yearly from 1967-2013 at 45°N and 39°N. The LUSI at 33°N is not included because there is not an extended downwelling phase during a year at this latitude.

TUMI

The total upwelled magnitude index (TUMI) is the sum of the UI over the duration of the upwelling season (e.g. LUSI). This index represents the total amount of upwelled water as an indicator of total upwelled nutrient availability to the photic zone for the year. At the southernmost station, TUMI has been variable with minima in 1992-1993 and 2004-2005 although no clear trend since 2007 (Figure OC23). TUMI at 39° N shows a decadal pattern with high values in the 1970s, low values in the 1980s-1998 and high values since 1999 with the exception of 2003-2004. At 45° N, TUMI had a minima in 1997 and a maxima in 2006. Since 2006, values have been below the mean but not extremely so. For the past 5 years, values have increased at all three locations. **For 2013, TUMI was high at all three locations, with central CA showing the highest value on record.** This further supports the evidence that 2013 was a year of high total upwelling as compared to previous years, with the southern portion being more intensified than the north.

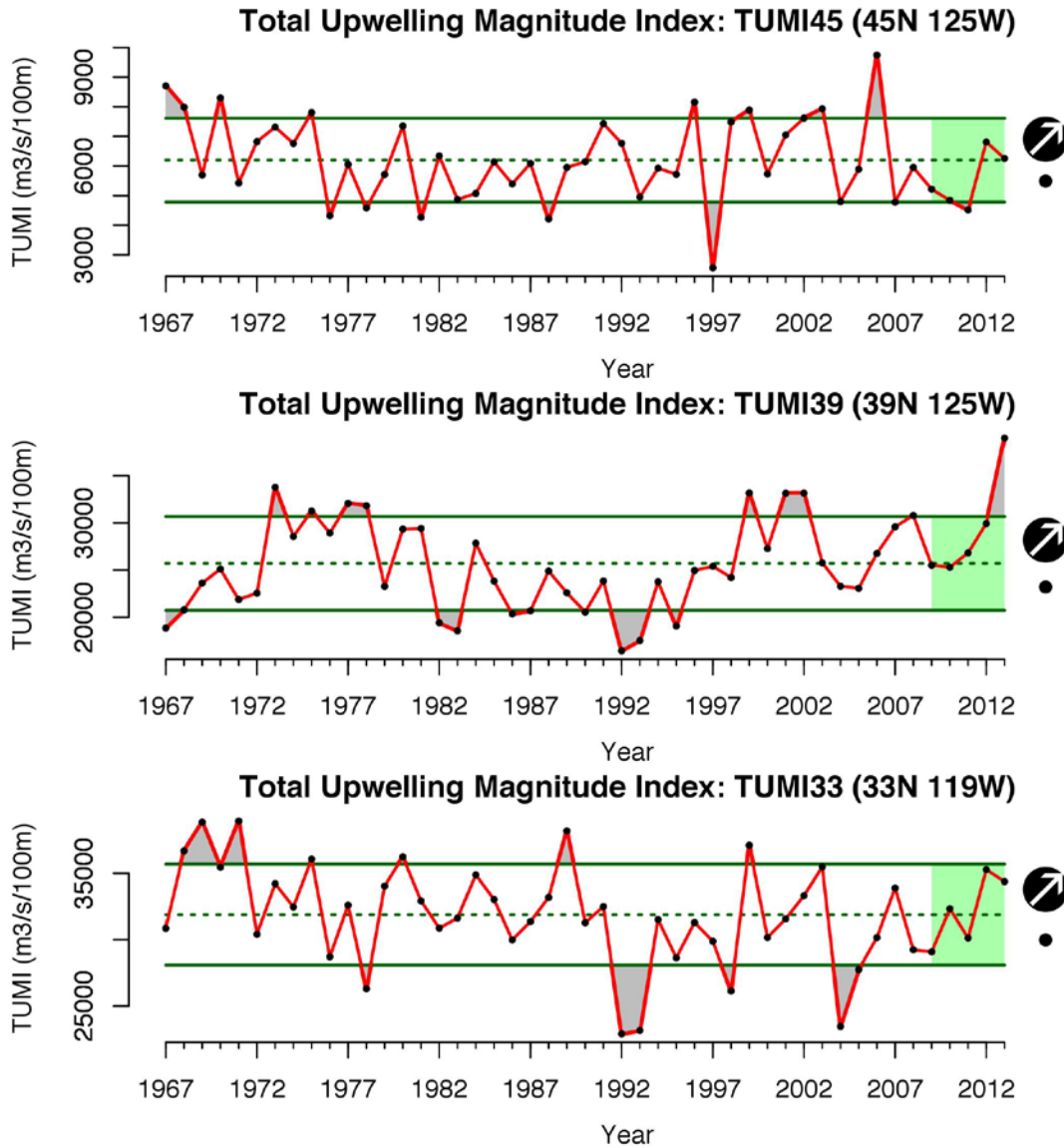


Figure OC 23. The total upwelled magnitude index (TUMI) calculated yearly from 1967-2013 at 45°N, 39°N and 33°N.

WINDS

Northerly winds in the CCLME result in offshore transport and upwelling of cold, nutrient rich water into the photic zone. In the winter, meridional (north/south) winds were consistently northward in 1998 and 2010, indicative of downwelling favorable conditions (positive MEI and NOI; Figures OC24 – OC26). In winter 2006, winds were also indicative of downwelling although less extreme than 1998 and 2010. In summer 2006 and winter 2007, there were highly favorable upwelling winds at the northern buoys (A and B). In summer 2010, upwelling favorable winds dominated all three buoys, although they declined at 39° N in 2011. **For 2013, meridional winds were more southward (e.g. more strongly towards negative values) except for the**

summertime values at the southernmost station, which were anomalously strongly northwards. *These observations support the evidence that 2013 was a year of atmospherically forced strong upwelling, which began early for most of the CCS, albeit with an altered anomalous state to the south.*

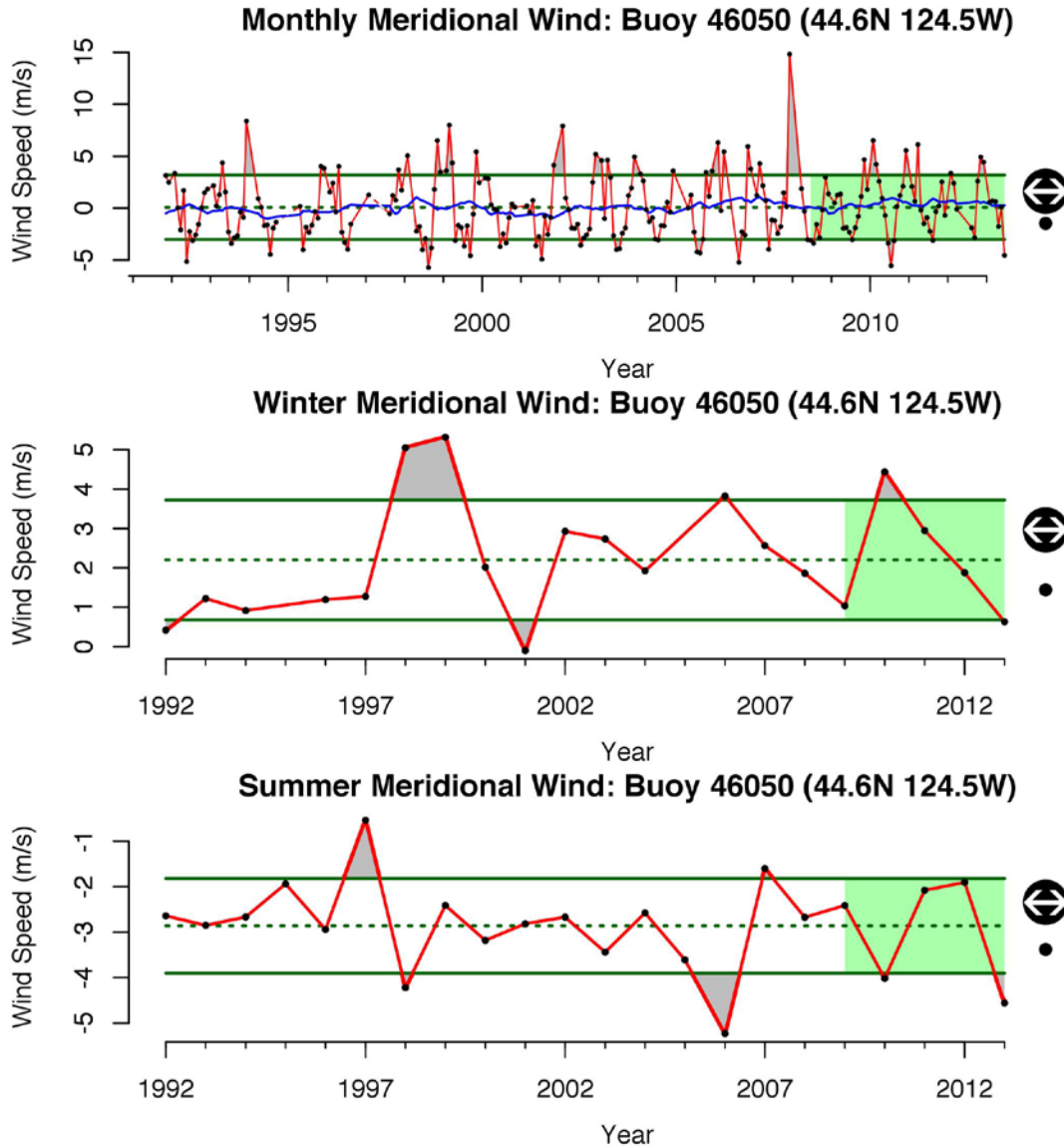


Figure OC 24. Alongshore, meridional winds buoy data from early 1990 -2013 for monthly, winter and summer means. Monthly values are included to show seasonal cycles and a continuous time series, and the blue line shows a running annual average. Buoy 46050 was chosen to illustrate patterns in the northern portion of the CCLME.

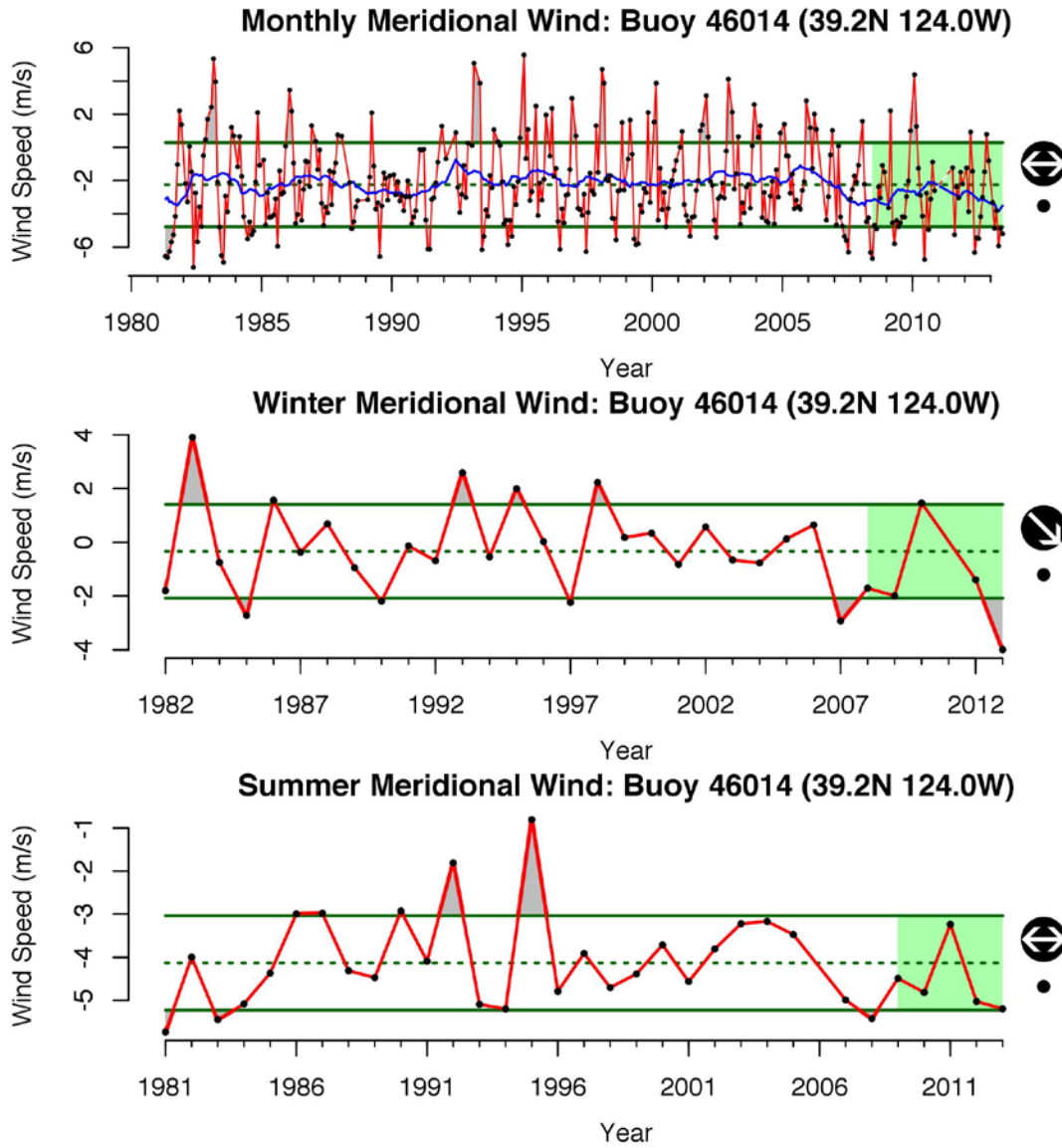


Figure OC 25. Alongshore, meridional winds buoy data from early 1990 -2013 for: monthly, winter and summer means. Monthly values are included to show seasonal cycles and a continuous time series, and the blue line shows a running annual average. Buoy 46014 was chosen to illustrate patterns in the central portion of the CCLME.

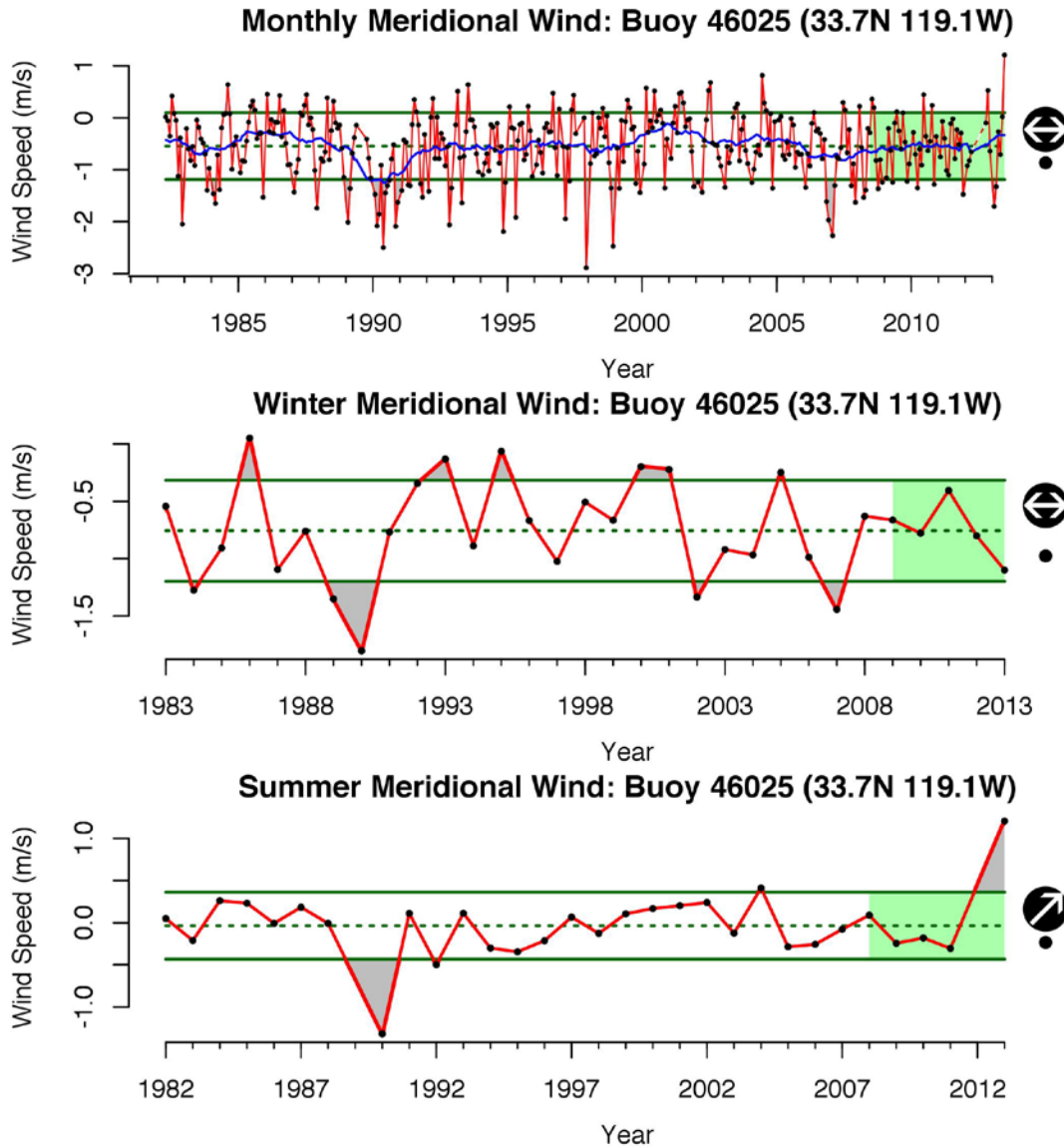


Figure OC 26. Alongshore, meridional winds buoy data from early 1990 -2013 for: monthly, winter and summer means. Monthly values are included to show seasonal cycles and a continuous time series, and the blue line shows a running annual average. Buoy 46025 was chosen to illustrate patterns in the southern portion of the CCLME.

TIMING AND FREQUENCY OF EL NIÑO EVENTS

BACKGROUND

El Niño Southern Oscillation (ENSO) events result from variations in sea level pressure, winds and sea surface temperatures between the eastern and western tropical Pacific. The resulting changes in the tropics have wide reaching consequences on the physical attributes in the CCLME. ENSO events can affect the CCLME through atmospheric teleconnections between the western

equatorial Pacific and the North Pacific and by the propagation of Kelvin waves from the equatorial Pacific. El Niño events result in ecosystem-wide effects from changes in species composition to lack of prey availability and breeding failure in top predators, while La Niña events can increase productivity in the system (Chavez et al. 2002).

EVALUATION AND SELECTION OF INDICATORS

Winter/summer means of the Northern Oscillation Index (NOI) and the Multivariate ENSO Index (MEI) are used as indicators for the timing and strength of El Niño and La Niña events. The NOI measures the teleconnection between the western equatorial Pacific and the north Pacific and is the difference between sea level pressure at the climatological location of the North Pacific High (NPH) and sea level pressure at Darwin Australia. Large positive (negative) values correspond to a strong (weak) NPH that will result in more (less) coastal upwelling. During an El Niño the influence of the NPH is diminished and the NOI has large negative values. The MEI is derived from several physical indicators and it does not have units. The MEI is one of many potential ENSO indicators (Wolter and Timlin 2011). Large positive values represent El Niño conditions while large negative values represent La Niña conditions. Local SST anomalies from satellite or buoy data also can serve as important local indicators of El Niño effects on the CCLME (Messié and Chavez 2011).

STATUS AND TRENDS

MEI

The Multivariate ENSO Index (MEI) describes ocean-atmosphere coupling in the equatorial Pacific. Positive values of the MEI represent El Niño conditions while negative values represent La Niña conditions. El Niño conditions in the CCLME are associated with warmer surface water temperatures and weaker upwelling winds. The MEI also had an increasing trend, with more positive values since 1977 (Figure OC27). Most recently, the MEI had a relatively strong negative value in the winter of 2008 indicating La Niña conditions that typically favor ocean/atmospheric teleconnections and high productivity coupled with subarctic conditions in the CCS. The MEI switched to positive indicating El Niño conditions in the beginning of 2010, which switched to a negative value in the summer of 2010. La Niña conditions continued through mid-2011 and have begun to return to neutral in late 2011. **The summer of 2012 saw higher values of the MEI, with average to low values of the MEI in the following summer and winters of 2013.** *Based on these recent MEI values, 2013 was not an El Niño year, which is supported by the relatively lower SSTs also observed during 2013.*

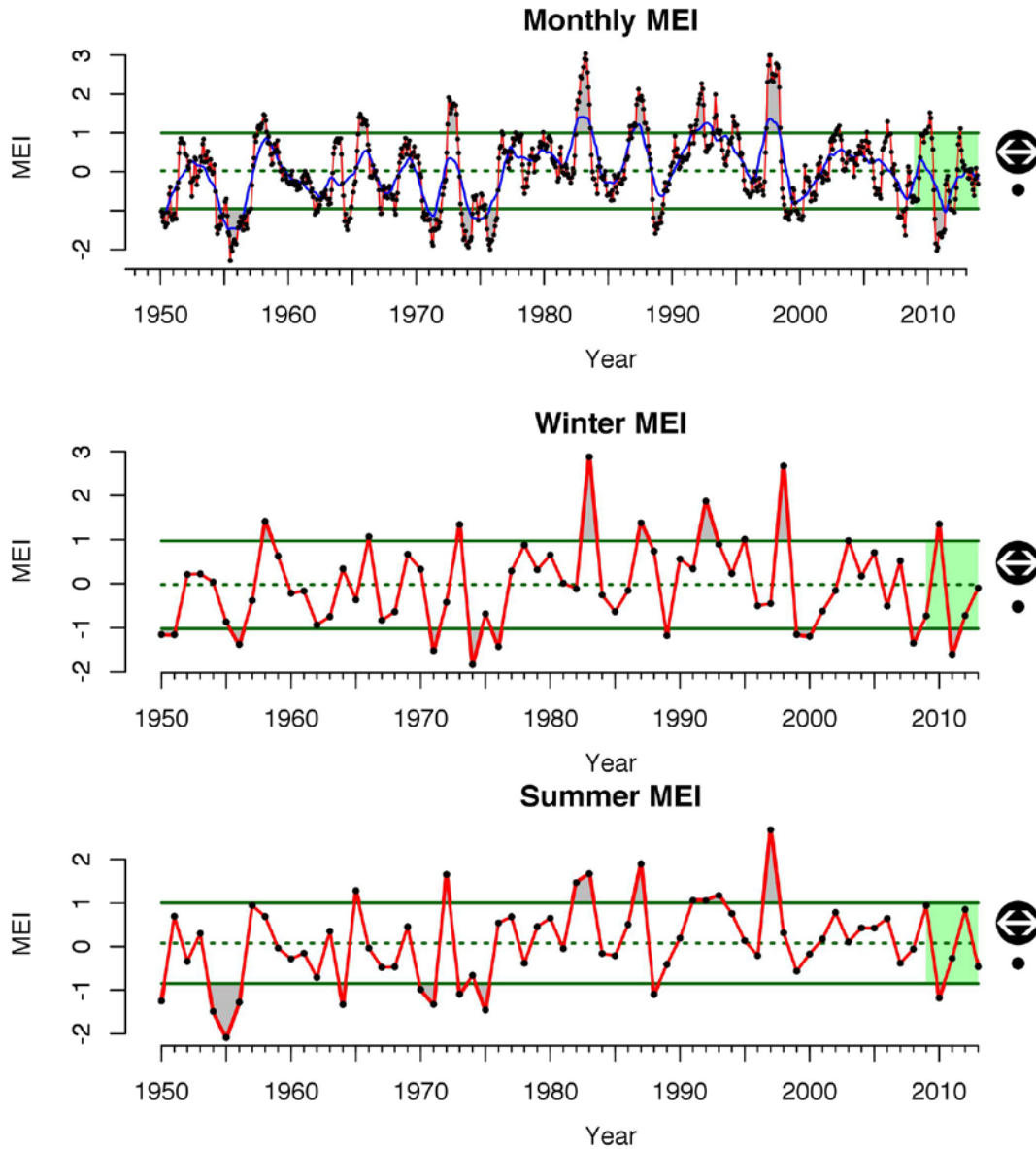


Figure OC 27. Multivariate ENSO Index values (MEI) from 1950-2013 for monthly, winter and summer means. For the monthly MEI the blue line shows a running annual average.

NOI

See sea surface temperature change above.

CHANGES IN SOURCE WATERS

BACKGROUND

Subarctic and tropical waters are important contributors of source waters to the CCLME at the upstream end and through local upwelling cells. Variations in the volume of subarctic waters occur both at the origination through ventilation (Bograd et al. 2008), transport eastward (Di Lorenzo et al. 2008) in the North Pacific Current (NPC) and as a function of where the NPC approaches the continental shelf and bifurcates into the southward-flowing California Current and the northward-flowing Alaska Current (Bi et al. 2011, Sydeman et al. 2011). Broad scale changes in nutrients and hypoxia in the California current are a function of source water changes and we have observed increased nutrients and decreased oxygen in the Southern California Bight over the past 25 years (Bograd et al. 2008). Earth system models have predicted further decreases in nutrients and oxygen over the next century (2001-2100) in part due to changes in offshore stratification and ventilation (Rykaczewski and Dunne 2011). Broad scale forcing (e.g. indexed by the Pacific Decadal Oscillation, PDO and North Pacific Gyre Oscillation, NPGO) can influence both the strength of transport and the location of bifurcation in the CCLME with downstream ecosystem consequences (King et al. 2011). Increases in subarctic source waters can result in changes in the food-web as cooler arctic waters carry larger, lipid-rich copepods and other plankton, compared to the smaller, often lipid-poor warm water copepods found offshore and to the south. Differences in copepod species composition can serve as ecological corroboration of changes in source water (Peterson and Keister 2003). The result is different trophic structure near the bifurcation (Bi et al. 2011). Dissolved Oxygen (discussed below) can also be used as an indicator of changes in source water (Bograd et al. 2008, Pierce et al. 2012)

EVALUATION AND SELECTION OF INDICATORS

There are a number of indicators that can assess the status of source waters flowing into the CC including temperature: salinity: oxygen relationships at depth (e.g. spiciness), bifurcation latitude of the NPC, nutrient content of source waters, dissolved oxygen (DO) of source waters, phases of the PDO and NPGO, and volume transport. We have narrowed the list to nutrient content, DO of source waters, copepod biomass anomaly and community structure data, and broad scale indices of the PDO and NPGO. As with previous indicators, the suite offers longevity with time, interpretability, but also measurements relevant to multiple spatial scales.

STATUS AND TRENDS

NPGO

The North Pacific Gyre Oscillation (NPGO) is a low frequency signal in sea surface heights over the Northeast Pacific. Positive (negative) values of the NPGO are linked with increased (decreased) surface salinities, nutrients, and chl-a values in the CCLME (Di Lorenzo et al. 2008). Many NPGO events since 1975 seem to have been more extreme or had a longer duration than those earlier in the time series (Figure OC28). Winter and summer trends were very similar with a broad low from 1991 to 1997 and a peak from 1998 to 2004. Since 2006, values have been increasing with the past 5 years falling around or above 1 standard deviation from the mean. **For 2013, the NPGO remained high and roughly similar to the previous several years.** *This suggests 2013 should have*

had high surface salinity, high nutrients, and resulting high chl-a values, further supporting the trends in upwelling strength that 2013 should have been a highly productive year.

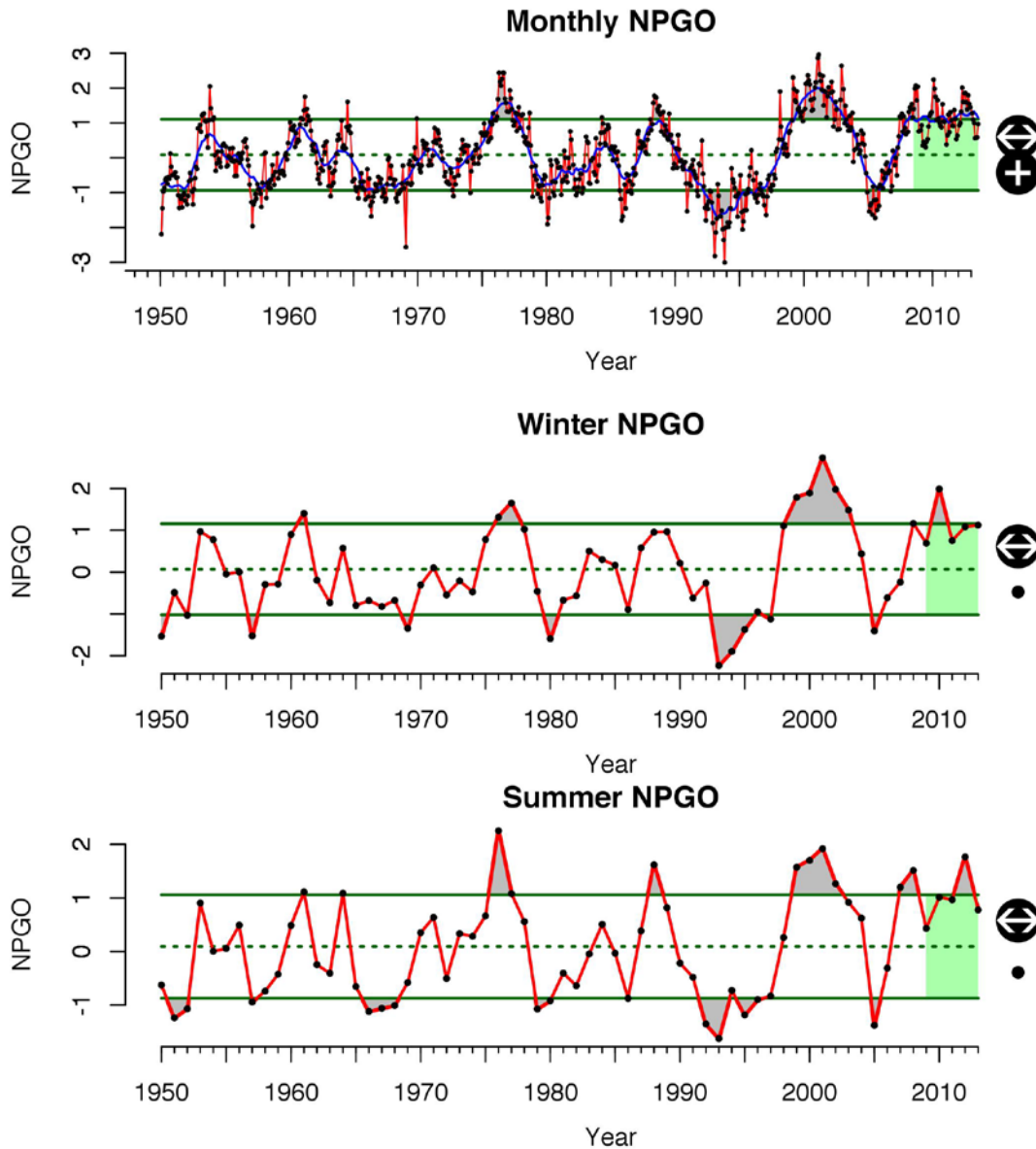


Figure OC 28. North Pacific Gyre Oscillation values (NPGO) from 1950-2013 for monthly, winter and summer means. For the monthly NPGO the blue line shows a running annual average.

NUTRIENT CONTENT

Nutrient content (represented by nitrate plus nitrite, NO_2 and NO_3) is a function of upwelling intensity and stratification, but also depends on the source waters that are upwelled. Deep casts at stations 93.30 in CALCOFI and NH25 (150 m) reflect the status of the source. CALCOFI

nutrients in central (station 67.55) and southern (station 93.30) California at 150 m depth show no long-term trend from the data available., but have generally increased over the past 5 years Central California nutrients peaked in 2009 and have declined since, while southern California nitrate and nitrite values had a large drop in 2008 and have increased through 2012 (Figures OC29-OC31). **For 2013, when and where we have data, nutrients remained high.** High nutrients during summer of 2013 support the contention that 2013 should have been a highly productive year.

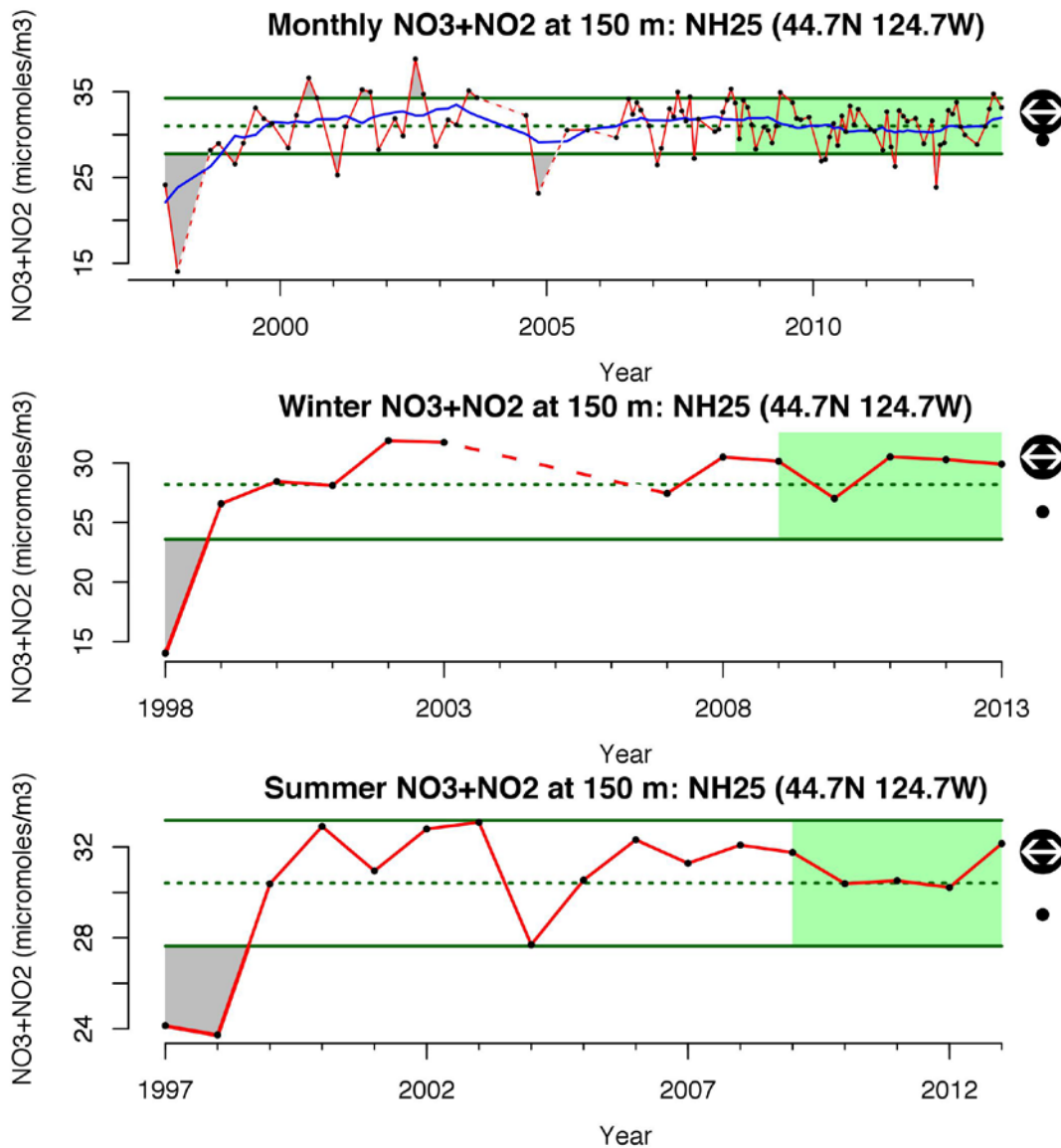


Figure OC 29. Nutrient data (nitrate + nitrite) at 150 m from 1997-2013 at station NH25 from the Newport line in the northern CCLME for monthly, winter and summer means. Monthly values are included to show seasonal cycles and a continuous time series, and the blue line shows a running annual average. Station NH25 illustrates patterns in the northern portion of the CCLME. Dashed lines show data gaps of greater than 2 years.

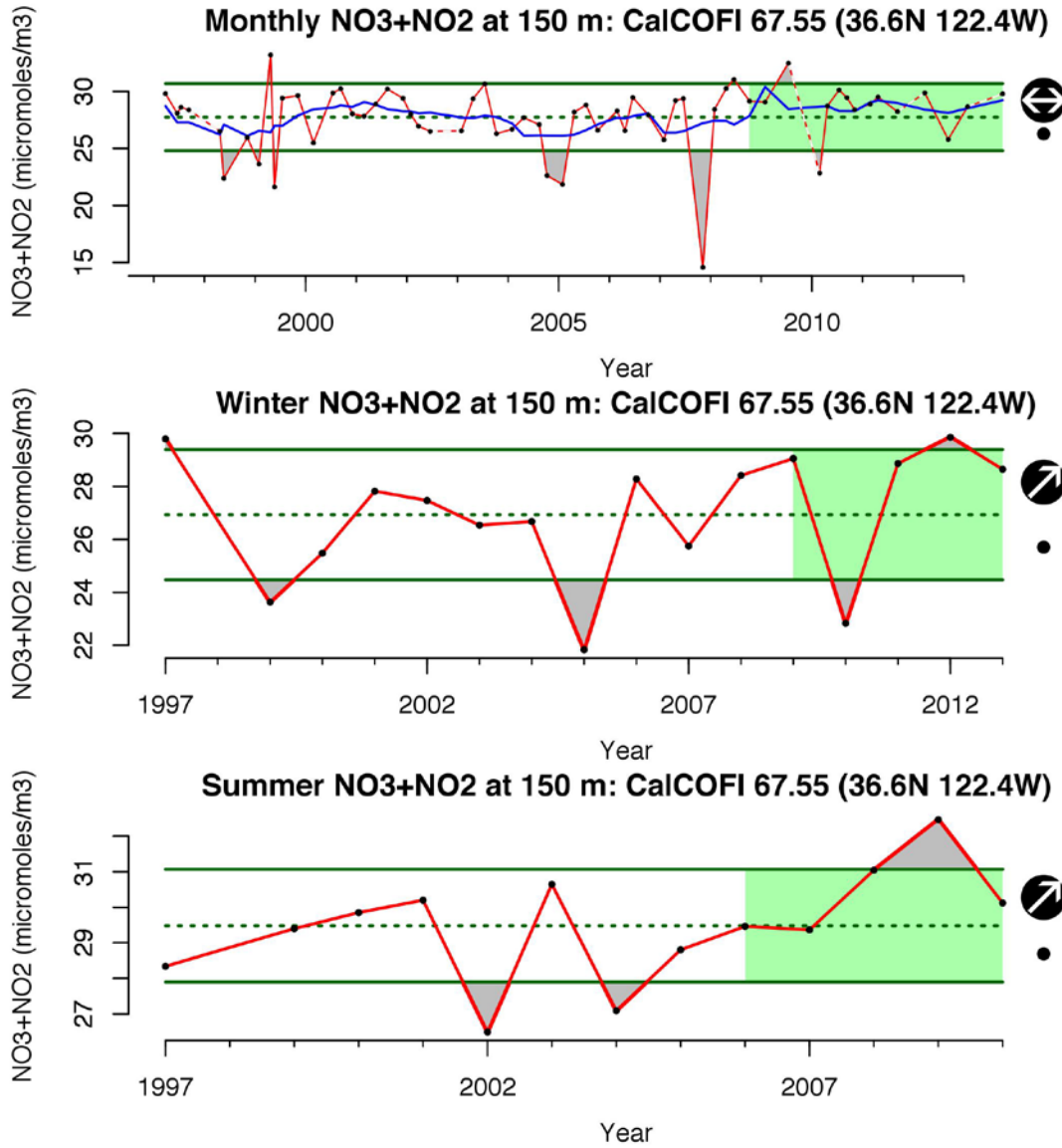


Figure OC 30. Nutrient data (nitrate + nitrite) at 150 m from 1997-2013 at CalCOFI station 67.55 representing central California for monthly, winter and summer means. Monthly values are included to show seasonal cycles and a continuous time series, and the blue line shows a running annual average. Station 67.55 illustrates patterns in the central portion of the CCLME. For the last 3 years sampling has not done at station 67.55 in the summer (Jun-Aug).

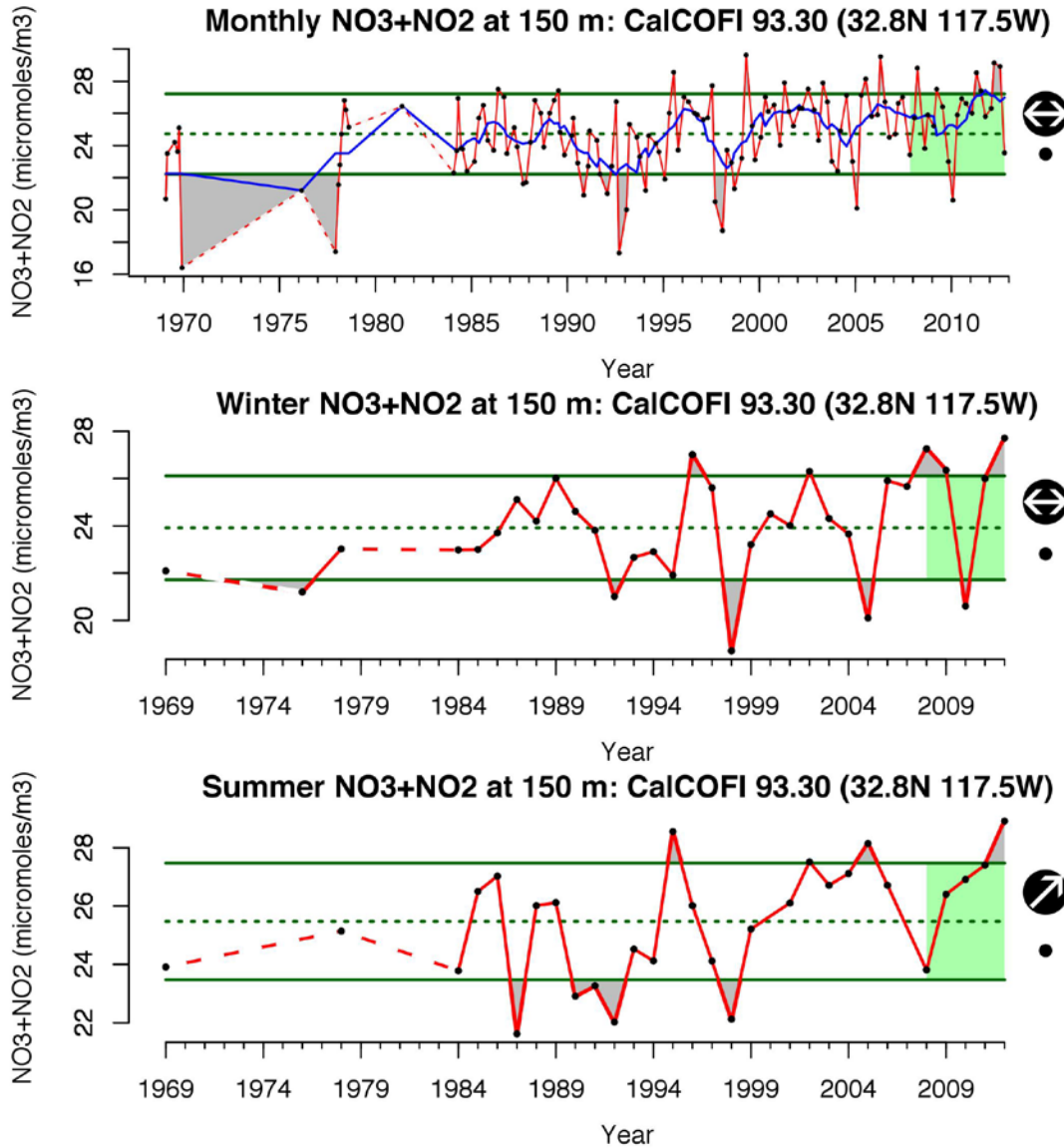


Figure OC 31. Nutrient data (nitrate + nitrite) at 150 m from 1997-2013 at CalCOFI station 93.30 representing southern California for: monthly, winter and summer means. Monthly values are included to show seasonal cycles and a continuous time series, and the blue line shows a running annual average. Station 93.30 illustrates patterns in the southern portion of the CCLME. Dashed lines show data gaps of greater than 2 years.

TOTAL COPEPOD BIOMASS AND SPECIES COMPOSITION

Copepod biomass and species composition vary seasonally with the highest biomass occurring in the summer months, when food is most plentiful, and the lowest biomass in the winter months (Figures OC32). Copepods are transported to the Oregon coast, either from the north/northwest or from the west/south. Copepods that arrive from the north are cold-water species with higher lipid stores and result in greater productivity of downstream predators; these

are referred to as the northern copepods. Copepods that arrive from the west or south are referred to as the southern copepods and are less rich in lipids. The cold-water group, the northern copepods, usually dominates the Washington/Oregon coastal zooplankton community in summer, whereas the warm-water southern copepods group usually dominates during winter (Peterson and Miller 1977, Peterson and Keister 2003, Peterson and Schwing 2003). However, the northern and southern copepod anomalies track the PDO and MEI fairly closely, thus this seasonal pattern in species composition can be altered during El Niño events or during periods when the PDO is consistently positive or negative. The copepod community index (CCI) is the x-axis score of a 2-dimensional ordination of the copepod species abundance data. The index has a strong seasonal cycle similar to the cyclicity in the monthly total copepod biomass shown below, however when the seasonal cycle is removed (by calculating monthly anomalies) as shown below, the monthly data (red line) track the PDO (compare to Fig OC7. This means that when the PDO is in positive phase, a community dominated by more southern copepods is present (indexed by positive values of the CCI); when the PDO is in negative phase, the copepod community is dominated by more northern species (indexed by negative values of the CCI). Note that during the large El Niño event of 1997-98 and during the summer of 2005 when upwelling was delayed that copepod biomass was low and the CCI was strongly positive. In general, higher abundances of the northern copepods (negative anomalies of the CCI) are indicative of favorable conditions for many upper trophic-level species, including salmon and seabirds. **Both copepod total biomass and community index remained similar to the past several years.**

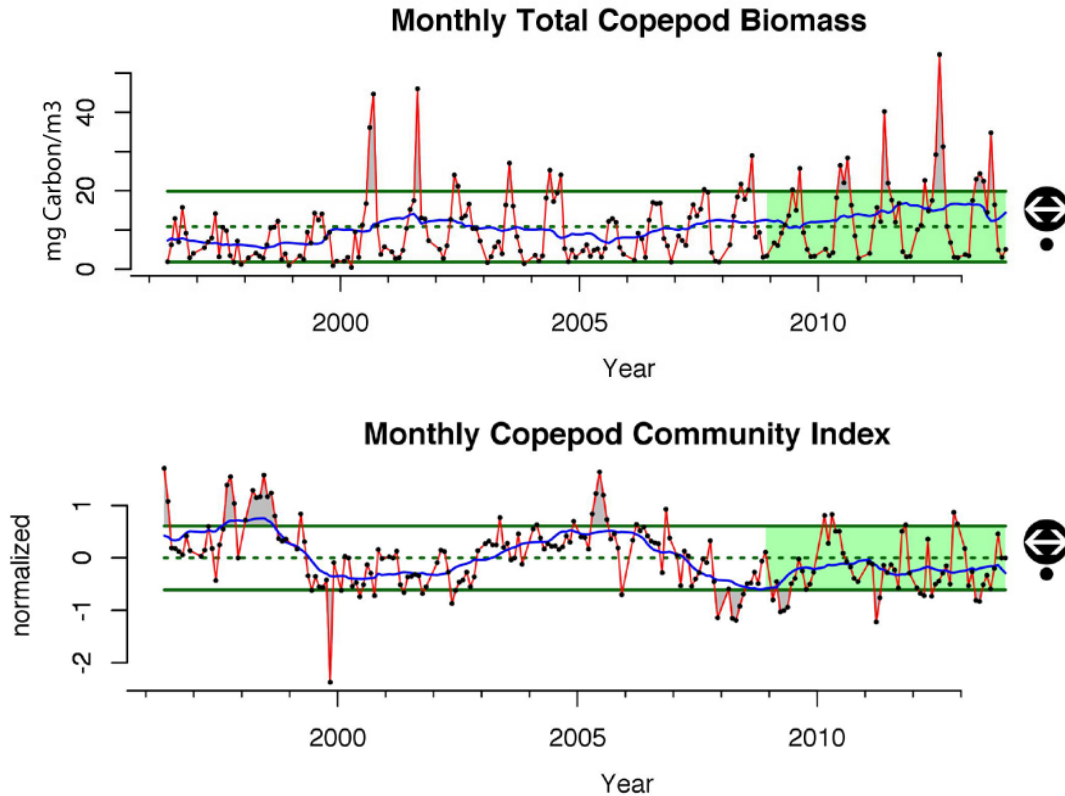


Figure OC 32. Top. total copepod biomass, and bottom. monthly anomaly of the copepod community index from 1996-2013 in the northern California current. The blue line shows a running annual average.

NORTHERN COPEPOD ANOMALY

During the 1997-98 El Niño event, the biomass anomalies of northern copepods was one order of magnitude lower than normal (Figure OC33). With the change in sign of the PDO from positive to negative in mid 1999, the northern copepods responded by showing consistently positive anomalies that prevailed through 2002 (Peterson et al. 2002, Peterson and Keister 2003). In late 2002, the PDO and MEI turned positive (indicating El Niño conditions) and the northern copepods showed negative anomalies. The anomalies were strongly negative during the summer of 2005, a summer characterized by a two-month delay to the start of upwelling (Kosro et al. 2006) and anomalous species composition among the zooplankton (Mackas et al. 2006). Over the past few years, the northern species have predominated with increases in biomass beginning in late 2006. High biomass values were observed for northern species both in 2008 and 2009 with a brief period of negative anomalies during the small El Niño from May 2009 through May 2010. The highest anomalies in the northern copepod biomass time series (since 1996) were observed in March and April 2011 and also the beginning of 2012, coincident with strongly negative PDO values. **For 2013, northern copepod biomass anomaly was again high.**

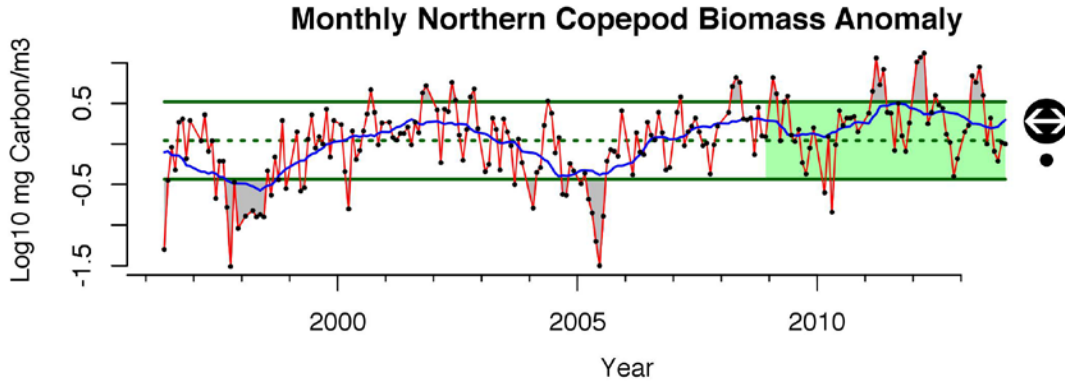


Figure OC 33. Northern Copepod Biomass Anomaly index monthly from 1996-2012 in the northern California current. The blue line shows a running annual average.

SOUTHERN COPEPOD ANOMALY

The highest positive anomalies of the southern species were observed during the 1997-1998 El Niño (Figure OC34). Consistently high positive anomalies of southern species were also observed from 2003 through 2006 coinciding with a period of positive PDO and mostly positive MEI. Over the past few years (since mid-to-late 2009) ocean conditions have been unsettled in that recently there was another small El Niño at the equator. MEI values were positive from May 2009 through May 2010 and the southern copepods responded quite strongly, having anomalies that were similar to those observed during the 1998 and extended (2003-2006) El Niño events. Both the MEI and PDO returned to negative values (signaling a cold ocean) in June 2010 and the southern copepod biomass anomaly became negative in early 2011 following the PDO and MEI sign change by about six months. **For 2013, southern copepod biomass anomaly was similarly low as compared to previous years.**

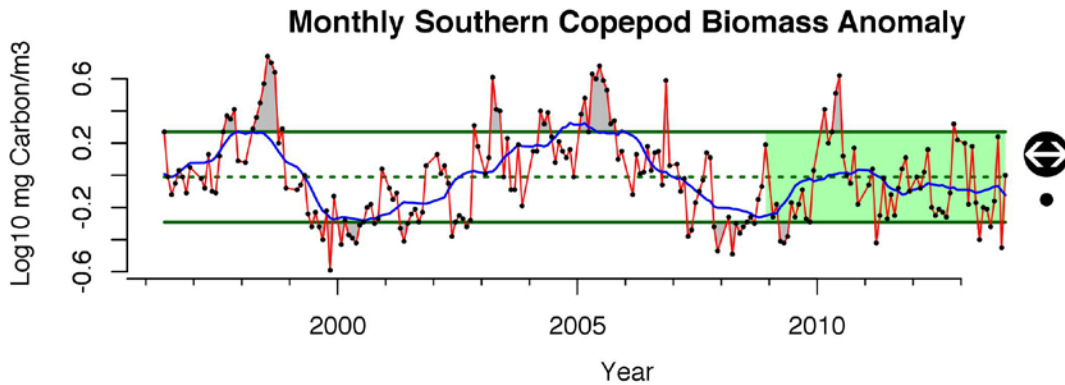


Figure OC 34. Southern Copepod Biomass Anomaly index monthly from 1996-2013 in the northern California current. The blue line shows a running annual average.

OCEAN ACIDIFICATION

BACKGROUND

For seawater, an increase in CO₂ leads to a decrease in pH (increased acidification) and carbonate concentration. Lower pH and reduced availability of carbonate negatively impacts organisms that rely on calcium carbonate (CaCO₃) for structural and protective shells (Barton et al. 2012); examples are coccolithophores and pteropods. Pteropods are important prey for several salmon species in the California Current ecosystem. Aragonite and calcite are the most common forms of CaCO₃ used by organisms. The ‘saturation-state’ of these minerals changes with pH, temperature and pressure. As ocean waters become more acidic they tend towards under saturation of CaCO₃ and protective shells and structural parts more readily dissolve. Many organisms, both calcifying and non-calcifying, may also be susceptible to a reduction in pH. Physiological stress through acid-base regulation and cellular ion exchange varies greatly among organisms. There are very limited data available on how different species compensate for this physiological stress from a lower pH environment, but the data that are available indicate that invertebrate species are likely the most susceptible, and in general, fish tend to be much less sensitive due to a better capacity for acid-base regulation (Pörtner 2008). However, there is potential for increased vulnerability during reproduction and early life history development, both of which are the focus of recent research.

EVALUATION AND SELECTION OF INDICATORS

The saturation state of aragonite and calcite, the pH, and the dissolved oxygen (DO) of waters in the California current all can serve as indicators of ocean acidification. It is likely that synergistic responses among these indicators will be quite difficult to isolate. Although some time series of calcium-carbonate chemistry (e.g. pCO₂, pH, alkalinity) have been started, we do not have enough data yet to say anything about status and trends. Because increases in CO₂ occur along with decreases in dissolved oxygen, we can use DO as a proxy for acidification in the California current. DO serves as an indicator of multiple pressures and also has a longer time series available than the other indicators of ocean acidification. Data are obtained from Newport, Oregon’s NH Line 25 nautical miles (46 km) offshore, from the central California CALCOFI station 67.55, and from the southern California Bight via CalCOFI’s station 93.30 at 22 km offshore.

DISSOLVED OXYGEN AND HYPOXIC EVENTS

BACKGROUND

Low dissolved oxygen concentration in coastal and shelf waters of the California Current ecosystem is a relatively recent issue (Grantham et al. 2004, Bograd et al. 2008). When dissolved oxygen concentrations fall below 1.4 ml L⁻¹, the waters are considered to be ‘hypoxic.’ Dissolved oxygen (DO) concentrations in the ocean are dependent on a number of physical and biological processes, including circulation, ventilation, air-sea exchange, production and respiration. Off Oregon, upwelling transports hypoxic waters onto productive continental shelves, where respiration can reduce water-column DO and thus subject coastal ecosystems to hypoxic or anoxic conditions. Off southern California, the boundary between oxygenated and hypoxic waters has shoaled in recent years. Some California Current nutrients are supplied from rivers and surface runoff, but these sources are minor inputs to the coastal and shelf ecosystem when compared to upwelling. This is in

contrast to the high riverine input in the Gulf of Mexico and Chesapeake Bay. For the northern California Current, upwelling primarily occurs during the summer months (May – Sept.) when the seasonal winds blow from the north. Towards the south, upwelling occurs throughout the year (Bograd et al. 2009). The deep, nutrient-rich waters that are brought up onto the shelf are often low in oxygen, but are rarely ‘hypoxic’ (Hales et al. 2006). Biochemical respiration in the water column and within the sediments draws the oxygen level down further, sometimes to hypoxic or anoxic levels (Connolly et al. 2010). The areas most vulnerable to hypoxia tend to be banks and wider shelf regions where water may be retained for extended periods of time with minimal ventilation from horizontal and vertical mixing (Grantham et al. 2004). There is evidence that the frequency, duration and spatial coverage of hypoxic events has been increasing over the last 20 years (Diaz and Rosenberg 2008), potentially due to increased stratification (reduced vertical mixing) and a decrease in the oxygen concentration of upwelled waters. In the southern portions of the California Current, the shoaling of the permanent Oxygen Minimum Zone is a contributing factor (Helly and Levin 2004, Bograd et al. 2008).

The impact of hypoxia on organisms in the California Current is poorly understood (Keller et al. 2010). Severe events have been shown to kill sessile and slow-moving benthic invertebrates and displace demersal fish species (Grantham et al. 2004, McClatchie et al. 2010). Studies from coastal regions of the Gulf of Mexico and Eastern United States indicate that a range of trophic levels, from plankton to fish, show behavioral changes, may be displaced or killed, or have negative impacts on early life history growth when exposed to low oxygen for extended periods (Rabalais and Turner 2001, Kidwell et al. 2009).

EVALUATION AND SELECTION OF INDICATORS

The indicators for DO are water column profiles of oxygen in % saturation or ml/L. We have chosen DO data from Newport, Oregon’s Newport Line at 25 nm (46 km) offshore, from central California’s 67.55, and from the southern California Bight via CalCOFI’s station 93.30 at 22 km offshore because of their long history and good spatial representation of two portions of the CCS. The data are from 150 meters as this depth as this common depth is targeted to sample source waters.

STATUS AND TRENDS

The northern CCLME has had increased continental shelf hypoxia and shoaling of the hypoxic boundary resulting from enhanced upwelling, primary production, and respiration over the past 15 years (Pierce et al. 2012). Severe and persistent anoxic events have had downstream effects on both demersal fish and benthic invertebrate communities off Oregon (Keller et al. 2010). For example, during a severe anoxic event in August 2006, surveys found an absence of rockfish on rocky reefs and a large mortality event of macroscopic benthic invertebrates (Chan et al. 2008). Seasonality in oxygen concentrations show oxygenated summer waters along the Newport Hydrographic Line since September 2005 (Figure OC35). In 2007, low oxygen concentrations were observed in the summer although the mean was above 1.4 ml/L. The 2011 data point had lower than average oxygen at NH25. Despite higher than average upwelling in 2008, boundary waters remained well oxygenated save two occasions.

In the southern CCLME (Bograd et al. 2008), deepening of the thermocline and decreased oxygen in deep source waters have resulted in decreased subsurface oxygen through 2007 (Figures OC35-OC37). Contrary to the past five years, large-scale wind forcing models predict hypoxia will

continue to expand under Intergovernmental Panel on Climate Change warming scenarios (Rykaczewski and Checkley 2008). **In the north the 2012 and 2013 DO values were slightly below average in the winter and increased to slightly above average in the summer. While in the central and southern regions the 2012 DO values were below average – the winter and summer values in 2012 for CALCOFI station 93.30 are below the long term mean.**

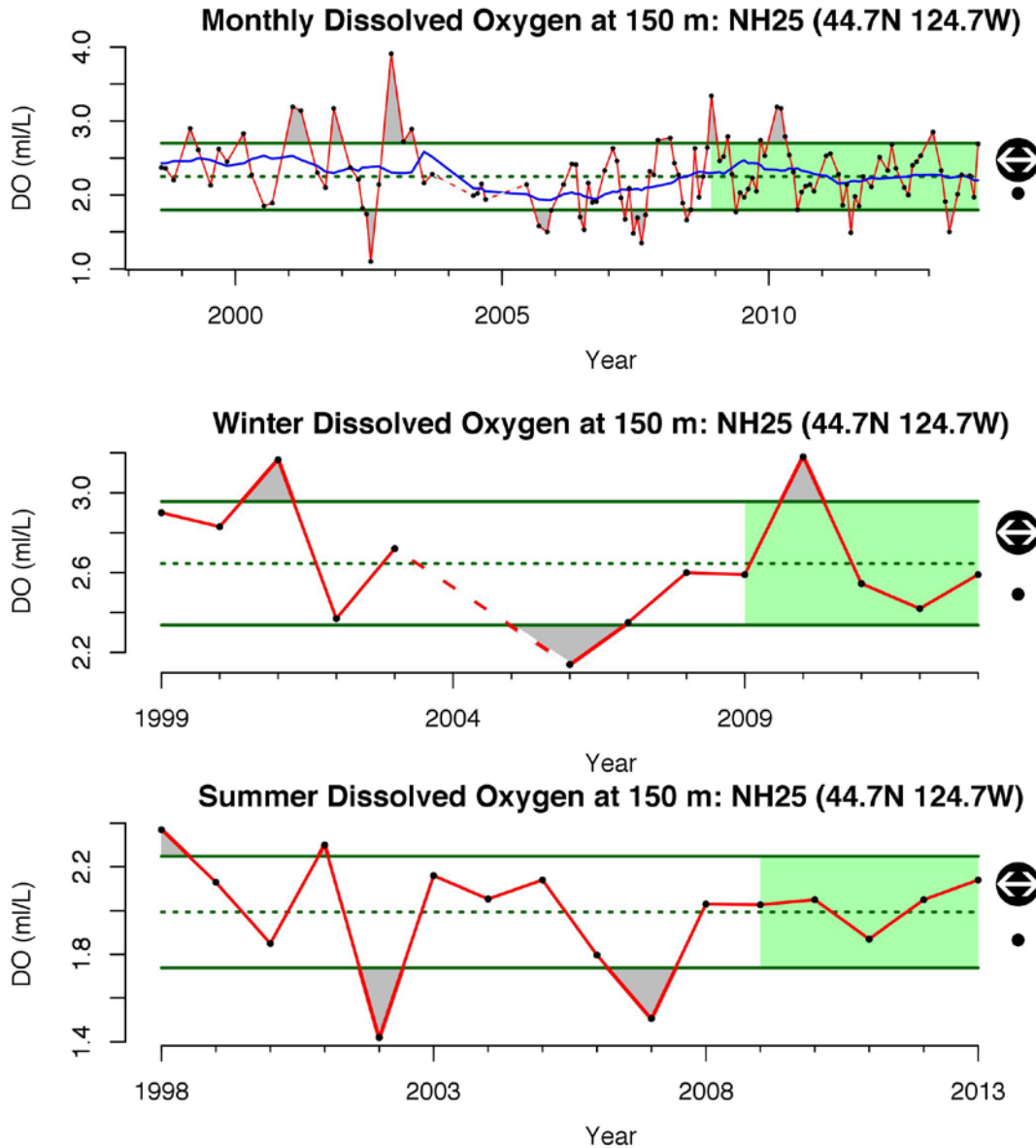


Figure OC 35. Newport line (Newport, Oregon NH25) dissolved oxygen at 150 m from 1999-2013 for monthly, winter and summer means. Monthly values are included to show seasonal cycles and a continuous time series, and the blue line shows a running annual average. Station NH25 illustrates patterns in the northern portion of the CCLME. Dashed lines show data gaps of greater than 2 years.

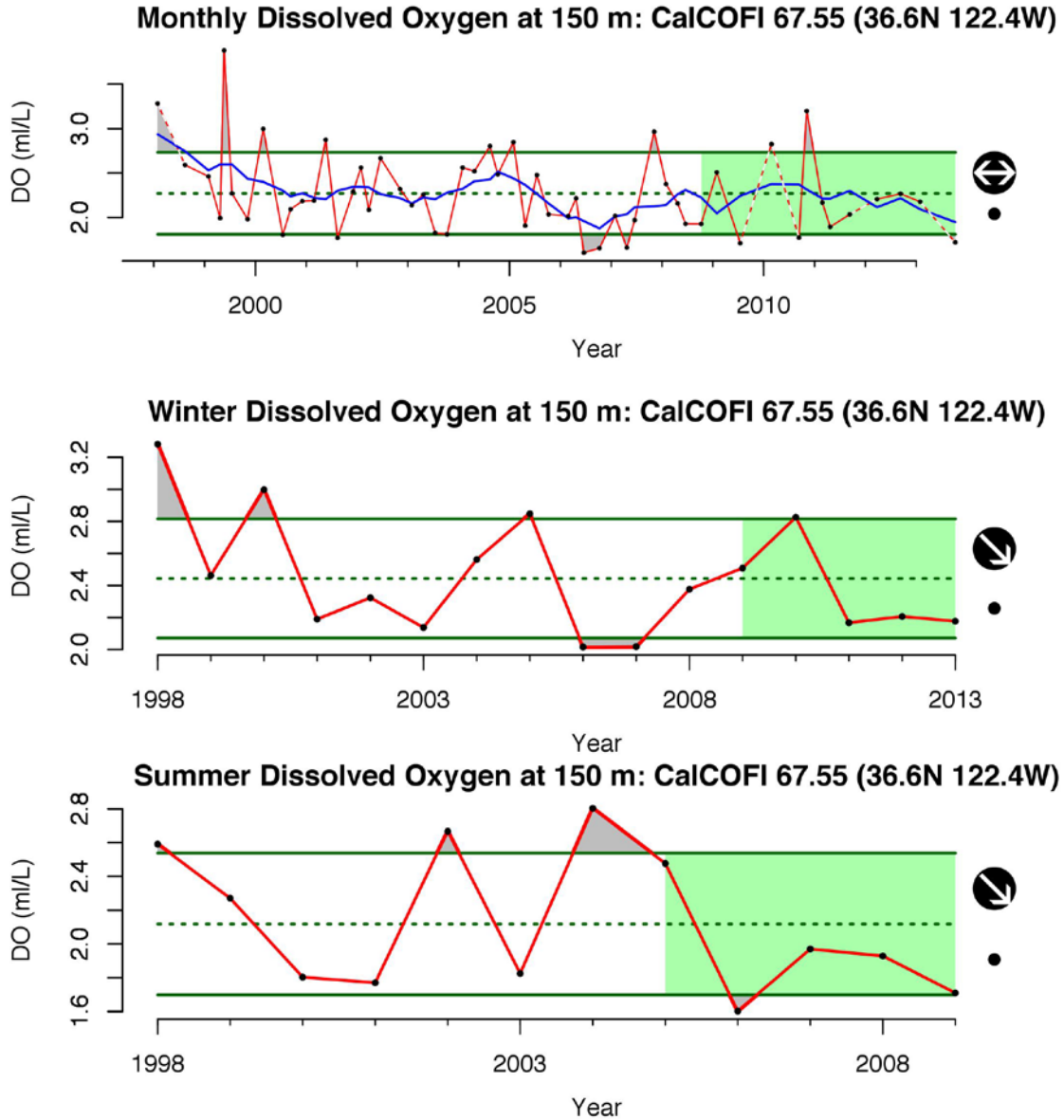


Figure OC 36. CALCOFI station 67.55 dissolved oxygen at 150 m from 1998–2012 for monthly, winter and summer means. Monthly values are included to show seasonal cycles and a continuous time series, and the blue line shows a running annual average. Station 67.55 illustrates patterns in the central portion of the CCLME.

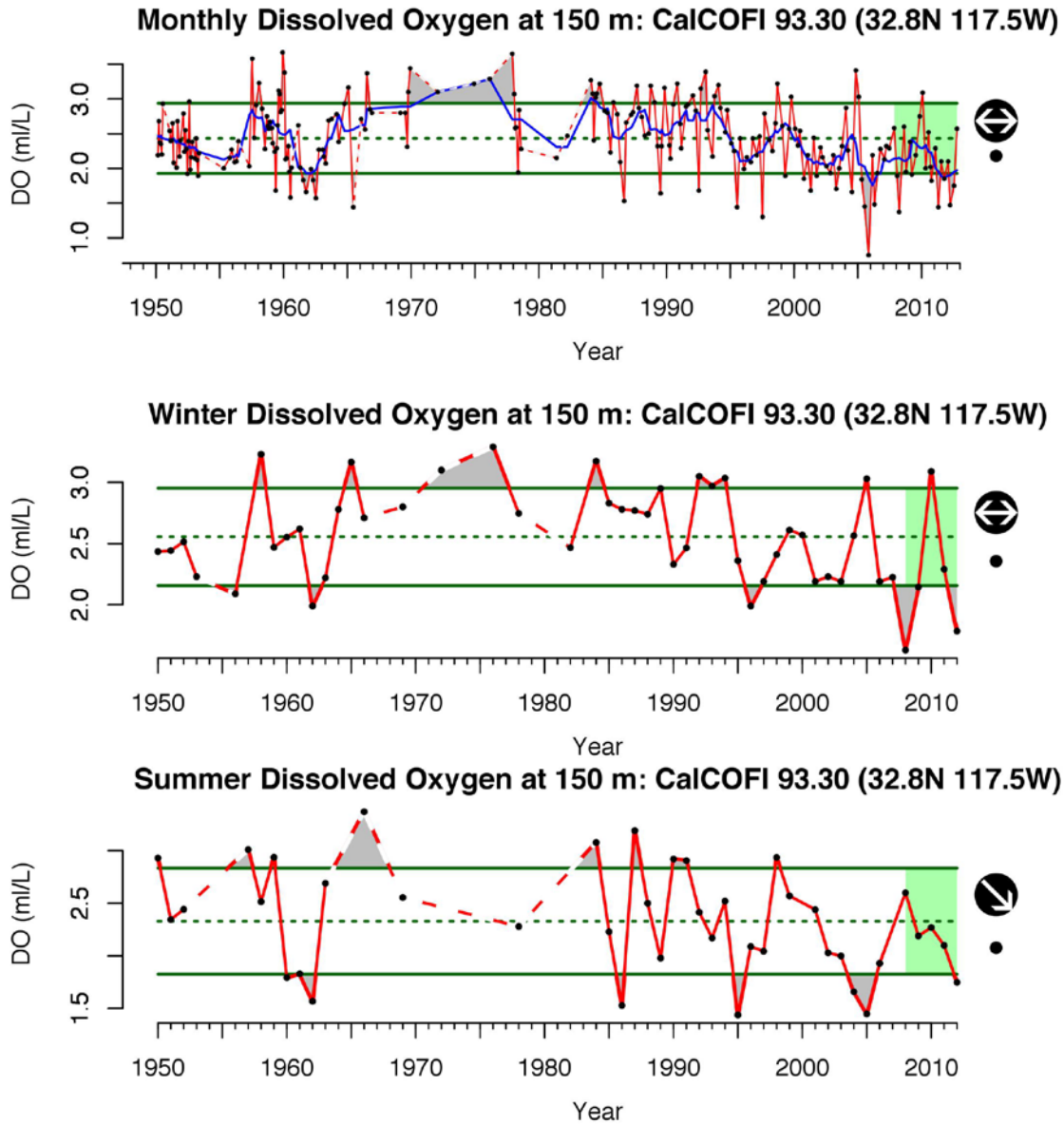


Figure OC 37. CALCOFI station 93.30 dissolved oxygen at 150 m from 1950–2012 for monthly, winter and summer means. Monthly values are included to show seasonal cycles and a continuous time series, and the blue line shows a running annual average. Station 93.30 illustrates patterns in the southern portion of the CCLME. Dashed lines show data gaps of greater than 2 years.

MULTIVARIATE OCEAN CLIMATE INDEX – MOCI

Towards furthering our goal of examining the cross-linkages between climate drivers and ecosystem response, a suite of 35 regional and local-scale anomaly indices were combined and examined using principal component analyses (PCAs) to create a **single** environmental indicator of ecosystem state in the central-northern ecoregion of the California Current (Sydeman et al. 2014). Generally, positive values of the MOCI represent a stronger subtropical influence, with warmer

temperatures, higher precipitation and generally weak winds with poor upwelling, while negative values indicate subarctic influence with cooler temperatures, stronger winds, and upwelling events. While MOCI is not well correlated with some variables such as bulk chl-a from remotely sensed datasets, and krill density for shipboard surveys, it is highly correlated with important biological time series such as the northern copepod index (Fig OC38) and the reproductive success of multiple species of seabirds (Sydeman et al. 2014). The seasonal MOCI represents important components of environmental variability in the CCE and could be a useful tool in understanding or potentially forecasting physical-biological interactions in the system.

From 2006-2010, the dominant signals were the strong upwelling and cold SST winters of 2007 and 2008, as well short-duration El Niño conditions quickly followed by La Niña conditions in late 2010. This is indicated by the positive trend in MOCI winter axis 1 towards warm, weaker upwelling conditions and negative trends in MOCI summer axis 1 towards stronger upwelling conditions. The utility of MOCI depends on continued monitoring of environmental variables and re-calculation of MOCI parameters beyond 2010 for future status reports.

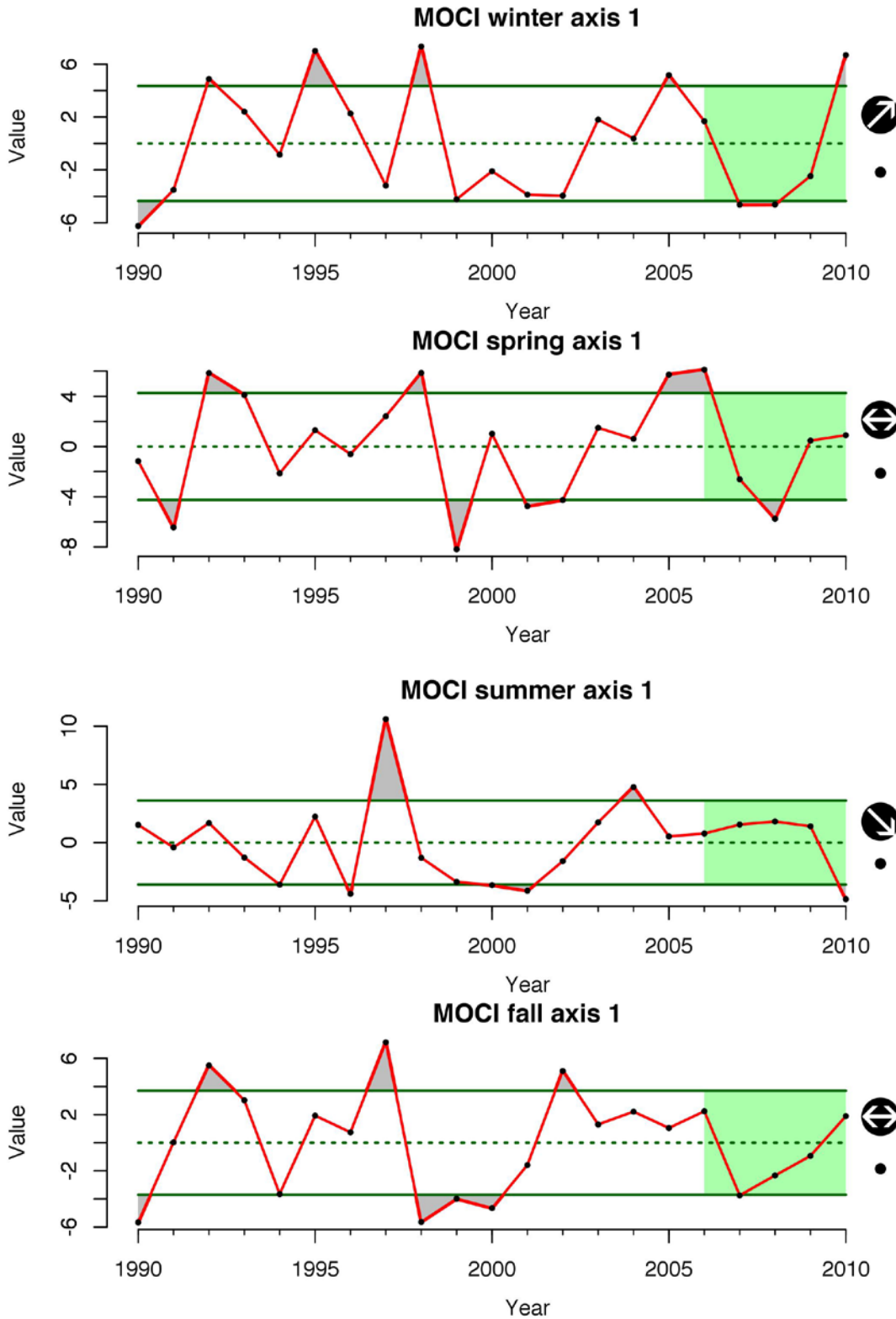


Figure OC 38. Multivariate Ocean Climate Index, axis 1, for winter, spring, summer and fall for the central-northern ecoregion of the CCLME from 1990-2010.

SPATIAL SATELLITE SEA SURFACE TEMPERATURE AND CHLOROPHYLL-A

BACKGROUND

So far in this section, time series from specific locations in the CCLME have been presented to establish the mean and trend over the last 5 years (2009-2013) for different physical processes. Satellite sampling allows for the extension of the IEA's indicator analysis to the whole CCLME. We will focus on satellite measured SST and chlorophyll-a (chl-a) sampled over 30-48°N and 130-116°W as indicators of productivity. The SST product, developed by the NOAA west coast Coastwatch node, is a blend of SST measurements from MODIS, AVHRR, and GOES satellite instruments and has 5-day means from July 2002 to the present. Chl-a data are daily data from July 2002 to the present and are measured by the Aqua MODIS satellite instrument. Monthly averages were used for both SST and chl-a to construct maps of anomalies for 2013, means over the last 5 years, and trends over the last 5 years for winter (Jan-Mar) and summer (Jun-Aug).

STATUS AND TRENDS

SST

The sea surface temperature (SST) for the winter of 2013 (Figure OC39) was cooler than the long-term mean (2002-2013), with SST anomalies of 1 °C or cooler occurring over a wide extent of coastal areas. The mean of the last 5 years (2009-2013) was slightly cooler than the long-term average but displayed no areas when the mean was below 1 standard deviation from the long-term mean. The trend over the last 5 years did display areas when the difference of the start and end dates of the trend was below 1 standard deviation. These areas occurred south of 40°N especially along the coast from 30-34°N. The cause of these negative trends is due to warm SST during the mild El Niño in the winter of 2010 being followed by exceptionally cool temperature in 2013 (see buoy SST above).

The SST anomalies for the summer of 2013 (Figure OC40) are generally warmer for the whole area except for cool areas along the coast in the north (42-45°N) and south (30-34°N). The anomalies for the satellite SST are in slight disagreement to the buoys. This is due to the fact that the summer means of the buoy data for July and August 2013 are missing and hence the buoy data missed a large increase in SST that occurred between July and August of 2013. The mean over the last 5 years was cooler for the whole region but without any grid cells below 1 standard deviation of the long-term mean. The trend over the last 5 years shows mostly positive trends in areas along the coast and areas of negative trends offshore in the south (centered around 32°N 122°W). The positive trends are due to the cool conditions experienced in the summer of 2010 followed by the warmer conditions in the summer of 2013.

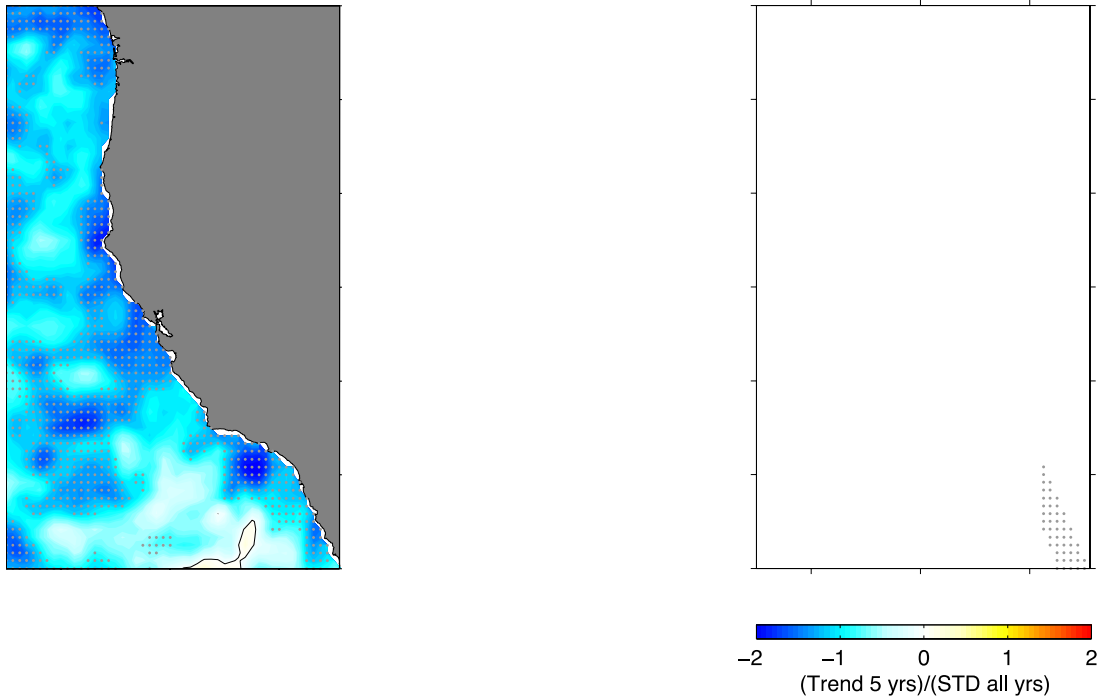


Figure OC 39. Blended satellite SST for: (left) winter 2013 SST anomalies, (middle) 5-year (2009-2013) winter SST means relative to the long-term standard deviation and (right) 5-year (2009-2013) winter SST trends relative to the long-term standard deviation. The value of each grid cell in the mean (center) and trend (right) maps has been normalized by the long-term standard deviation of the winter time series at that grid cell. In the anomaly map the zero contour is drawn in black and a gray dot marks a grid cell where the 2013 anomaly exceeds 1 standard deviation of the long-term mean. The plus/minus 1 contour is drawn in black for the trend map and a gray dot marks any grid location that has a trend exceeding 1 standard deviation from the long-term value.

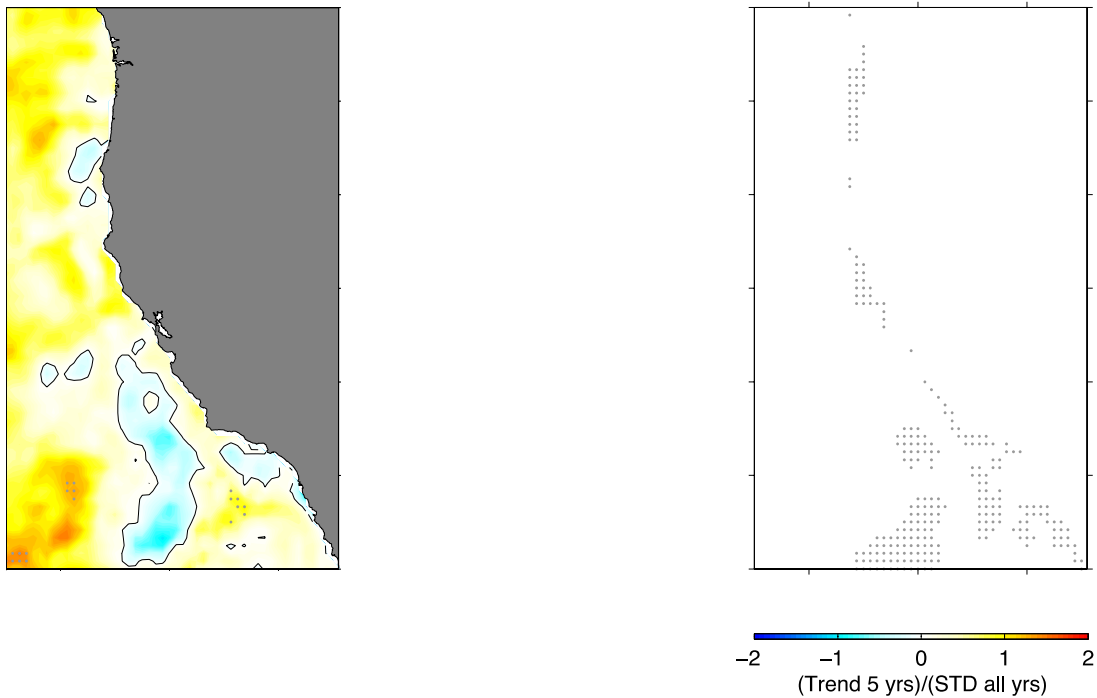


Figure OC 40. Blended satellite SST for: (left) summer 2013 SST anomalies, (middle) 5-year (2009-2013) summer SST means relative to the long-term standard deviation and (right) 5-year (2009-2013) summer SST trends relative to the long-term standard deviation. The value of each grid cell in the mean (center) and trend (right) maps has been normalized by the long-term standard deviation of the summer time series at that grid cell. In the anomaly map the zero contour is drawn in black and a gray dot marks a grid cell where the 2013 anomaly exceeds 1 standard deviation of the long-term mean. The plus/minus 1 contour is drawn in black for the trend map and a gray dot marks any grid location that has a trend exceeding 1 standard deviation from the long-term value.

CHL-A

The winter chl-a anomalies for 2013 (Figure OC41) were exceptionally high for three areas along the coast (47-48°N, 39-42°N, and 36-38°N). The winter mean for the last 5 years generally had more positive than negative values, but the mean did not exceed 1 standard deviation of the long-term mean for any grid cell. The winter trend over the last 5 years had positive trends along the coast and negative trends offshore. The coastal areas when the difference of the start and end dates of the trend was above 1 standard deviation occurred in the same three locations as the positive anomalies for 2013. These positive trends are due to the high chl-a values experienced in the winter of 2013. The offshore negative trends are due to high chl-a experienced during the winter of 2010 being followed by low chl-a values in the winters of 2012 and 2013.

The summer chl-a anomalies for 2013 (Figure OC42) have low anomalies along the coast between 40-47°N and 37-38°N. High anomalies along the coast between 47-48°N persisted in this region from the winter. The summer mean for the last 5 years was mostly below the long-term mean for areas

along the coast. Though, none of these means exceeded 1 standard deviation of the long-term mean. Negative trends of the last 5 years were observed along the coast between 43-47°N and 30-33°N, while positive trends were found along the coast in areas of strong upwelling (38-39°N and 35-36°N). The areas of positive summer trends resulted due to low chl-a values in 2009 followed by the high values in 2013.

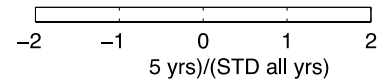
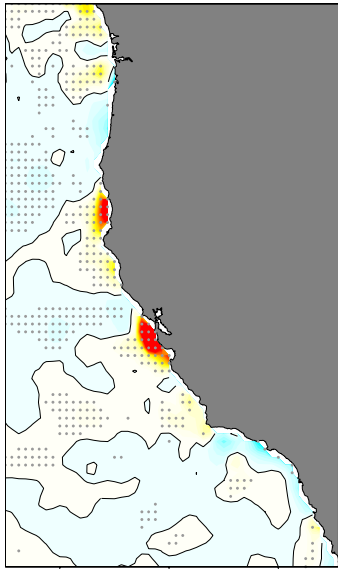


Figure OC 41. Aqua MODIS satellite chl-a for: (left) winter 2013 chl-a anomalies, (middle) 5-year (2009-2013) winter chl-a means relative to the long-term standard deviation and (right) 5-year (2009-2013) winter chl-a trends relative to the long-term standard deviation. The value of each grid cell in the mean (center) and trend (right) maps has been normalized by the long-term standard deviation of the winter time series at that grid cell. In the anomaly map the zero contour is drawn in black and a gray dot marks a grid cell where the 2013 anomaly exceeds 1 standard deviation of the long-term mean. The plus/minus 1 contour is drawn in black for the trend map and a gray dot marks any grid location that has a trend exceeding 1 standard deviation from the long-term value.

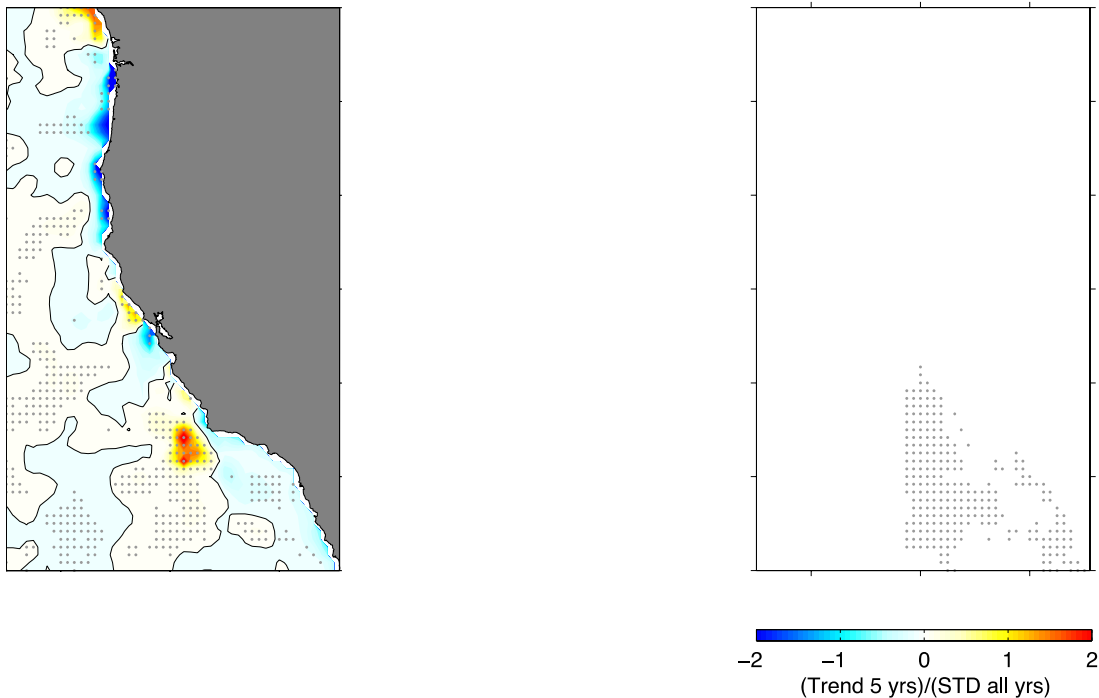


Figure OC 42. Aqua MODIS satellite chl-a for: (left) summer 2013 chl-a anomalies, (middle) 5-year (2009-2013) summer chl-a means relative to the long-term standard deviation and (right) 5-year (2009-2013) summer chl-a trends relative to the long-term standard deviation. The value of each grid cell in the mean (center) and trend (right) maps has been normalized by the long-term standard deviation of the summer time series at that grid cell. In the anomaly map the zero contour is drawn in black and a gray dot marks a grid cell where the 2013 anomaly exceeds 1 standard deviation of the long-term mean. The plus/minus 1 contour is drawn in black for the trend map and a gray dot marks any grid location that has a trend exceeding 1 standard deviation from the long-term value.

EFFECTS OF ANTHROPOGENIC CLIMATE CHANGE

Ocean temperatures have increased, and are likely to continue to increase for the foreseeable future. Land is expected to heat faster than the ocean and these contrasts in temperatures may result in higher wind speeds (Bakun 1990, Snyder et al. 2003). Warmer waters are also increasing stratification (Roemmich and McGowan 1995, McGowan et al. 2003). The effects of stronger winds and increased stratification on upwelling, temperature, and primary productivity in the CCLME are not well known (Schwing and Mendelssohn 1997, Mendelssohn and Schwing 2002), but clearly will have ecosystem consequences beyond warming surface temperatures. It is important to note that dynamics in the CCS are often dominated by changing wind patterns at local, regional, and basin scales which have masked long-term thermodynamic-forced trends apparent in other ocean ecosystems.

The timing of the seasonal cycle of productivity is changing (GRL 2006, Bograd et al. 2009). Just as terrestrial biological systems are experiencing earlier phenology (IPCC 2007), we may

observe an earlier start to the upwelling season in the CCLME, and these patterns may vary by ecoregion. If upwelling occurs earlier, this could result in an earlier seasonal cycle, from earlier phytoplankton blooms to earlier peaks in zooplankton abundance. In contrast, as noted previously, if the efficacy of upwelling is weakened or delayed by increased water stratification, the seasonal cycle of different organisms may be offset, leading to mismatches among trophic levels in both abundance and availability of prey (Bograd 2010).

We are already seeing changes in nutrient values and shoaling of hypoxic zones in many parts of the California Current (Bograd et al. 2008, Chan et al. 2008). These trends are predicted to increase as decreased ventilation of the North Pacific will lead to greater nutrient concentrations in CCLME source waters (Rykaczewski and Dunne 2010). Predicted increases in nitrate are accompanied by decreased DO and increased ocean acidification leading to the potential for multiple stressors on the California Current ecosystem (Doney 2010, Halpern et al. 2010, Keeling et al. 2010).

With these varied scenarios in mind, there is the potential for increased interannual variability in the CCLME upwelling (Bograd et al. 2009, Bograd 2010). A more volatile climate with more extreme events will impact biological systems of the CCLME (Francis and Mantua 2003). Increased upwelling has been hypothesized and predicted in some global climate models (Bakun et al. 2010, Rykaczewski and Dunne 2010, Doney et al. 2012), but there is still much debate as to the ultimate effects of global climate change on upwelling intensity. In addition, evidence of variability and declines in biological systems in the CCLME since about 1990 has already been observed (Sydeman and Bograd 2009). Such changes and others (e.g., range shifts in species' distributions) are likely to continue.

LINKS TO DATA, AS APPROPRIATE

Table OC 1. Top indicators for ocean and climatic pressures. Three stations were chosen when possible for northern, central, and southern portions of the California current. Time series availability often differed across the three locations.

Pressure	Indicator	Definition and source of data	Time series	Sampling frequency
Ocean acidification	DO	Newport line station NH25 and at 150 meters deep as representative of the northern CCLME.	1998 - 2011	monthly
		CALCOFI station 93.30 at 150 meters as representative of the southern CCLME.	1984 - 2012	quarterly
		CALCOFI station 67.55 at 150 meters as representative of the central CCLME.	1998 - 2011	quarterly
Decreasing oxygen	DO	Newport line station NH25 and at 150 meters as representative of the northern CCLME.	1998 - 2013	monthly
		CALCOFI station 93.30 at 150 meters as representative of the southern CCLME.	1984 - 2012	quarterly
		CALCOFI station 67.55 at 150 meters as representative of the central CCLME.	1998 - 2013	quarterly
Sea level rise	Coastal Sea Level	Sea Level measured by tide gauges at South Beach, OR.	1967 - 2013	daily
		Sea Level measured by tide gauges at San Francisco, CA.	1897 - 2013	daily
		Sea Level measured by tide gauges at San Diego, CA. Data were obtained from UHawaii Sea Level Center: http://uhslc.soest.hawaii.edu/home	1906 - 2013	daily
Temperature change	Sea surface buoy temperatures	Sea surface temperatures measured by NDBC buoy 46050 (44.639° N 124.534° W; 37 km from land).	1991 - 2013	hourly
		Sea surface temperatures measured by NDBC buoy 46014 (39.235° N 123.974° W; 17 km from land).	1981 - 2012	hourly
		Sea surface temperatures measured by NDBC buoy 46025 (22.749° N 119.053° W; 40 km from land). Data are available at National Data Buoy Center: http://ndbc.noaa.gov	1982 - 2013	hourly
	PDO	Pacific Decadal Oscillation (PDO) is the dominant pattern of North Pacific SST anomalies. Data are available at: http://jisao.washington.edu/pdo/	1900 - 2013	monthly
	NOI	Northern Oscillation Index (NOI) measures atmospheric teleconnections between North Pacific High and northeast Pacific. Data are available at: http://coastwatch.pfeg.noaa.gov/erddap/index.html	1967 - 2013	monthly

	MEI	Multivariate ENSO Index (MEI) reports on the status of the coupled ocean-atmosphere ENSO events. Data are available at: http://www.esrl.noaa.gov/psd/enso/mei/mei.html	1950 - 2013	monthly
	Satellite sea surface temperatures	Blend of SST measurements from MODIS, AVHRR, and GOES satellite instruments. Data are available at: http://coastwatch.pfeg.noaa.gov/erddap/griddap/erdBASsta5day.graph	2002-2013	5-day means
Water column structure	Pycnocline depth	Three stations, Newport NH25, CALCOFI 93.30, and 67.55 were used for water column structure.	1984 - 2013	quarterly
	Pycnocline strength	Three stations, Newport NH25, CALCOFI 93.30, and 67.55 were used for water column structure.	1984 - 2013	quarterly
Changes in source waters	Nutrient content (NO ₂ +NO ₃)	Three stations, Newport NH25, CALCOFI 93.30, and 67.55 were used for water column structure. Nitrate+nitrite concentrations at 150 m show variations in source water.	1984 - 2013	quarterly
	Zooplankton community structure	Newport line data are compiled into four indices (total biomass, northern anomaly, southern anomaly, and copepod index).	1998 - 2013	monthly
	NPGO	North Pacific Gyre Oscillation (NPGO) explains variations in the circulation of the North Pacific Gyre. The NPGO describes nutrient concentrations in the CCS. Data are available at: http://www.o3d.org/npgo/	1950 - 2013	monthly
Changes in CC transport & mesoscale variability	EKE	Eddy Kintectic Energy (EKE) was calculated over three spatial locations (6 degree mean), at 33°, 39° and 45° N. Meridional and zonal geostrophic velocities used in the EKE calculations are distributed by Aviso at: http://www.aviso.oceanobs.com/duacs/	1992 - 2013	daily
Timing and strength of upwelling	meridional	North winds are drive much of coastal upwelling and are measured by NDBC buoy 46050 (44.639° N 124.534° W; 37 km from land)	1991 - 2013	hourly
		North winds are measured by NDBC buoy 46014 (39.235° N 123.974° W; 17 km from land)	1981 - 2013	hourly
		North winds are measured by NDBC buoy 46025 (22.749° N 119.053° W; 40 km from land). Data are available at National Data Buoy Center: http://ndbc.noaa.gov	1982 - 2013	hourly
	UI	Upwelling Index (UI) denote the strength of coastal upwelling and downwelling; data are presented at 33°, 39° and 45° N.	1967-2013	daily
	STI	Spring Transition Index (STI) denotes the start of the upwelling season .It is derived from the daily UI and data are presented at 33°, 39° and 45° N.	1967-2013	yearly
	TUMI	Total Upwelling Magnitude Index (TUMI) is the amount of upwelling between the spring and fall transition dates. It is derived from the daily UI at 33°, 39° and 45° N.	1967-2013	yearly

	LUSI	Length of Upwelling Index (LUSI) is the number of days during the upwelling season. It is derived from the daily UI at 33°, 39° and 45° N. Data are available at: http://www.pfeg.noaa.gov/products/las.html	1967-2013	yearly
Timing and frequency of El Niño events	MEI	Multivariate ENSO Index (MEI) measures the magnitude and duration of El Niño and La Niña events. Data are available at: http://www.esrl.noaa.gov/psd/enso/mei/	1950 - 2012	monthly
	NOI	Northern Oscillation Index (NOI) measures atmospheric teleconnections between North Pacific High and northeast Pacific. Large negative values usually occur during an El Niño event. Data are available at http://coastwatch.pfeg.noaa.gov/erddap/index.html	1950 - 2012	monthly
Productivity	MOCI	Multivariate Ocean Climate Index (MOCI) is a PCA of 35 separate regional and local indicators of ecosystem status for the central-northern ecoregion of the California Current.	1990-2010	yearly
Primary Productivity	CHL-A	Chlorophyll-a measured by the Aqua MODIS satellite data available at: http://coastwatch.pfeg.noaa.gov/erddap/griddap/erdMHchla1day.graph	2002-2013	daily

REFERENCES CITED

- Bakun, A. 1975. Daily and weekly upwelling indices, west coast of North America, 1967-73. NMFS, Washington, DC.
- Bakun, A. 1990. Global Climate Change and Intensification of Coastal Ocean Upwelling. *Science* **247**:198-201.
- Bakun, A., D. B. Field, A. Redondo - Rodriguez, and S. J. Weeks. 2010. Greenhouse gas, upwelling - favorable winds, and the future of coastal ocean upwelling ecosystems. *Global Change Biology* **16**:1213-1228.
- Barth, J. A., B. A. Menge, J. Lubchenco, F. Chan, J. M. Bane, A. R. Kirincich, M. A. McManus, K. J. Nielsen, S. D. Pierce, and L. Washburn. 2007. Delayed upwelling alters nearshore coastal ocean ecosystems in the northern California current. *Proceedings of the National Academy of Sciences* **104**:3719-3724.
- Barton, A., B. Hales, G. G. Waldbusser, C. Langdon, and R. A. Feely. 2012. The Pacific oyster, *Crassostrea gigas*, shows negative correlation to naturally elevated carbon dioxide levels: Implications for near-term ocean acidification effects. *Limnology And Oceanography* **57**:698-710.
- Behrenfeld, M. J., R. T. Malley, D. A. Siegel, C. R. McClain, J. L. Sarmiento, G. C. Feldman, A. J. Milligan, P. G. Falkowski, R. M. Letelier, and E. S. Boss. 2006. Climate-driven trends in contemporary ocean productivity. *Nature* **444**:752-755.
- Bi, H., W. T. Peterson, and P. T. Strub. 2011. Transport and coastal zooplankton communities in the northern California Current system. *Geophysical Research Letters* **38**:5 PP.-5 PP.
- Bjorkstedt, E. P., R. Goericke, S. McClatchie, E. Weber, W. Watson, N. Lo, B. Peterson, B. Emmett, R. Brodeur, J. Peterson, M. Litz, J. Gómez-Valdéz, G. Gaxiola-Castro, B. E. Lavaniegos, F. Chavez, C. Collins, J. Field, K. Sakuma, S. J. Bograd, F. B. Schwing, P. Warzybok, R. Bradley, J. Jahncke, G. S. Campbell, J. A. Hildebrand, W. J. Sydeman, S. A. Thompson, J. L. Largier, C. Halle, S. Y. Kim, and J. Abell. 2011. State of the California Current 2010-2011: Regionally variable responses to a strong (but fleeting?) La Niña. *CalCOFI Rep* **52**:36-68.
- Black, B. A., I. D. Schroeder, W. J. Sydeman, S. J. Bograd, B. K. Wells, and F. B. Schwing. 2011. Winter and summer upwelling modes and their biological importance in the California Current Ecosystem. *Global Change Biology*.
- Bograd, S. J. 2010. PICES report: Marine Ecosystems of the North Pacific Ocean 2003-2008. California Current, Chapter 3. Online at http://www.pices.int/publications/special_publications/default.aspx. Marine Ecosystems of the North Pacific Ocean, 2003-2008.
- Bograd, S. J., C. G. Castro, E. Di Lorenzo, D. M. Palacios, H. Bailey, W. Gilly, and F. P. Chavez. 2008. Oxygen declines and the shoaling of the hypoxic boundary in the California Current. *Geophysical Research Letters* **35**:1-6.
- Bograd, S. J., I. Schroeder, N. Sarkar, X. Qiu, W. J. Sydeman, and F. B. Schwing. 2009. Phenology of coastal upwelling in the California Current. *Geophysical Research Letters* **36**.
- Brodeur, R. D. 1990. Abundance and distribution patterns of zooplankton along the Oregon and southern WA coasts during the summer of 1981. Univ. Wash. Fish. Res. Inst. Tech. Rep. **9003**.

- Brodeur, R. D. and W. G. Pearcy. 1992. Effects of environmental variability on trophic interactions and food web structure in a pelagic upwelling ecosystem. *Marine Ecology Progress Series* **84**:101-119.
- Bromirski, P. D., A. J. Miller, and R. E. Flick. 2012. Understanding North Pacific sea level trends. *Eos, Transactions American Geophysical Union* **93**.
- Chan, F., J. A. Barth, J. Lubchenco, A. Kirincich, H. Weeks, W. T. Peterson, and B. A. Menge. 2008. Emergence of Anoxia in the California Current Large Marine Ecosystem. *Science* **319**:920-920.
- Chavez, F. P., J. T. Pennington, C. G. Castro, J. P. Ryan, R. P. Michisaki, B. Schlining, P. Walz, K. R. Buck, A. McFadyen, and C. A. Collins. 2002. Biological and chemical consequences of the 1997-1998 El Niño in central California waters. *Progress In Oceanography* **54**:205-232.
- Chavez, F. P., J. Ryan, S. E. Lluch-Cota, and M. Niquen C. 2003. From Anchovies to Sardines and Back: Multidecadal Change in the Pacific Ocean. *Science* **299**:217-221.
- Checkley, D. M. and J. A. Barth. 2009. Patterns and processes in the California Current System. *Progress In Oceanography* **83**:49-64.
- Chenillat, F., P. Rivière, X. Capet, E. D. Lorenzo, and B. Blanke. 2012. North Pacific Gyre Oscillation modulates seasonal timing and ecosystem functioning in the California Current upwelling system. *Geophysical Research Letters* **39**:6 PP.-6 PP.
- Connolly, T. P., B. M. Hickey, S. L. Geier, and W. P. Cochlan. 2010. Processes influencing seasonal hypoxia in the northern California Current System. *Journal of Geophysical Research* **115**:C03021-C03021.
- Cummins, P. F. and H. J. Freeland. 2007. Variability of the North Pacific Current and its bifurcation. *Progress In Oceanography* **75**:253-265.
- Di Lorenzo, E., N. Schneider, K. M. Cobb, P. J. S. Franks, K. Chhak, A. J. Miller, J. C. McWilliams, S. J. Bograd, H. Arango, E. Curchitser, T. M. Powell, and P. Rivière. 2008. North Pacific Gyre Oscillation links ocean climate and ecosystem change. *Geophysical Research Letters* **35**:6 PP.-6 PP.
- Diaz, R. J. and R. Rosenberg. 2008. Spreading Dead Zones and Consequences for Marine Ecosystems. *Science* **321**:926-929.
- Domingues, C. M., J. A. Church, N. J. White, P. J. Gleckler, S. E. Wijffels, P. M. Barker, and J. R. Dunn. 2008. Improved estimates of upper-ocean warming and multi-decadal sea-level rise. *Nature* **453**:1090-1093.
- Doney, S. C. 2010. The growing human footprint on coastal and open-ocean biogeochemistry. *Science* **328**:1512-1516.
- Doney, S. C., M. Ruckelshaus, J. Emmett Duffy, J. P. Barry, F. Chan, C. A. English, H. M. Galindo, J. M. Grebmeier, A. B. Hollowed, N. Knowlton, J. Polovina, N. N. Rabalais, W. J. Sydeman, and L. D. Talley. 2012. Climate Change Impacts on Marine Ecosystems. *Annual review of marine science* **4**:11-37.
- Douglas, B. C. 1991. Global Sea-Level Rise. *Journal of Geophysical Research Oceans* **96**:6981-6992.
- Foy, R. J. and B. L. Norcross. 1999. Spatial and temporal variability in the diet of juvenile Pacific herring (*Clupea pallasii*) in Prince William Sound, Alaska. *Canadian Journal of Zoology* **77**:697-706.

- Francis, R. C. and N. J. Mantua. 2003. Climate and Extinction Risk for Salmon Populations of the Northeast Pacific. Eds. A. D. MacCall and T. C. Wainwright. Assessing extinction risk for West Coast salmon: Proceedings of the workshop, Nov 13-15, 1996, Seattle, WA. U.S. Dep. Commer., NOAA Tech. Memo **NMFS-NWFSC-56: 37-76**.
- García-Reyes, M. and J. L. Largier. 2012. Seasonality of coastal upwelling off central and northern California: New insights, including temporal and spatial variability. *Journal of Geophysical Research* **117**:17 PP.-17 PP.
- Grantham, B. A., F. Chan, K. J. Nielsen, D. S. Fox, J. A. Barth, A. Huyer, J. Lubchenco, and B. A. Menge. 2004. Upwelling-driven nearshore hypoxia signals ecosystem and oceanographic changes in the northeast Pacific. *Nature* **429**:749-754.
- GRL. 2006. Warm Ocean Conditions in the California Current in Spring/Summer 2005: Causes and Consequences. *Geophysical Research Letters* **33**.
- Hales, B., L. Karp-Boss, A. Perlin, and P. A. Wheeler. 2006. Oxygen production and carbon sequestration in an upwelling coastal margin. *Global Biogeochemical Cycles* **20**:GB3001-GB3001.
- Halpern, B. S., C. V. Kappel, K. A. Selkoe, F. Micheli, C. M. Ebert, C. Kontgis, C. M. Crain, R. G. Martone, C. Shearer, and S. J. Teck. 2009. Mapping cumulative human impacts to California Current marine ecosystems. *Conservation Letters* **2**:138-148.
- Halpern, B. S., S. E. Lester, and K. L. McLeod. 2010. Placing marine protected areas onto the ecosystem-based management seascape. *Proceedings of the National Academy of Sciences of the United States of America* **107**:18312-18317.
- Halpern, B. S., S. Walbridge, K. A. Selkoe, C. V. Kappel, F. Micheli, C. D'Agrosa, J. F. Bruno, K. S. Casey, C. Ebert, H. E. Fox, R. Fujita, D. Heinemann, H. S. Lenihan, E. M. P. Madin, M. T. Perry, E. R. Selig, M. Spalding, R. Steneck, and R. Watson. 2008. A global map of human impact on marine ecosystems. *Science* **319**:948-952.
- Haney, R. L., R. A. Hale, and D. E. Dietrich. 2001. Offshore propagation of eddy kinetic energy in the California Current. *Journal of Geophysical Research* **106**:PP. 11,709-711,717-PP. 711,709-711,717.
- Hazen, E. L., S. Jorgensen, R. R. Rykaczewski, S. J. Bograd, D. G. Foley, I. D. Jonsen, S. A. Shaffer, J. P. Dunne, D. P. Costa, L. B. Crowder, and B. A. Block. 2012. Predicted habitat shifts of Pacific top predators in a changing climate. *Nature Climate Change*.
- Helly, J. and L. Levin. 2004. Global distribution of naturally occurring marine hypoxia on continental margins. *Deep Sea Research Part I: Oceanographic Research Papers* **51**:1159-1168.
- Hickey, B. M. 1979. The California current system—hypotheses and facts. *Progress In Oceanography* **8**:191-279.
- Hooff, R. C. and W. T. Peterson. 2006. Copepod biodiversity as an indicator of changes in ocean and climate conditions of the northern California current ecosystem. *Limnology And Oceanography* **51**:2607-2620.
- Huyer, A. 1983. Coastal Upwelling in the California Current System. *Progress In Oceanography* **12**:259-284.
- IPCC. 2007. Climate Change 2007: The Physical Science Basis. Contribution of Working Group I to the Fourth Assessment Report of the Intergovernmental Panel on Climate Change. **AR4**:996-996.

- Jahncke, B. L. Saenz, C. L. Abraham, C. Rintoul, R. W. Bradley, and W. J. Sydeman. 2008. Ecosystem responses to short-term climate variability in the Gulf of the Farallones, California. *Progress In Oceanography* **77**:182-193.
- Kappes, M. A., S. A. Shaffer, Y. Tremblay, D. G. Foley, D. M. Palacios, P. W. Robinson, S. J. Bograd, and D. P. Costa. 2010. Hawaiian albatrosses track interannual variability of marine habitats in the North Pacific. *Progress In Oceanography* **86**:246-260.
- Keeling, R. E., A. Körtzinger, and N. Gruber. 2010. Ocean deoxygenation in a warming world. *Annual review of marine science* **2**:199-229.
- Keister, J. E., E. Di Lorenzo, C. A. Morgan, V. Combes, and W. T. Peterson. 2011. Zooplankton species composition is linked to ocean transport in the Northern California Current. *Global Change Biology* **17**:2498-2511.
- Keller, A. A., V. Simon, F. Chan, W. W. Wakefield, M. E. Clarke, J. A. Barth, D. Kamikawa, and E. L. Fruh. 2010. Demersal fish and invertebrate biomass in relation to an offshore hypoxic zone along the US West Coast. *Fisheries Oceanography* **19**:76-87.
- Kershner, J., J. F. Samhuri, C. A. James, and P. S. Levin. 2011. Selecting Indicator Portfolios for Marine Species and Food Webs: A Puget Sound Case Study. *PLoS ONE* **6**.
- Kidwell, D. M., A. J. Lewitus, E. B. Jewett, S. B. Brandt, and D. M. Mason. 2009. Ecological impacts of hypoxia on living resources. *Journal of Experimental Marine Biology and Ecology* **381**:S1-S3-S1-S3.
- King, J. R., V. N. Agostini, C. J. Harvey, G. A. McFarlane, M. G. G. Foreman, J. E. Overland, E. Di Lorenzo, N. A. Bond, and K. Y. Aydin. 2011. Climate Forcing and the California Current Ecosystem. *ICES Journal of Marine Science: Journal du Conseil* **68**:1199-1216.
- Kosro, P. M., W. T. Peterson, B. M. Hickey, R. K. Shearman, and S. D. Pierce. 2006. Physical versus biological spring transition: 2005. *Geophysical Research Letters* **33**.
- Levin, P. S., A. James, J. Kershner, S. O'Neill, T. Francis, J. F. Samhuri, and C. J. Harvey. 2011. The Puget Sound ecosystem: What is our desired future and how do we measure progress along the way? In *Puget Sound Science Update*, Chapter 1a. Online at <http://www.psp.wa.gov/scienceupdate.php> [accessed 17 August 2012].
- Levin, P. S. and F. B. Schwing. 2011. Technical background for an integrated ecosystem assessment of the California Current: Groundfish, salmon, green sturgeon, and ecosystem health. U.S. Dept. of Commerce, NOAA Tech. Memo., NMFS-NWFSC-109, 330 p.
- Levitus, J. I. Antonov, T. P. Boyer, R. A. Locarnini, H. E. Garcia, and A. V. Mishonov. 2009. Global ocean heat content 1955–2008 in light of recently revealed instrumentation problems. *Geophysical Research Letters* **36**:1-5.
- Mackas, D. L., W. T. Peterson, M. D. Ohman, and B. E. Lavaniegos. 2006. Zooplankton anomalies in the California Current system before and during the warm ocean conditions of 2005. *Geophysical Research Letters* **33**:7 PP.-7 PP.
- Mantua, N. J., S. R. Hare, Y. Zhang, J. M. Wallace, and R. C. Francis. 1997. A Pacific Interdecadal Climate Oscillation with Impacts on Salmon Production. *Bulletin of the American Meteorological Society* **78**:1069-1079.
- Marchesiello, P., J. C. McWilliams, and A. Shchepetkin. 2003. Equilibrium Structure and Dynamics of the California Current System. *Journal of Physical Oceanography* **33**:753-783.

- McClatchie, S., R. Goericke, R. Cosgrove, G. Auad, and R. Vetter. 2010. Oxygen in the Southern California Bight: Multidecadal trends and implications for demersal fisheries. *Geophysical Research Letters* **37**.
- McGowan, J. A., S. J. Bograd, R. J. Lynn, and A. J. Miller. 2003. The biological response to the 1977 regime shift in the California Current. *Deep Sea Research Part II: Topical Studies in Oceanography* **50**:2567-2582.
- Mendelssohn and F. B. Schwing. 2002. Common and uncommon trends in SST and wind stress in the California and Peru–Chile current systems. *Progress In Oceanography* **53**:141-162.
- Mendelssohn, R., F. B. Schwing, and S. J. Bograd. 2003. Spatial structure of subsurface temperature variability in the California Current, 1950–1993. *Journal of Geophysical Research* **108**:3093-3093.
- Messié, M. and F. Chavez. 2011. Global Modes of Sea Surface Temperature Variability in Relation to Regional Climate Indices. *Journal of Climate* **24**:4314-4331.
- Palacios, D. M., S. J. Bograd, R. Mendelssohn, and F. B. Schwing. 2004. Long-term and seasonal trends in stratification in the California Current, 1950–1993. *Journal of Geophysical Research* **109**.
- Parker, B. B. 1991. Sea Level As an Indicator of Climate and Global Change. *Marine Technology* **25**:13-24.
- Peterson, W. J., R. Emmett, R. Goericke, E. Venrick, A. W. Mantyla, S. J. Bograd, F. B. Schwing, R. Hewitt, N. Lo, W. Watson, J. Barlow, M. Lowry, S. Ralston, K. A. Forney, B. E. Lavanigos, W. J. Sydeman, D. Hyrenbach, R. W. Bradley, P. Warzybok, F. Chavez, K. Hunter, S. Benson, M. Weise, J. Harvey, G. Gaxiola-Castro, and R. Durazo. 2006. State of the California Current, 2005-2006: Warm in the north, cool in the south. *California Cooperative Oceanic Fisheries Investigations Reports* **47**:30-74.
- Peterson, W. J. and C. B. Miller. 1977. Seasonal cycle of zooplankton abundance and species composition along the central Oregon coast. *Fishery Bulletin* **74**:717-724.
- Peterson, W. T. 2009. Copepod species richness as an indicator of long term changes in the coastal ecosystem of the northern California Current. *Reports of California Cooperative Oceanic Fisheries Investigations* **50**:73-81.
- Peterson, W. T. and J. E. Keister. 2003. Interannual variability in copepod community composition at a coastal station in the northern California Current: a multivariate approach. *Deep Sea Research Part II: Topical Studies in Oceanography* **50**:2499-2517.
- Peterson, W. T., J. E. Keister, and L. R. Feinberg. 2002. The effects of the 1997–99 El Niño/La Niña events on hydrography and zooplankton off the central Oregon coast. *Progress In Oceanography* **54**:381-398.
- Peterson, W. T., C. A. Morgan, J. O. Peterson, J. L. Fisher, B. J. Burke, and K. L. Fresh. 2012. Ocean ecosystem indicators of salmon marine survival in the northern California Current. NOAA/NMFS/Fish Ecology Division. Accessed 22 March 2012: http://www.nwfsc.noaa.gov/research/divisions/fed/oeip/documents/peterson_etal_2011.pdf.
- Peterson, W. T. and F. B. Schwing. 2003. A new climate regime in northeast pacific ecosystems. *Geophysical Research Letters* **30**:1896-1896.
- Pierce, S. D., J. A. Barth, R. K. Shearman, and A. Y. Erofeev. 2012. Declining Oxygen in the Northeast Pacific. *Journal of Physical Oceanography* **42**:495-501.

- Pond and G. L. Pickard. 1983. *Introductory Dynamical Oceanography*. Pergamon Press.
- Pörtner, H.-O. 2008. Contribution to the Theme Section 'Effects of ocean acidification on marine ecosystems' Ecosystem effects of ocean acidification in times of ocean warming: a physiologist's view. *Marine Ecology Progress Series* **373**:203-217.
- Rabalais, N. N. and R. E. Turner. 2001. *Coastal Hypoxia: Consequences for Living Resources and Ecosystems*. American Geophysical Union.
- Radić, V. and R. Hock. 2011. Regionally differentiated contribution of mountain glaciers and ice caps to future sea-level rise. *Nature Geoscience* **4**:91-94.
- Rijnsdorp, A. D., M. A. Peck, G. H. Engelhard, C. Mollmann, and J. K. Pinnegar. 2009. Resolving the effect of climate change on fish populations. *ICES Journal of Marine Science* **66**:1570-1583.
- Roemmich and J. McGowan. 1995. Climatic warming and the decline of zooplankton in the California current. *Science* **267**:1324-1326.
- Roth, J. E., K. L. Mills, and W. J. Sydeman. 2007. Chinook salmon (*Oncorhynchus tshawytscha*) - seabird covariation off central California and possible forecasting applications. *Canadian Journal of Fisheries and Aquatic Sciences* **64**:1080-1090.
- Rykaczewski, R. R. and D. M. Checkley. 2008. Influence of ocean winds on the pelagic ecosystem in upwelling regions. *Proceedings of the National Academy of Sciences of the United States of America* **105**:1965-1970.
- Rykaczewski, R. R. and J. P. Dunne. 2010. Enhanced nutrient supply to the California Current Ecosystem with global warming and increased stratification in an earth system model. *Geophysical Research Letters* **37**:1-5.
- Rykaczewski, R. R. and J. P. Dunne. 2011. A measured look at ocean chlorophyll trends. *Nature* **472**:E5-E6; discussion E8-E9.
- Saraceno, P. T. Strub, and P. M. Kosro. 2008. Estimates of sea surface height and near-surface alongshore coastal currents from combinations of altimeters and tide gauges. *Journal of Geophysical Research* **113**:1-20.
- Schwing, F. B. and R. Mendelssohn. 1997. Increased coastal upwelling in the California Current System. *Journal of Geophysical Research* **102**:3421-3438.
- Schwing, F. B., T. Murphree, and P. M. Green. 2002. The Northern Oscillation Index (NOI): a new climate index for the northeast Pacific. *Progress In Oceanography* **53**:115-139.
- Snyder, M. A., L. C. Sloan, N. S. Diffenbaugh, and J. L. Bell. 2003. Future climate change and upwelling in the California Current. *Geophysical Research Letters* **30**:1-4.
- Song, H., A. J. Miller, S. McClatchie, E. D. Weber, K. M. Nieto, and D. M. C. Jr. 2012. Application of a data-assimilation model to variability of Pacific sardine spawning and survivor habitats with ENSO in the California Current System. *Journal of Geophysical Research* **117**:C03009-C03009.
- Spence, B. C. and J. D. Hall. 2010. Spatiotemporal patterns in migration timing of coho salmon (*Oncorhynchus kisutch*) smolts in North America. *Canadian Journal of Fisheries and Aquatic Sciences* **67**:1316-1334.

- Strub, P. T. and C. James. 2000. Altimeter-derived variability of surface velocities in the California Current System: 2. Seasonal circulation and eddy statistics. *Deep Sea Research Part II: Topical Studies in Oceanography* **47**:831-870.
- Sunday, J. M., A. E. Bates, and N. K. Dulvy. 2012. Thermal tolerance and the global redistribution of animals. *Nature Climate Change*.
- Sydeman, W. J., R. W. Bradley, P. Warzybok, C. L. Abraham, J. Jahncke, K. D. Hyrenbach, V. Kousky, J. M. Hipfner, and M. D. Ohman. 2006. Planktivorous auklet *Ptychoramphus aleuticus* responses to ocean climate, 2005: Unusual atmospheric blocking? *Geophysical Research Letters* **33**:5 PP.-5 PP.
- Sydeman, W. J. and M. L. Elliott. 2008. Developing the California current integrated ecosystem assessment, module I: Select time-series of ecosystem state., Farallon Institute for Advanced Ecosystem Research, Final report to NOAA/NMFS/Environmental Research Division, Petaluma, CA.
- Sydeman, W. J. and S. A. Thompson. 2010. The California Current integrated ecosystem assessment (IEA) module II: Trends and variability in climate-ecosystem state. Farallon Institute for Advanced Ecosystem Research, Final report to NOAA/NMFS/Environmental Research Division, Petaluma, CA.
- Sydeman, W. J., S. A. Thompson, J. C. Field, W. T. Peterson, R. W. Tanasichuk, H. J. Freeland, S. J. Bograd, and R. R. Rykaczewski. 2011. Does positioning of the North Pacific Current affect downstream ecosystem productivity? *Geophysical Research Letters* **38**:L12606-L12606.
- Sydeman, W. J., S. A. Thompson, M. García-Reyes, M. Kahru, W. T. Peterson, and J. L. Largier. 2014. Multivariate ocean-climate indicators (MOCI) for the central California Current: Environmental change, 1990–2010. *Progress In Oceanography* **120**:352-369.
- Teck, S. J., B. S. Halpern, C. V. Kappel, F. Micheli, K. A. Selkoe, C. M. Crain, R. Martone, C. Shearer, J. Arvai, B. Fischhoff, G. Murray, R. Neslo, and R. Cooke. 2010. Using expert judgment to estimate marine ecosystem vulnerability in the California Current. *Ecological Applications* **20**:1402-1416.
- Thompson, S. A., W. J. Sydeman, J. A. Santora, B. A. Black, R. M. Suryan, J. Calambokidis, W. T. Peterson, and S. J. Bograd. 2012. Linking predators to seasonality of upwelling: Using food web indicators and path analysis to infer trophic connections. *Progress In Oceanography* **101**:106-120.
- Wells, B. K., J. C. Field, J. A. Thayer, C. B. Grimes, S. J. Bograd, W. J. Sydeman, F. B. Schwing, and R. Hewitt. 2008. Untangling the relationships among climate, prey and top predators in an ocean ecosystem. *Marine Ecology Progress Series* **364**:15-29.
- Wolter, K. and M. S. Timlin. 2011. El Niño/Southern Oscillation behaviour since 1871 as diagnosed in an extended multivariate ENSO index (MEI.ext). *International Journal of Climatology* **31**:1074-1087.